NAVAL POSTGRADUATE SCHOOL
Monterey, California

THESIS

THE EFFECTS OF FREESTREAM TURBULENCE ON
AIRFOIL BOUNDARY LAYER BEHAVIOR
AT LOW REYNOLDS NUMBERS

by

David W. Kindelspire

September 1988

Thesis Advisor: Prof. R. M. Howard

88 12 27 131

REPORT DOCUMENTATION PAGE

1a REPORT SECURITY CLASSIFICATION UNCLASSIFIED		1b RESTRICTIVE MARKINGS			
2a SECURITY CLASSIFICATION AUTHORITY		3 DISTRIBUTION/AVAILABILITY OF REPORT Approved for public release; distribution is unlimited.			
2b DECLASSIFICATION / DOWNGRADING SCHEDULE					
4 PERFORMING ORGANIZATION REPORT NUMBER(S)		5 MONITORING ORGANIZATION REPORT NUMBER(S)			
6a NAME OF PERFORMING ORGANIZATION Naval Postgraduate School	6b OFFICE SYMBOL (If applicable)	7a NAME OF MONITORING ORGANIZATION Naval Postgraduate School			
6c ADDRESS (City, State, and ZIP Code) Monterey, CA 93943-5000		7b ADDRESS (City, State, and ZIP Code) Monterey, CA 93943-5000			
8a NAME OF FUNDING/SPONSORING ORGANIZATION	8b OFFICE SYMBOL (If applicable)	9 PROCUREMENT INSTRUMENT IDENTIFICATION NUMBER			
8c ADDRESS (City, State, and ZIP Code)		10 SOURCE OF FUNDING NUMBERS			
		PROGRAM ELEMENT NO	PROJECT NO	TASK NO	WORK UNIT ACCESSION NO

11 TITLE (Include Security Classification) THE EFFECTS OF FREESTREAM TURBULENCE ON AIRFOIL BOUNDARY LAYER BEHAVIOR AT LOW REYNOLDS NUMBERS

12 PERSONAL AUTHOR(S) Kindelspire, David W.

13a TYPE OF REPORT Master's Thesis	13b TIME COVERED FROM _____ TO _____	14 DATE OF REPORT (Year, Month, Day) September 1988	15 PAGE COUNT 117

16 SUPPLEMENTARY NOTATION The views expressed in this thesis are those of the author and do not reflect the official policy or position of the Department of Defense or the U.S. Government.

17 COSATI CODES			18 SUBJECT TERMS (Continue on reverse if necessary and identify by block number)
FIELD	GROUP	SUB-GROUP	Reynolds Numbers; Laminar flow, Boundary Layer; Transition
			Turbulence;

19 ABSTRACT (Continue on reverse if necessary and identify by block number) An experimental study was conducted to determine the effects of freestream turbulence on airfoil boundary layer behavior. Freestream turbulence intensity levels up to approximately 4% and length scales up to approximately two inches were generated using turbulence-generating grids. Data were collected using a single-wire hot-wire probe in conjunction with a three-dimensional traversing system. Increased levels of freestream turbulence were found to cause correspondingly earlier transition to a turbulent boundary layer. Boundary layer growth was found to be unaffected by freestream turbulence levels up to 4% at length scales an order of magnitude greater than the boundary layer thickness. For length scales on the order of boundary layer thickness, a 12% increase in the turbulent boundary layer thickness was found with an increase in turbulence intensity from 0.23% to 0.5%. Keywords:

Theses, Computer programs,

20 DISTRIBUTION/AVAILABILITY OF ABSTRACT ☒ UNCLASSIFIED/UNLIMITED ☐ SAME AS RPT ☐ DTIC USERS	21 ABSTRACT SECURITY CLASSIFICATION Unclassified	
22a NAME OF RESPONSIBLE INDIVIDUAL R.M. Howard	22b TELEPHONE (Include Area Code) (408) 646-2870	22c OFFICE SYMBOL 67HO

DD FORM 1473, 84 MAR   83 APR edition may be used until exhausted   SECURITY CLASSIFICATION OF THIS PAGE
All other editions are obsolete

UNCLASSIFIED

The Effects of Freestream Turbulence
on Airfoil Boundary Layer Behavior
at Low Reynolds Numbers

by

David W. Kindelspire
Lieutenant, United States Navy
B.S., Southeast Missouri State University, 1980

Submitted in partial fulfillment of the
requirements for the degree of

MASTER OF SCIENCE IN AERONAUTICAL ENGINEERING
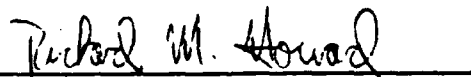
from the

NAVAL POSTGRADUATE SCHOOL
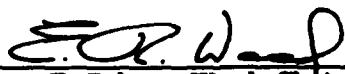September 1988

Author: _____

David W. Kindelspire

Approved By: _____

Richard M. Howard, Thesis Advisor

_____

E. Roberts Wood, Chairman,
Department of Aeronautics and Astronautics

_____

Gordon E. Schacher,
Dean of Science and Engineering

ii

ABSTRACT

An experimental study was conducted to determine the effects of freestream turbulence on airfoil boundary layer behavior. Freestream turbulence intensity levels up to approximately 4% and length scales up to approximately two inches were generated using turbulence-generating grids. Data were collected using a single-wire hot-wire probe in conjunction with a three-dimensional traversing system. Increased levels of freestream turbulence were found to cause correspondingly earlier transition to a turbulent boundary layer. Boundary layer growth was found to be unaffected by freestream turbulence levels up to 4% at length scales an order of magnitude greater than the boundary layer thickness. For length scales on the order of boundary layer thickness, a 12% increase in the turbulent boundary layer thickness was found with an increase in turbulence intensity from 0.23% to 0.5%.

QUALITY SPECTED

```
Accession For
NTIS   GRA&I        ☑
DTIC TAB            ☐
Unannounced         ☐
Justification

By
Distribution/
  Availability Codes
       Avail and/or
 Dist    Special

A-1
```

iii

TABLE OF CONTENTS

ACKNOWLEDGEMENT

This paper would not have been possible without the invaluable assistance of a number of individuals who deserve special thanks and recognition. The following NPS Aeronautical Engineering technicians provided invaluable assistance in design, manufacture, and implementation of the hardware used in this research:

- Mr. Pat Hickey
- Mr. Alan M'Guire
- Mr. Ron Ramaker
- Mr. John Moulton
- Mr. Don Harvey
- Mr. Jack King

Additionally, the support, wisdom, and guidance of my thesis advisor, Professor Rick Howard is greatly appreciated.

Finally, I wish to thank my wife, ███ and my children for their infinite patience during the long periods of time I was working toward reaching this goal.

I. INTRODUCTION

A. BACKGROUND

In recent years, interest in low Reynolds number aerodynamics has risen dramatically due to the changing flight regimes of today's flight vehicles. Low Reynolds numbers are typically thought of as being 500,000 or less and occur when there is a low free-stream velocity, low air density (high altitude), or a small airfoil chord normally associated with high aspect ratio wings.

Within the civilian community, the growing popularity of radio-controlled model aircraft, sailplanes, and manned ultra-lights has resulted in a myriad of slow-flight high aspect ratio aircraft designed specifically for flight in the low Reynolds number regime. Additionally, the recent successes of such experimental aircraft as the man-powered Gossomer Condor and the record-setting Voyager have demonstrated the feasibility of efficient low Reynolds number flight and have sparked renewed interest in research and development in this field. [Ref. 1]

Military interest, too, is at an all-time high due to the increased operational role projected for Remotely Piloted Vehicles (RPVs). In the past, the role of the military RPV has been limited to such missions as target drone and weather reconnaissance. However, given the ever-increasing cost per flight hour for manned aircraft, in both materials and manpower, military strategists and long-range planners are now taking a

1

much closer look at the utilization of the RPV in support of manned flight operations. The future role of the military RPV now includes such missions as communication relay, aircraft identification and tracking, laser target identification, defense suppression, long-range open-ocean surveillance, and photo/radar imagery [Ref 1]. Flight profiles for these unmanned vehicles will be dictated by the particular mission assignments and will include extended flight at high altitude, low speed flight at low altitude, or combinations of both. All profiles will result in low Reynolds numbers.

B. TURBULENCE

Flow in which there are random, small-scale velocity fluctuations about the mean freestream flow velocity is said to be turbulent. In order to characterize the amount of turbulence present in the flow field, two parameters are normally used. The first, turbulence intensity (T_u), is normally expressed as a percentage and used as a measure of the relative magnitude of the velocity fluctuations. Turbulence intensity is defined as the root-mean-square (rms) value of the fluctuations divided by the mean velocity of the flow field. [Ref. 2]

The second term used in characterizing turbulence is the turbulence length scale. The length scale is used to describe the dimensional parameters of the fluctuations, i.e. space and time, relative to the size of the body in the flow field. Large length scale perturbations are considered to be of a size comparable to or larger than the body. Since

velocity perturbations can be thought of as turbulent eddies existing in the flow field, large length scale values can be associated with large eddies that take a relatively long period of time to pass over the body in the flow field. Therefore, they tend to affect the entire body in the flow over a longer period of time than small length scale perturbations. This is analogous to changing the entire flow field for a relatively long period of time.

Small length scale turbulence has a spatial dimension that is much smaller than the body in the flow field and its effects on the body are quite different from large length scale turbulence. Small length scale turbulence has a spatial dimension on the order of boundary layer thickness and its effects on the body are felt for very short periods of time. This type of turbulence effects only the flow around the body--not the body itself. Thus, boundary layer formation, transition, and separation are greatly affected by small length scale turbulence. [Refs. 2 and 3]

Turbulence, to some degree, is present in all wind tunnels. Sources of the turbulence can be inherent to the tunnel (flow straighteners, turning vanes, or mechanical vibrations) or intentionally generated by using turbulence-generating grids [Refs. 4 and 5]. In his Master's thesis, Roane [Ref. 3] experimentally "mapped" the turbulence of the Naval Postgraduate School wind tunnel for four different turbulence generating grids. Figure 1 and Figure 2 show the wind tunnel's turbulence intensity and turbulence length scales as functions of position in the test

3

section. With no grid installed, turbulence intensity in the wind tunnel is constant at 0.23% (not shown in Figure 1) [Ref. 3]. The grids used to generate wind tunnel turbulence will be discussed in more detail in the hardware section of this report.

C. RELATED WORK

Historically, the vast majority of aerodynamic research, and in particular research pertaining specifically to boundary layer studies, has been conducted in the high Reynolds number regime (Reynolds numbers in excess of 1,000,000). This research has resulted in a variety of very accurate flow-modelling techniques with which to mathematically predict wing performance prior to construction or wind tunnel testing. However, these modelling techniques, such as lifting-line theory, vortex-lattice theory, and wing panelling methods, are all inviscid flow modelling techniques based upon potential flow theory. They are independent of Reynolds number effects until combined with existing boundary layer codes. The effect of Reynolds numbers does not play a large role in solutions obtained with these flow-modelling techniques alone because they assume a "natural" boundary layer transition from laminar to turbulent flow. [Ref. 5]

This natural boundary layer transition begins downstream of the leading edge and is usually located at or near the point of minimum pressure. In the high Reynolds number regime this natural boundary
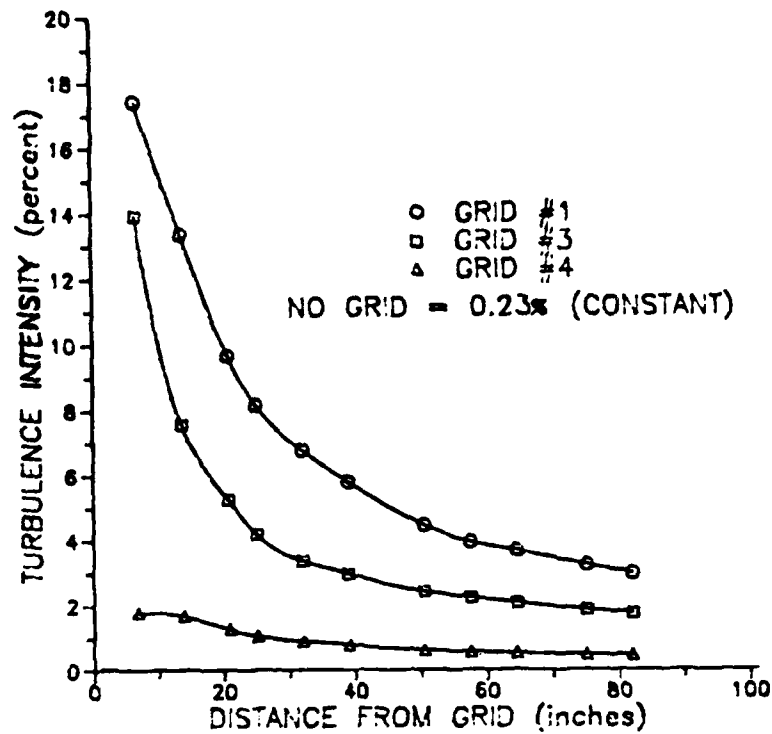
Figure 1. Grid-Generated Turbulence Intensity [Ref. 3]
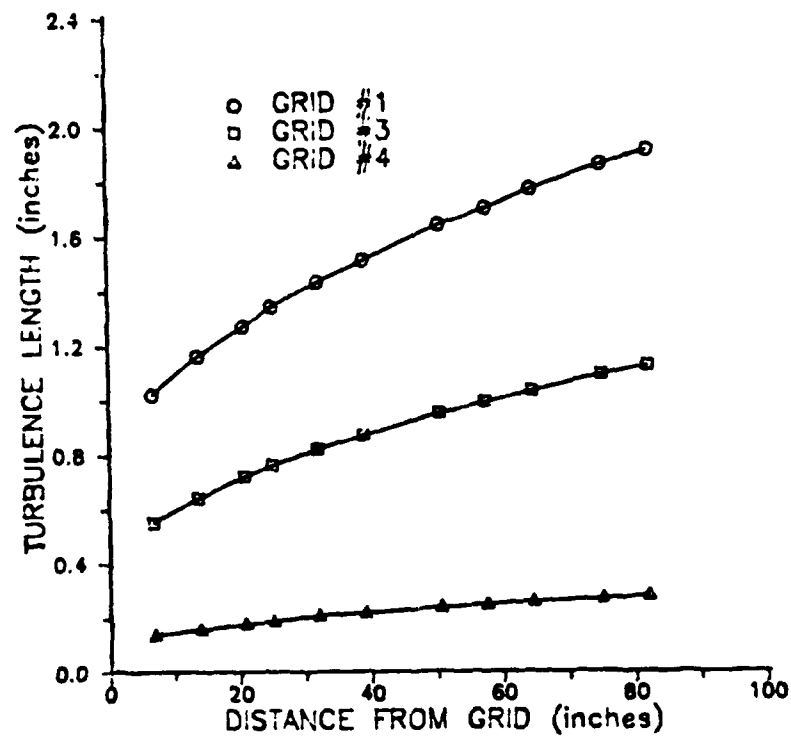
Figure 2. Grid-Generated Length Scale [Ref. 3]

5

layer transition is not normally characterized by separated flow behavior. The attached laminar boundary layer transitions to an attached turbulent boundary layer. Separation will occur farther downstream when the attached turbulent layer can no longer overcome the adverse pressure gradient. [Ref. 5]

Quite unlike high Reynolds number flow, transition at low Reynolds numbers from a laminar to a turbulent boundary layer is not a well-understood process. Several airfoils which operate efficiently at low Reynolds numbers, particularly the Wortmann FX 63-137, the Miley airfoil, and the Lissaman airfoil, exhibit a laminar separation region phenomenon during transition commonly referred to as the "laminar separation bubble". This phenomenon is characterized by a separation of the laminar boundary layer followed by transition to a turbulent shear layer (i.e., a "detached" boundary layer). This turbulent shear layer will, given the right conditions, reattach to the airfoil surface creating a separated "bubble" region between the laminar separation point and the turbulent reattachment point. The conditions required for reattachment are not yet fully understood. However, if the reattachment does occur, the overall performance of the airfoil is significantly increased over the performance of one in which the turbulent shear layer remains separated. This boundary layer phenomenon, though unique to low Reynolds number flows, has been experimentally demonstrated in only a relatively few cases. [Ref. 1]

Brendel and Mueller [Refs. 6 and 7] have done extensive research in this field, particularly with the Wortmann airfoil. They have described two types of separation bubbles, short and long bubbles, and have shown these bubbles occupying up to 15% of the airfoil chord depending on experimental conditions. Schmidt, O'Meara, and Mueller investigated the NACA 66_3-018 airfoil in the low Reynolds number regime and reported on several criteria influencing the formation and size of the laminar portion of the separation bubbles. Among the criteria cited in their report are chord Reynolds number and the freestream disturbance environment [Ref. 9]. Crouch and Saric investigated separation bubbles on the Wortmann airfoil using hot-wire anemometry [Ref. 10]. Their research, conducted primarily at Reynolds numbers of approximately 150,000, shows that separation bubbles are generally smaller and are formed farther downstream with increasing Reynolds numbers. They concluded that disturbances within the boundary layer must reach a critical amplitude in order to trigger flow separation and bubble formation.

Mueller gives an excellent summary of much of the research conducted in the low Reynolds numbers regime [Ref. 1]. His characterization of boundary layer behavior, particularly in relation to laminar separation bubbles, highlights the critical role played by these separation bubbles in overall airfoil performance and notes the importance of free stream parameters (velocity, turbulence, Reynolds numbers, etc.) on separation bubble formation and behavior. More experimental studies need to be undertaken in order to more fully

7

understand these phenomena to effectively predict and control boundary layer behavior in low Reynolds number flow.

D. PURPOSE OF EXPERIMENT

The main purpose of this project is to investigate airfoil performance, specifically the boundary layer development and behavior, at low Reynolds numbers in the presence of high turbulence levels. The experimental Reynolds numbers will be approximately 500,000 and steady-state levels of freestream turbulence up to 4% will be generated using turbulence grids. Data collected will help to form a data base for follow-on research and testing at higher levels of both steady and unsteady turbulence. Additionally, experimental data can be utilized by Computational Fluid Dynamicists (CFD) working on algorithms to simulate actual flows at low Reynolds numbers with elevated levels of freestream turbulence.

II. EXPERIMENTAL APPARATUS

A. EXPERIMENTAL HARDWARE

The experimental hardware for this experiment can be divided into five major subdivisions. These are the wind tunnel, the wing/wing mount, the anemometry system, the 3-D traverser, and the turbulence grids. Each of these will be individually discussed in the following sections.

1. Wind Tunnel

The Naval Postgraduate School's 32-inch by 45-inch low-speed wind tunnel was used during this research. The tunnel, shown schematically in Figure 3, is a single return tunnel measuring 64 feet in length with the width varying from 21.5 feet to 24.5 feet. The tunnel is powered by a 100 horsepower electric motor coupled to a three-bladed variable pitch fan by a four-speed Dodge transmission. [Ref. 4]

As the flow moves downstream of the fan blades, it passes through one set of stators and three sets of turning vanes which turn the flow 270° for entry into the contraction cone and test section. The stators, more commonly called the flow straighteners, are designed and installed to remove the swirling velocities imparted to the flow by the fan. The turning vanes used are plane curved sheets with segmented trailing edges for minor flow adjustments. Working in conjunction, the stators and the turning vanes minimize tunnel turbulence.

9
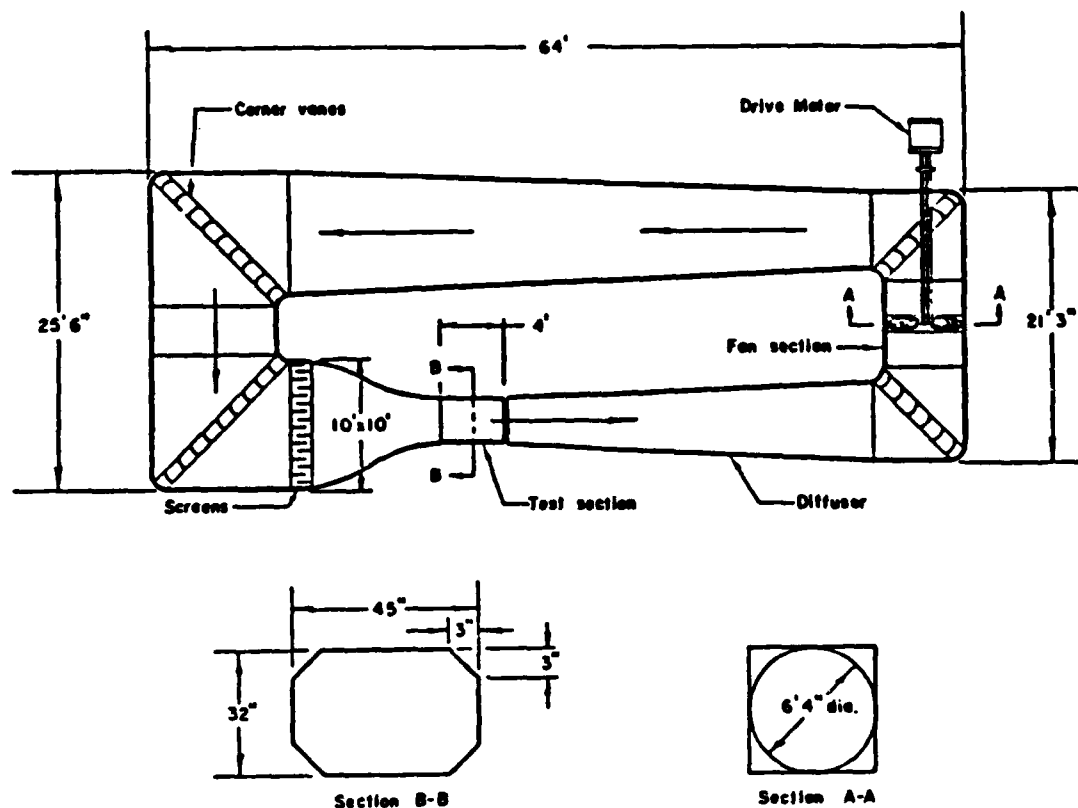
Figure 3. NPS Wind Tunnel Schematic Drawing [Ref. 4]

In the settling chamber, where the tunnel cross section is the largest, the flow velocity is lower than any other place in the tunnel. Installed here are two additional fine-mesh wire screens, shown in Figure 3, designed to smooth the flow even more. The screens are positioned six inches apart and effectively break down any large velocity perturbations (turbulence) into smaller ones that are quickly dissipated as heat energy.

The smoothed flow then enters the contraction cone leading into the test section. The function of the contraction cone is to accelerate the flow to the desired velocity in the test section. The contraction ratio of the NPS tunnel is approximately 10 to 1.

The test section, which operates at atmospheric pressure due to a circumferential breather slot located just downstream, has a floor-mounted reflection plane and slightly divergent walls to compensate for the effective area contraction due to boundary layer growth along the walls of the wind tunnel. The reflection plane has a flush-mounted turntable and balance plate installed that was not utilized in this experiment. The test section also has a pitot-static system connected to an airspeed indicator, providing an indication of tunnel velocity. For this experiment, a separate pitot-static system was installed and used in the calibration procedure to be discussed in a later section.

2. Wing/Wing Mount Assembly

The airfoil originally selected for this experiment was the Wortmann FX 63-137. However, due to the unavailability of the Wortmann model at the time of testing, an alternate airfoil section was selected. The airfoil chosen was a tail rotor section from a Bell helicopter. The tail rotor airfoil is shown in Figure 4 and the X-Y coordinates are given in Table A-1, Appendix A. It has a 10-inch chord and was cut to a 24-inch span, filled, sanded, smoothed, and finished with a coating of black lacquer paint. The black lacquer was chosen due to its reflectivity.

11
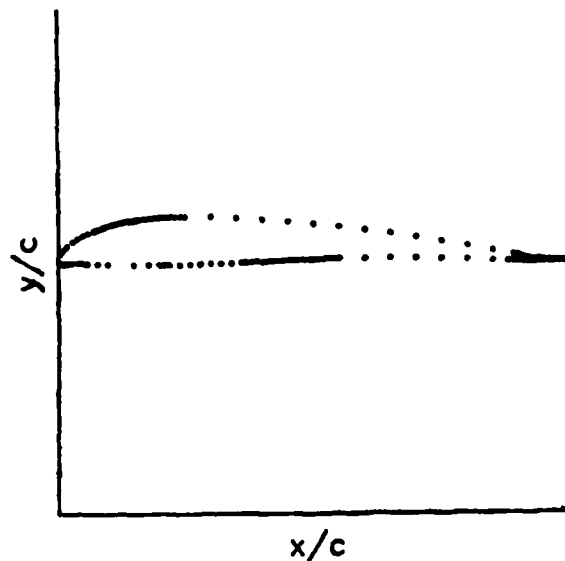
Figure 4. Experimental Airfoil Section

The reflectivity of the surface is important during hot-wire probe movements into the boundary layer. In order to get the probe as close as possible to the surface of the wing, the operator must look through a surveyor's transit scope as the probe and its reflection off the wing moved toward each other. By using graduated marking on the scope's reticle, it was possible to get the probe to within approximately 0.005 inches of the surface. These graduated marks were also a useful tool in ensuring that boundary layer data originated from the same distance above the wing each time for each chord location chosen. It is noted here that additional tunnel lighting was required to clearly see both the probe and its reflection. Figure 5 shows the probe and its reflection as they appear just prior to a data collection run.
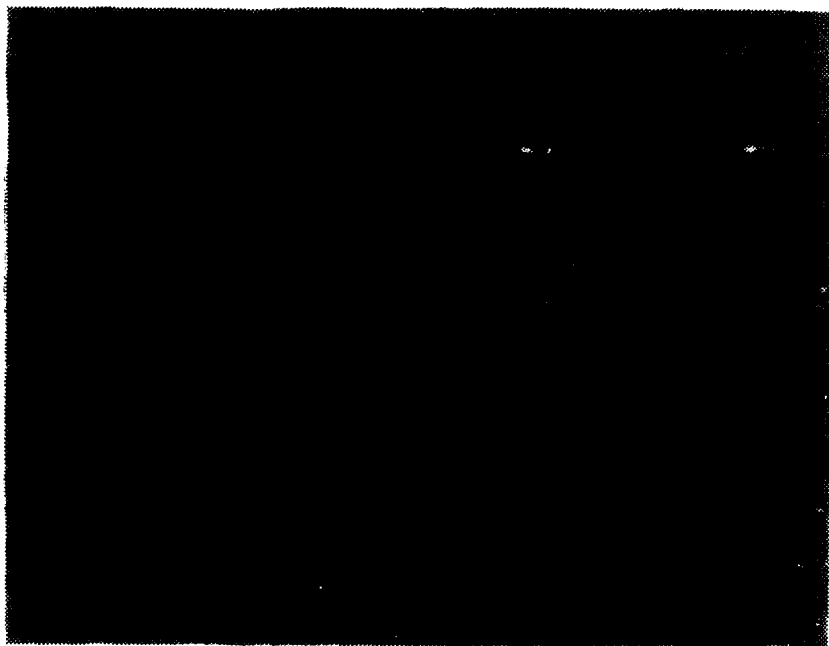
Figure 5. Hot-Wire Probe/Reflection

The open ends of the 24-inch tail rotor section were capped with aluminum inserts containing round metal studs. The studs were inserted in and secured to the mounting bracket assemblies.

The mounting brackets were designed by the author and manufactured by technicians at the Naval Postgraduate School. They are constructed of 1/4-inch and 1/2-inch aluminum and are mounted vertically in the wind tunnel from the reflection plane on the floor to the ceiling as shown in Figure 6. The leading edges of all sections of the brackets are rounded to minimize flow disturbance near the airfoil. A general rule-of-thumb noted here is that flow disturbance due to end plates may be evident up to approximately one chord length from the mount. All data collected during this experiment was taken at the mid-span of the airfoil

13
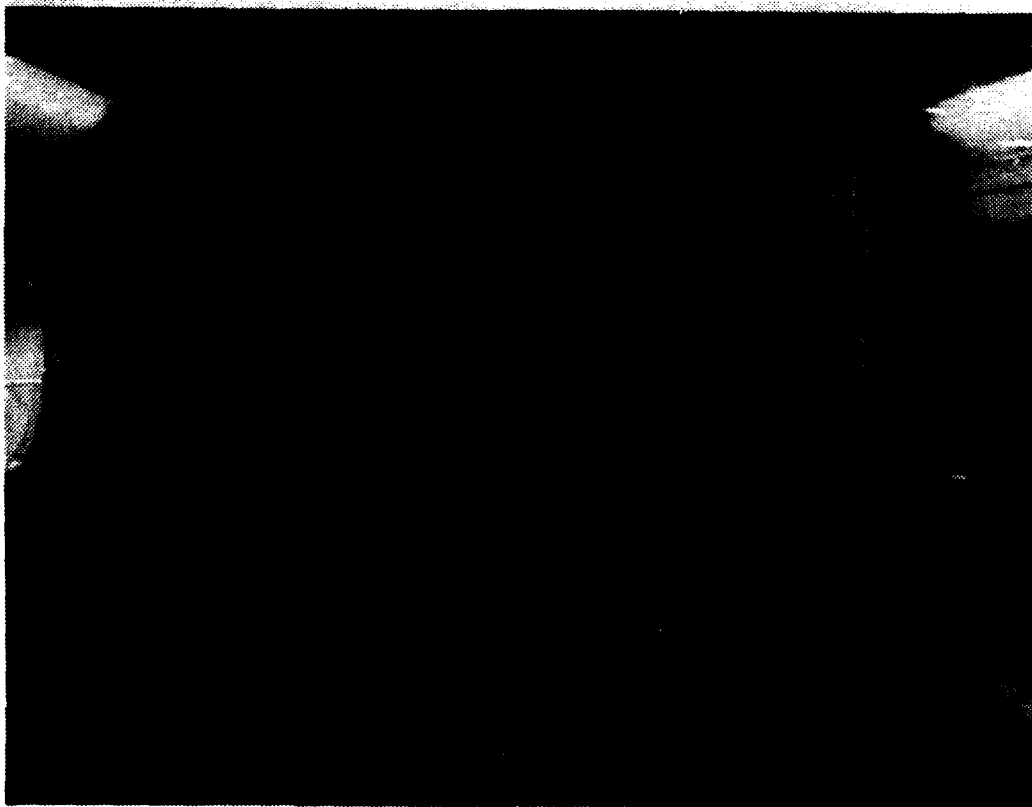
Figure 6. Wing/Wing Mount Installed in NPS Wind Tunnel

section, a sufficient distance away from the mounts (approximately 1.2 chord lengths).

The metal studs on the airfoil endcaps were fitted into an adjustable portion of the mounting hardware capable of adjusting the angle-of-attack (AOA) from +35° to -15°. Figure 7 shows a side view of the wing mounts and the AOA adjustment ring. Graduated markings on the outer cylinder are used in conjunction with a fixed mark on the mount to set AOA. Data collected were taken at 6° AOA for this experiment. Six degrees was chosen to ensure boundary layer transition

Figure 7. Side View of Wing Mount

at some point on the surface and to minimize the chance for separated flow (complete airfoil stall) over the airfoil surface.

3. Hot-Wire Anemometry System

Figure 8 shows the TSI Inc. IFA-100 Model 158 constant temperature anemometer system used in this experiment. Model 158 is a high performance, low noise system featuring digital readout of the hot-wire voltage and operator-selectable signal conditioning circuitry. [Ref. 11]

Hot-wire anemometry is a flow velocity measurement technique in which a very small tungsten or platinum-coated wire (usually on the order of 5 microns in diameter) is suspended perpendicular to the flow field between two support structures as shown in Figure 9. The support structures are typically stainless steel needle-like structures designed for minimum flow obstruction. The distance between the probe tips can

15

Figure 8. IFA-100 Anemometry System

vary, but for accurate velocity measurements and minimum interference from the supports, the ratio of wire length to wire diameter should be greater than 200. [Ref. 2]

The probe is electrically connected to an output/control amplifier through a Wheatstone bridge circuit and is heated by the current flow provided by the amplifier. As the flow velocity across the wire increases, the wire is cooled by the flow and its

Figure 9. Hot-Wire Probe

resistance decreases. The response of the output/control amplifier to this inbalance in the bridge potential is an increase in current flow through

16
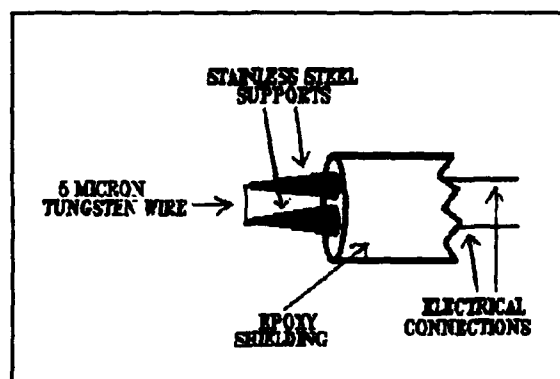
the bridge circuit in order to rebalance the bridge electrically. A typical constant-temperature bridge circuit is shown in Figure 10.

The operator inputs the desired operating resistance of the probe which sets the resistance of the control resistor (Rc). The output of the Wheatstone bridge is connected directly to the control amplifier. As the flow velocity over the wire increases, the hot-wire cools and its resistance is lowered. This decrease in resistance on one branch of the bridge circuit decreases the voltage input to the control amplifier. The amplifier then increases the current flow into the bridge via the feedback loop in order to rebalance the voltage potential across the bridge. This increase in current flow on the bridge will heat the wire, returning the wire to
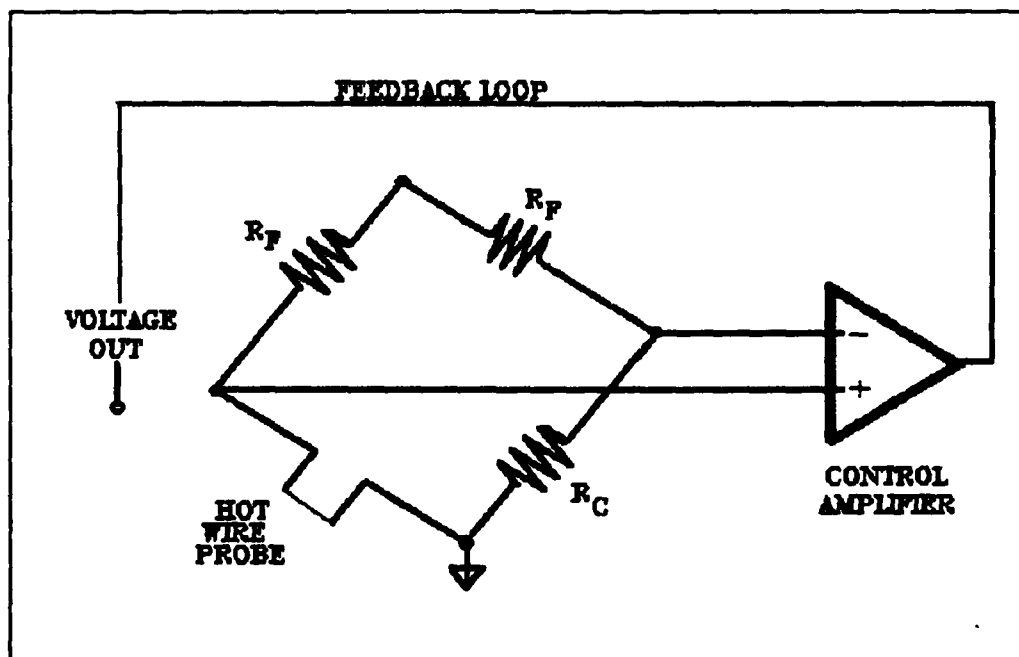
Figure 10. Bridge Circuit

17

the appropriate temperature, thus increasing its resistance and rebalancing the bridge. [Ref. 11]

The output of the constant-temperature anemometer system is the voltage output of the control amplifier which is directly proportional to the amount of current required to maintain a balanced voltage potential across the bridge. The flow velocity associated with a given control amplifier output voltage will determine the calibration curve for that particular probe. The methodology of calibration will be addressed in Section III of this report.

The major benefit of selecting a constant-temperature anemometry system, as opposed to a constant-current system, is the high levels of frequency response achieved by using a feedback loop in association with the control amplifier. With modern solid state components, particularly in a rapidly fluctuating flow field (i.e., turbulent flow), frequency responses as high as 500 KHz can be achieved. Additional benefits of the constant-temperature system include the system's ability to accurately measure very large velocity fluctuations and the lower inherent noise levels of the system. [Ref.11]

The type of hot-wire probe used was the Dantec Single-Wire Sensor 55 P-11. The control amplifier output voltage range for this probe, over the span of velocities expected to be encountered, was found to be less than one volt. Therefore, with the turbulence grids in place, the voltage fluctuations (due to turbulence) in this limited voltage range made data collection very difficult. However, by using the signal

18

conditioning circuitry of the IFA-10C system, the displayed output voltage range was adjusted to be zero volts with no flow in the tunnel and approximately five volts at the higher flow velocities. System settings for this response were an offset of one volt and a gain of six. Using these signal conditioning settings, observed voltage outputs within the boundary layer ranged from 3 volts to 4.5 volts. Since the data recorded by the author was manually read and input, the wider range of output voltages made for easier and more accurate readings.

Signal filtering, another selectable option of the signal conditioning circuitry of the IFA-100, was used to prevent any aliasing of the rms signals and to filter out unwanted noise present in the system. Filters selected for this experiment were a 100 KHz AC low-pass filter and a DC high-pass filter. Figure 11 shows the overall data collection system and signal transfer paths.

Two additional pieces of hardware were used in conjunction with the anemometry system and are also shown in Figure 8. An oscilloscope was used as a visual indication to the operator of the relative turbulence level present in the tunnel. An oscilloscope will show a near-flat voltage trace outside the boundary layer with little or no turbulence present (no grid). At higher turbulence levels, voltage traces of the turbulence appear as random amplitude fluctuations of the trace. As the probe entered the top of the boundary layer, the oscilloscope trace changed from the free stream turbulence trace, thus providing the operator an easy reference to the approximate height of the boundary layer at a

19

given chord location. The oscilloscope reading was then confirmed by a check of the hot-wire control amplifier voltage output. The mean output voltage of the hot-wire also changed from the free stream value as the probe entered the boundary layer.

The last piece of hardware used in the data collection system was the Fluke 8050A Digital Multimeter (DMM). During data collection, the IFA-100 system indicated DC voltage output of the control amplifier. The DMM was also connected to the control amplifier output through a coaxial cable connection on the front of the IFA-100 monitor. The DMM was configured to read only the AC component of the output voltage. The DMM read the AC component, then computed and displayed rms
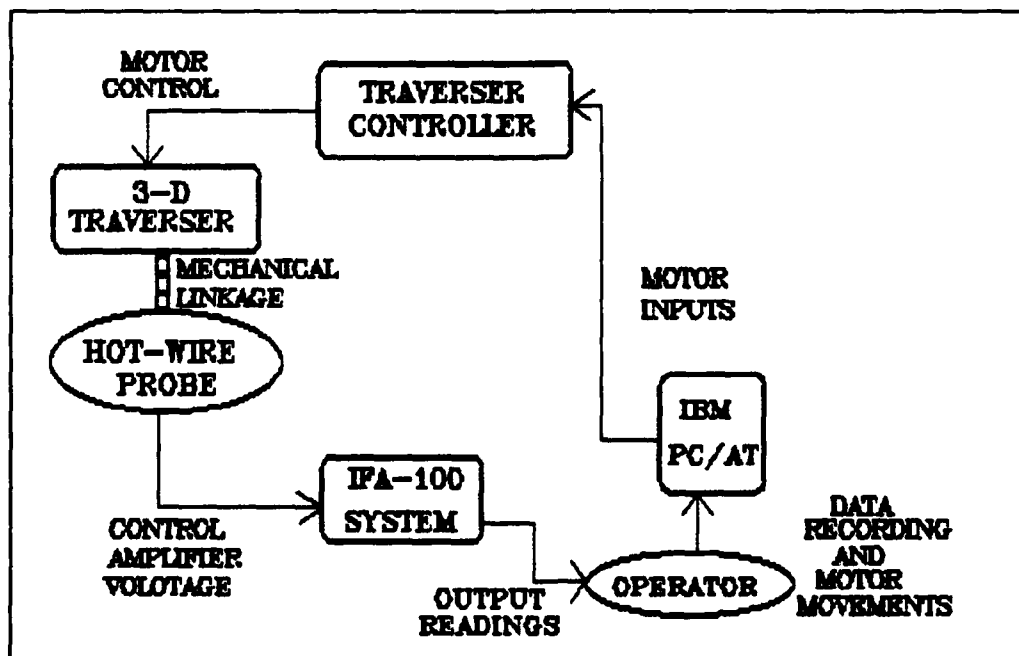
Figure 11. Data Aquisition/Signal Flow Schematic

values of the voltage fluctuations. These rms values were later used in plots to give representing relative turbulence levels at any given point in the sampled boundary layer.

4. Three-Dimensional Traverser

To accurately and effectively move the hot-wire probe through the boundary layer, the probe was attached to a Velmex 8300 Control/Driver. The 8300 is a 3-D traversing system using three microcomputer-controlled stepping motors (one for each axis of movement). The system is composed of the motor controller assembly and the traversing assembly as shown in Figure 12.
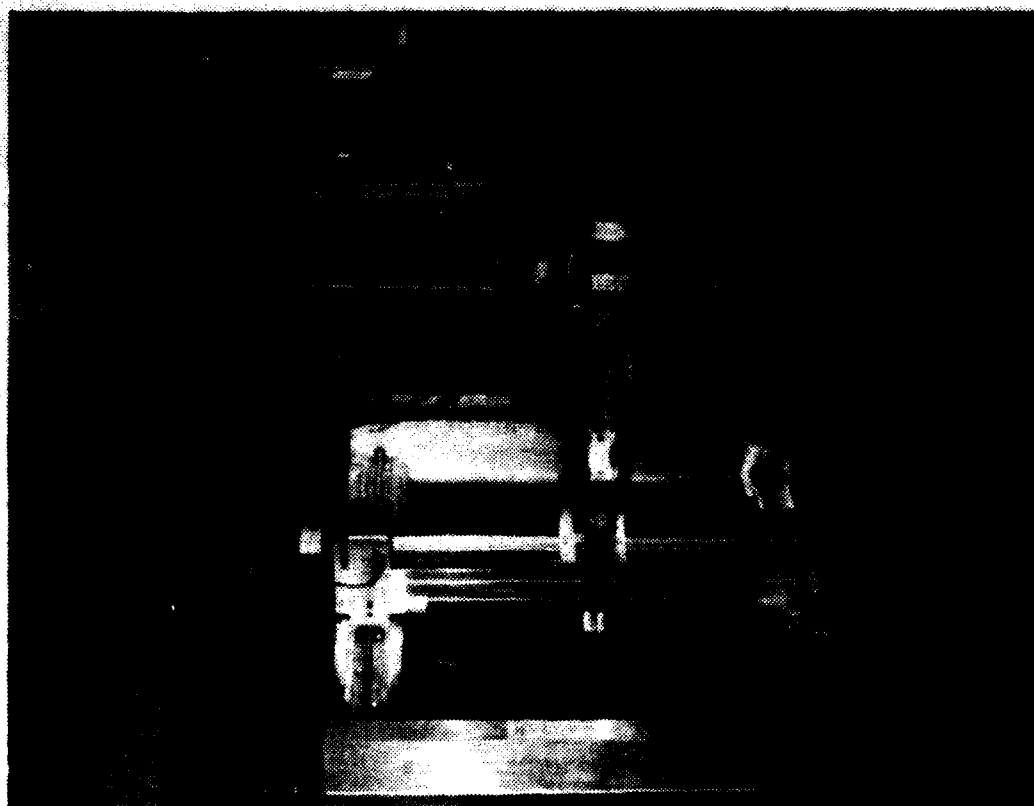
Figure 12. Velmex 8300 3-D Traverser Assembly

21

The motor controller assembly is the interface unit between the operator and the motors. The controller is capable of interpreting motor movement commands from a host computer or from a remote terminal. Data communication between the controller assembly and a remote terminal is made through a full-duplex RS-232C port located on the front of the controller assembly. Operator-initiated manual motor movements are input via switches also located on the front panel.

The resident BASIC interpreter software program contains the necessary motor movement subroutines and is responsible for monitoring motor status. Fault lights on the front panel indicate parity or data bus errors and a ready light indicates the previous motor movement is completed and the controller is ready to accept the next input. Additionally, the controller has 12K of custom hardware and 20K of ROM contained on a 6502-based microchip for interactive pre-programmed motor control. Operator-selectable motor variables, accessible through software commands, include motor velocity, motor acceleration, increment distance, and incremental units (motor steps or inches). [Ref. 12]

The traverser assembly is a stainless steel and aluminum assembly consisting of three separate motor/jackscrew assemblies. Each motor/jackscrew combination moves the traverser along one of the axes depending on the connections made to the controller. Each motor is a 200 step-per-revolution, ten amp stepper motor with a maximum velocity of 3000 steps/sec. Minimum motor movement is one motor step (1/200 of a revolution) which equates to approximately 0.000125 inches. [Ref. 12]

22

Several minor modifications were made to the 8300 system for use in conjunction with the Naval Postgraduate School wind tunnel. To move the hot-wire into the boundary layer on the upper surface of the wing, the traverser assembly was mounted on top of the tunnel. Two one-inch aluminum bars were attached to the base of the traverser and mounted to existing hardware located on top of the tunnel. The assembly was mounted in a position such that tunnel-induced vibrations on the traverser were minimized, thus reducing hot-wire probe vibrations during data collection.

With the traverser and controller assemblies mounted on top of the tunnel, a 25-foot RS-232C cable enabled motor movements to be made from a computer terminal terminal located next to the tunnel. Additionally, a one-foot extension bar was inserted between the traverser mounting bracket and the hot wire probe mounting tube to allow the probe to reach the trailing edge of the airfoil at very high angles of attack. Access into the wind tunnel was made through a small slot cut into a plexiglass sheet fitted into the top of the tunnel, as shown in Figure 12.

Motor movements were controlled via the controller assembly from an IBM PC/AT computer located adjacent to the tunnel. The author created a program, to be discussed in detail in the software section of this report, that allowed for both manual motor movements (i.e., one entry--one movement) and computer-controlled movements through the boundary layer. Motor movements in the computer

23

controlled option depend on operator inputs of the number of data points desired and the size of the boundary layer to be measured. In order to avoid distance ambiguities with extremely small motor movements, all computer-controlled movements were limited to 0.0002 inches (approximately twice the published minimum motor movement).

5. Turbulence-Generating Grids

Three different turbulence-generating grids, shown in Figure 13, were used during this experiment. The grids were constructed by Roane [Ref. 3] and used by him and Rabang [Ref. 13] to study the effects of
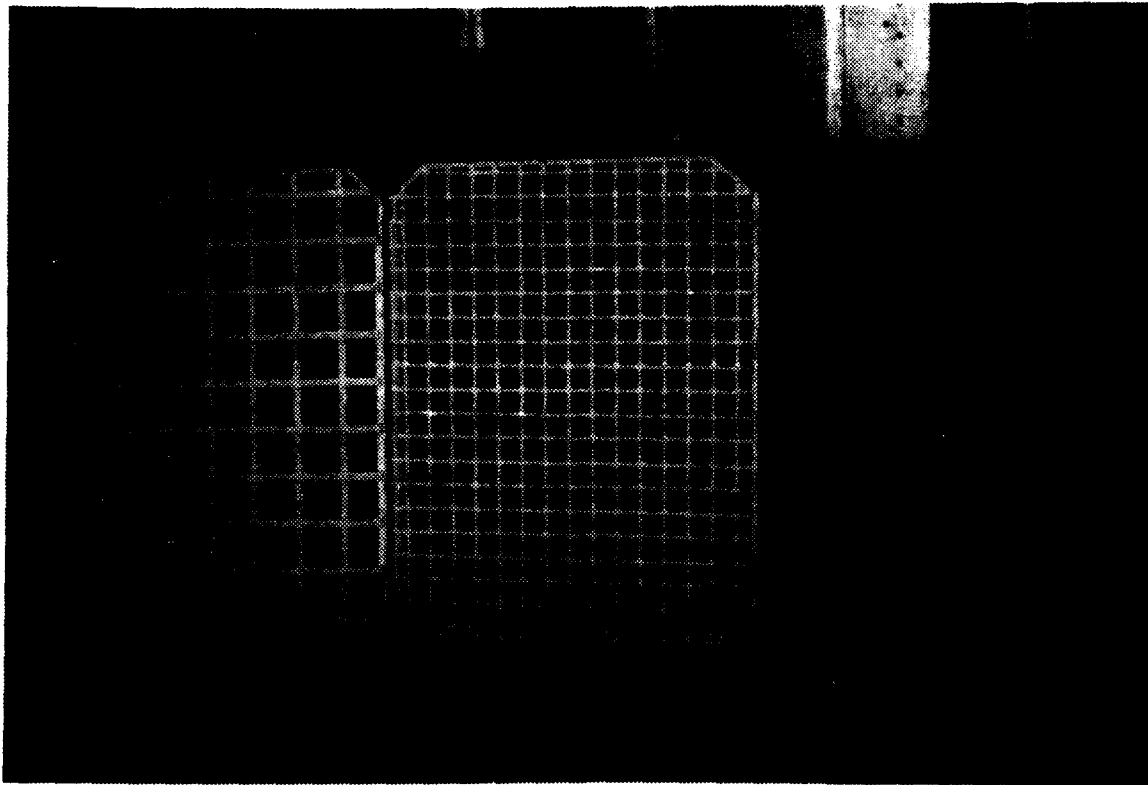
Figure 13. Turbulence Grids

turbulence on vertically launched missiles. Two of the grids were wooden, square-mesh, biplanar grids and the third was a wire, square-mesh, round-axis grid. The grids were installed in the wind tunnel just ahead of the test section and were located approximately 72 inches upstream of the mid-chord line of the airfoil. Figure 14 shows the wing installed in the tunnel with a turbulence grid upstream.
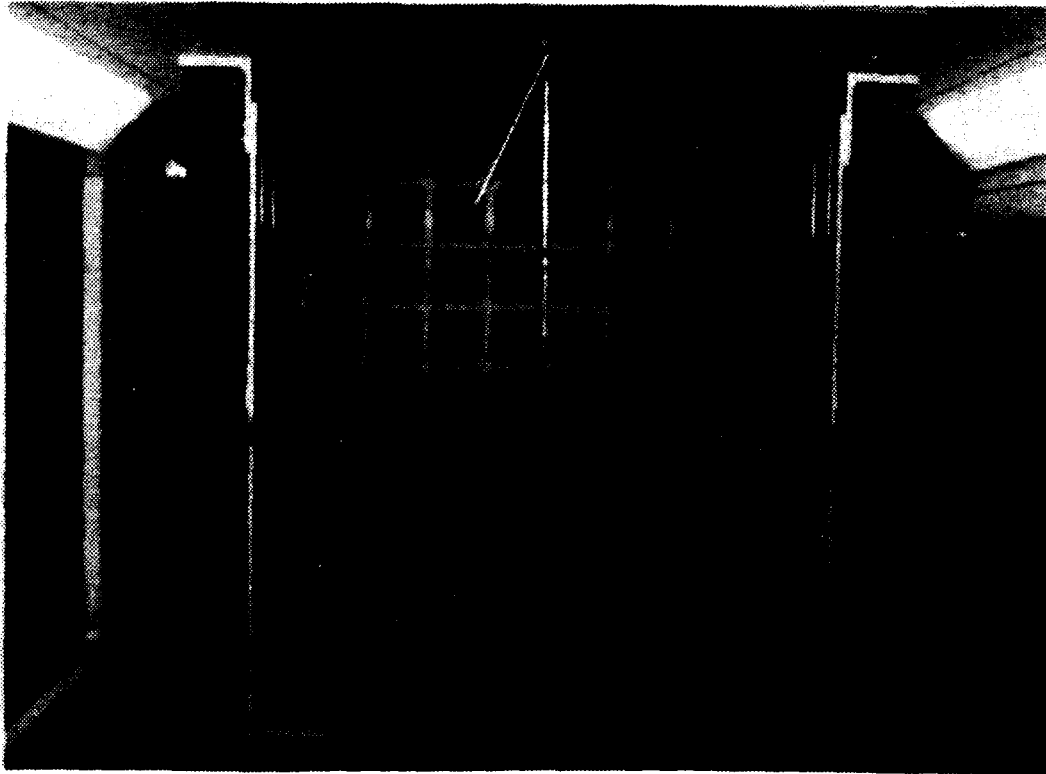
Figure 14. Turbulence Grid Installed in Tunnel

The two wooden grids were similarly constructed and differed only in mesh size and cross-member diameter. The mesh-to-diameter (M/D) ratio for both grids is five. The biplanar design was chosen to provide nearly isotropic tunnel turbulence, with the level of turbulence a

25

function of the grid mesh size and bar diameter [Ref. 2]. From Figure 1, it can be seen that approximate turbulence intensity levels at the airfoil correspond to 3.5%, 1.9%, and 0.5% for grid 1, grid 3, and grid 4 respectively. Turbulence length scales for the grids, from Figure 2, are estimated to be 1.8, 1.2, and 0.5 inches. Figure 15 shows a schematic drawing of the wooden grids. Table 1 lists grid specifications for each of the grids used.

(M)
MESH
WIDTH

(D)
BAR
DIAMETER
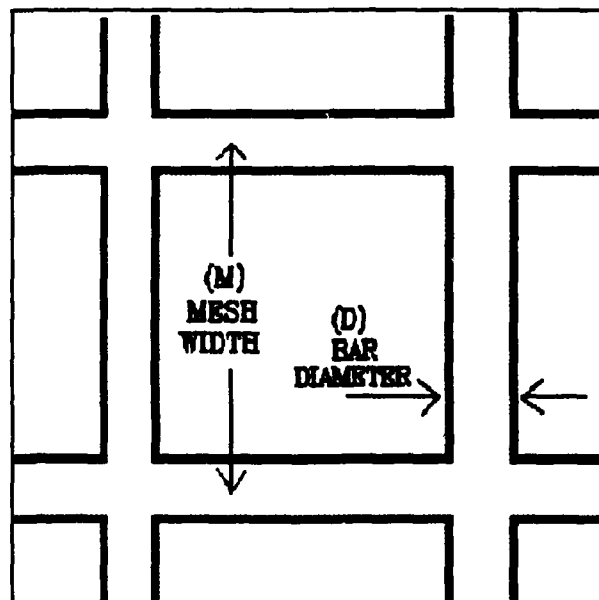
Figure 15. Grid Schematic [Ref. 3]

TABLE 1. Grid Specifications [Ref. 3]

Grid No.	M (in)	D (in)	M/D	Material
1	5.0	1.0	5	wood
3	2.5	0.5	5	wood
4	1.0	0.0625	16	wire

B. EXPERIMENTAL SOFTWARE

The software program "TRAVERSE", written by the author to serve as the interface between the operator and the motor controller assembly, is listed in Appendix D. The highly interactive program was used for motor movement control, data recording, and data reduction. It was written in advanced BASIC (BASICA) and allows the operator precise control of hot-wire movement via the 3-D traverser controller unit. Much of the initial portion of the program is dedicated to operator-selectable options (i.e. motor velocity, motor acceleration, etc.) available for each motor. However, default values for each option are provided in the programming and the operator can select the defaults for all motors with one keystroke.

The program gives the operator a choice of manual input (meaning one motor movement for each operator input) or computer-controlled movement through a boundary layer. The manual movements were used to pre-position the hot-wire probe prior to data collection runs through the boundary layer. The operator used the surveyor's transit scope to monitor probe movement as the probe was manually moved to the bottom of the boundary layer for the start of a data collection run. Figure 16 shows the hot-wire probe in position for data collection.

After pre-positioning the probe, the operator selected the computer-controlled boundary layer movement option. This option uses a sine function-based algorithm to compute individual motor movements through the layer. The algorithm uses a sine function as its base to concentrate

27

**Figure 16. Hot-Wire Positioned for
Data Collection**

many smaller motor movements at the bottom of the boundary layer and gradually increase motor increments toward the top of the layer. Therefore, more data points are sampled nearer the surface.

The program prompts the operator to input the number of data points desired and the thickness of the boundary layer to be measured for each chord location. The basic motor movement algorithm is given below as Equation 1.

$$Z(J) = BL * \{1 - [\sin(pi/2) * (1 + J/N)]\} \quad (1)$$

where: $Z(J)$ = incremental distance
          BL = estimated boundary layer height
          N = number of data points desired
          J = incremental data point

After each individual motor movement is completed, the program prompts the user for hot-wire voltage and rms voltage inputs. Voltages were read from the IFA-100 display and then entered manually by the operator. The probe position (relative to the bottom of the boundary layer) and the voltages are written to "raw" data files by the software program. Once the required voltages are input, a single keystroke will move the probe to the next data point and the process is repeated.

After voltages for each data point have been input, the program converts the "raw" data into the non-dimensional quantities normally used in boundary layer studies. These non-dimensional quantities include normalized distance above the airfoil surface (y/c), normalized velocity (u/U_e), and normalized velocity fluctuation, or turbulence intensity (rms/U_e). The data recorded for each sampled data point were non-dimensionalized by dividing by the airfoil chord length (in this case 10 inches) or the boundary layer edge velocity (U_e).

The velocity at each data point is computed by an algorithm incorporating the calibration curve equation for the hot-wire probe used. System vibration and high dynamic loading on the probes caused several of the probes to fail during this experiment. Each time a different probe was used, the system was recalibrated and the software program was updated to include the new calibration curve. Non-dimensional velocities for each data point were then computed by dividing each "raw" velocity by the edge velocity.

29

The rms values input by the user are actually the AC component of the velocity fluctuations sensed by the hot-wire. The magnitude of the rms values can be associated with the magnitude of the velocity fluctuations at any given point. Conversion of these "raw" rms values into a non-dimensional rms was accomplished by taking the "raw" rms inputs, multiplying them by the slope of the calibration curve at each data point, and dividing by U_e. This method compensates (at each data point) for the change in slope due to a non-linear calibration curve.

The non-dimensional values were then written to a data file by the software program. These data were then used as input to a graphics program to produce boundary layer profile and turbulence intensity plots, as seen in the experimental results section of this report.

III. RESULTS AND DISCUSSION

A. CALIBRATION

The calibration of a constant temperature hot-wire system is a procedure whose ultimate goal is to generate a calibration curve relating hot-wire voltage output to wind tunnel flow velocity. The calibration curve equation can then be used in all subsequent data reduction computations to transform voltage data into velocity data. An important point to note here is that calibration should be performed over the entire range of velocities expected to be encountered during the experiment.

As stated earlier in this report, the high dynamic loading on the hot-wire probes due to the grid-generated turbulence appeared to cause several of the hot-wires to break during the experiment. This section will discuss procedures used to calibrate the hot-wire probe used with no grid installed in the tunnel. These same procedures were used to calibrate all of the wires used during this experiment.

The calibration procedure can be divided into several different steps as outlined in the IFA-100 Instruction Manual [Ref. 11]. These steps are:

- To determine anemometry system cable resistance
- To determine hot-wire probe total resistance (R_{tot})
- To compute hot-wire probe operating resistance

- To collect hot-wire voltage outputs at a number of known
  wind tunnel velocities over the range of velocities expected

- Plot voltage vs velocity to obtain a calibration curve equation

The first three steps of the calibration procedure are performed using the IFA-100 hardware with no flow in the wind tunnel. The cable resistance is measured directly by the IFA-100 system by inserting a shorting probe in the hot-wire support. The operator then displayed and entered cable resistance into IFA-100 memory via selections located on the front panel. The cable resistance was then automatically subtracted from all subsequent probe resistance measurements [Ref. 11]. The cable used throughout this experiment had a resistance of 0.868 ohms.

Hot-wire probe total resistance (R_{tot}), also referred to as "cold" resistance, is the resistance of the wire at zero flow velocity and is also directly measured by the IFA-100 system. After removing the shorting probe and inserting the hot-wire probe, R_{tot} was displayed on the IFA-100 front panel. This resistance value was used only to calculate operating resistance of the hot-wire and not entered into the memory circuitry of the system.

The hot-wire probe operating resistance (R_{op}) is computed from the following relationship [Ref. 11]:

$$R_{op} = R_{lot} + [alpha_{20} * R_{20} * (T_a - T_o)] \qquad (2)$$

where: T_a = desired operating temperature (250° C)

               T_o = room temperature (20° C)

and $alpha_{20}$ and R_{20} are the temperature coefficient
               and probe total resistance at 20° C supplied by
               the probe manufacturer

A check of the operating resistance computed was then performed using the hot-wire "overheat ratio". The overheat ratio is defined as the ratio of the probe operating resistance to the probe total (cold) resistance. Normal overheat ratio values for tungsten wires range from 1.5 to 2.0 [Ref 11]. For the no grid calibration run, probe total resistance was measured at 4.597 ohms and probe operating resistance was computed to be 7.495 ohms. The overheat ratio for this wire was 1.63.

The next step in the calibration procedure was to run the wind tunnel at known velocities and record hot-wire voltage output at each velocity. A reference pitot-static probe was inserted into the top of the wind tunnel and connected to a water-filled slant manometer. This pitot-static system was used throughout the experiment to provide a reference pressure differential for adjusting the tunnel flow velocity. The hot-wire probe was traversed to a position adjacent to the pitot-static probe but outside any flow perturbations caused by the probe. Figure 17 shows the hot-wire and pitot-static probe in position for a calibration run.

33
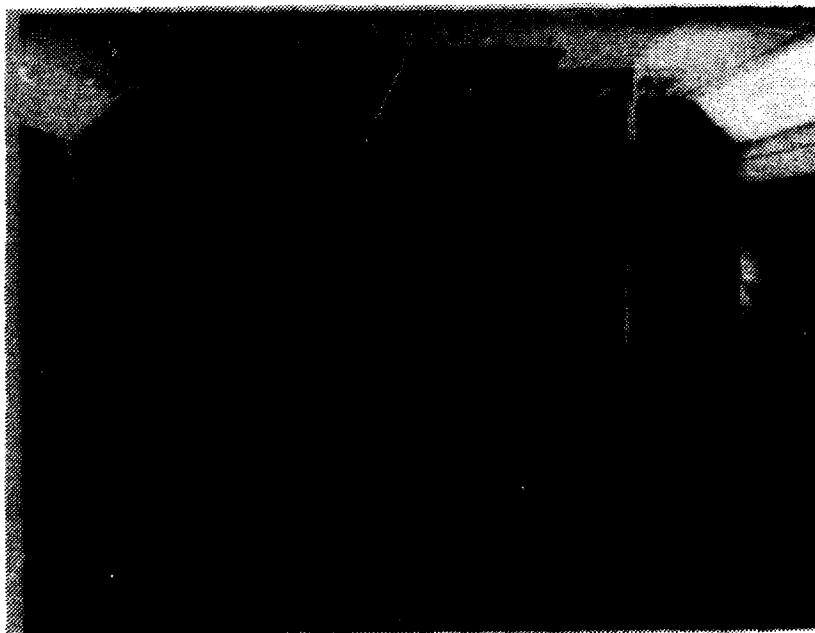
Figure 17. Hot-Wire Calibration Configuration

The slant manometer was set at 40° inclination and calibration data were obtained at 0.5 inch increments, as read on the manometer, up to a maximum differential of 10 inches. At each incremental pressure (height) differential, hot-wire voltage output was recorded. Actual tunnel flow velocity was then computed by the relationship:

$$\text{vel (ft/sec)} = \left[\frac{(2)*(62.43)*(h*\sin 40)}{(12) * (\text{rho})}\right]^{.5} \qquad (3)$$

where: h = height difference of water in slant tube
          rho = density

Table 2 shows the no grid calibration data collected. Note that the velocity range of the calibration run extends from approximately 33 ft/sec to 153 ft/sec--covering the entire range of velocities expected.

TABLE 2. No Grid Calibration Data

Del-h (in)	Hot-Wire volts	Vel (ft/sec)	Del-h (in)	Hot-Wire volts	Vel (ft/sec)
0.38	2.601	33.01	4.60	4.331	114.84
0.79	3.083	47.59	4.97	4.385	119.36
1.22	3.363	59.14	5.56	4.471	126.25
1.62	3.557	68.15	5.98	4.528	130.93
2.01	3.711	75.91	6.30	5.579	134.39
2.40	3.829	82.95	6.78	4.640	139.41
2.88	3.968	90.86	7.18	4.688	143.47
3.25	4.069	96.52	7.58	4.737	147.41
3.79	4.174	104.24	7.84	4.782	149.92
4.20	4.261	109.73	8.27	4.837	153.97

By plotting velocity against hot-wire voltage output a non-linear form of the calibration curve equation was obtained. Figure 18 shows the non-linear calibration curve and illustrates the greater probe sensitivity at lower flow velocities. A quick check on the calibration curve obtained was run by plotting voltage squared against the square-root of velocity (commonly called a "fourth order fit"). A reliable calibration curve will result in a nearly straight-line fit [Ref. 11]. Figure 19 shows the fourth order fit and the linear results obtained.

This same calibration procedure was used each time a different hot-wire probe was used. Because of the relatively low tunnel velocities used during this experiment (approximately 100 ft/sec), the non-linear form of the calibration curve was used in data reduction. Calibration data and curves for the other wires used can be found in Appendix B.

B. DATA ANALYSIS

Boundary layer data were collected at nine airfoil chord locations ranging from 0.25c to 0.65c in 0.05c increments. The boundary layer at
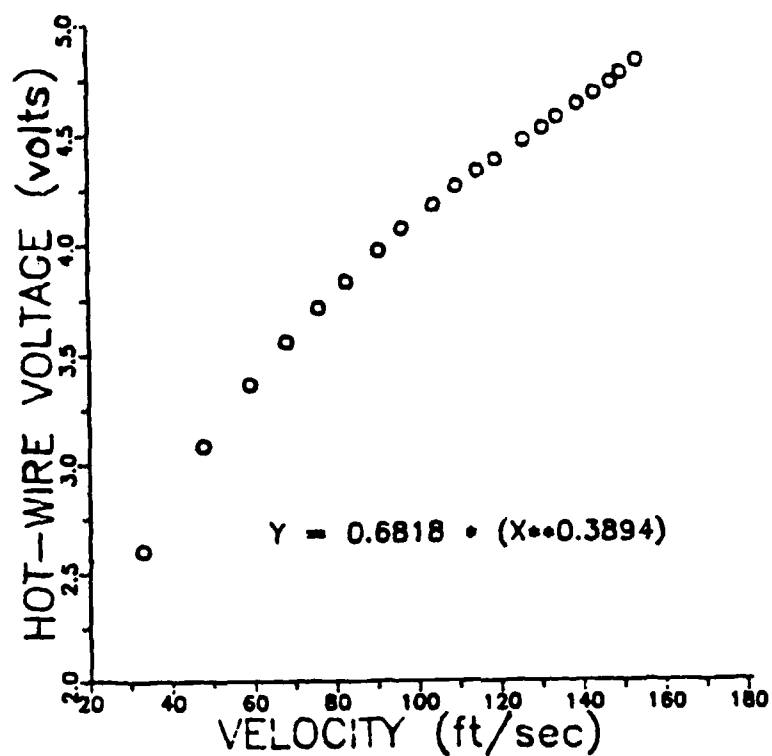
Figure 18. Non-Linear Calibration Curve

$Y = 0.6818 \cdot (X**0.3894)$
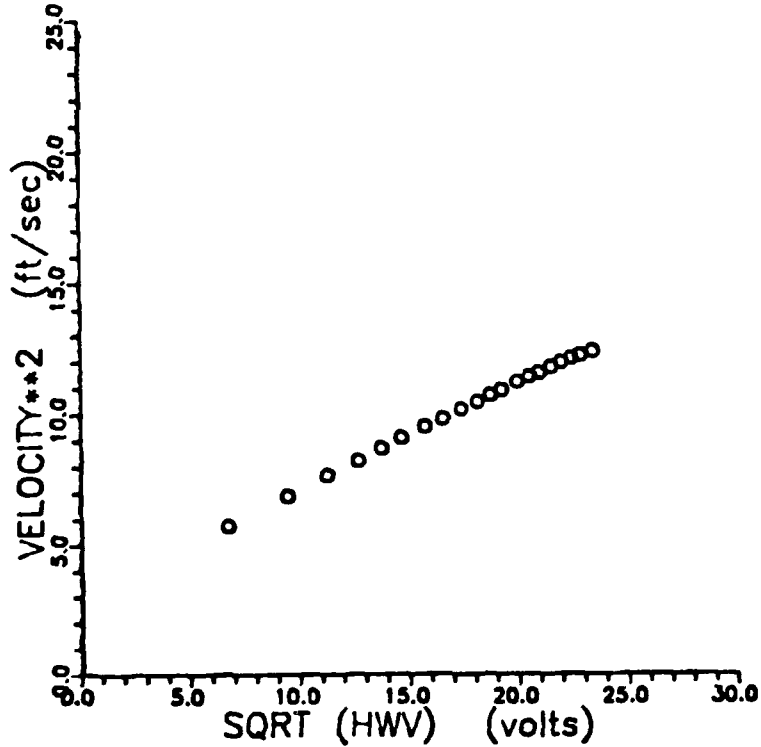
Figure 19. Fourth-Order Curve Fit

36

each chord location was sampled at four different wind tunnel configurations: with no grid installed and with each of the three grids described in Section II of this report. As described in Section II, raw data consisted of hot-wire voltage output, rms voltage, and probe distance above airfoil surface. The raw data were used as input into a software program incorporating the calibration equation to output wind tunnel velocity data and the non-dimensional quantities previously discussed. These data are provided in Appendix C. Table 3 shows the chord locations, height of boundary layer sampled, and number of data points taken for each wind tunnel configuration.

TABLE 3. Data Sampling Table

				Chord Locations*					
	.25	.30	.35	.40	.45	.50	.55	.60	.65
NO	.20	.25	.25	.25	.30	.30	.30	.35	.30
GRID	35	35	35	35	40	40	40	40	40
GRID	.20	.20	.20	.21	.225	.225	.25	.25	.25
#1	30	30	35	35	35	35	35	35	35
GRID	.20	.20	.22	.25	.30	.35	.35	.30	.30
#3	30	30	30	35	40	40	40	40	40
GRID	**	.20	.20	.30	.30	.30	.30	.30	.30
#4	**	30	30	35	35	35	35	40	35

* Boundary layer height (inches) and number of data points given for each chord location sampled.

** Data unavailable

The data collected will be presented and discussed in two formats. The first, mean boundary layer velocity profiles, will show boundary layer development, transition, and overall behavioral characteristics of the flow within the boundary layer. The second format, turbulence intensity profiles, will show relative turbulence levels existing within each sampled boundary layer. The discussion will emphasize similarities and differences in profile characteristics due to the different wind tunnel configurations.

Each of the plots corresponds to one particular wind tunnel configuration (i.e., no grid, grid 1, etc.). The various profiles shown on each plot correspond to the different chord locations sampled at a given wind tunnel configuration. Chord locations are noted above each profile on the plots. The profiles were spread along the horizontal axis by adding a constant (0.3) to all data at each sequential chord location--0.3 added at the .30c position, 0.6 added at the .35c position, 0.9 added at the .40c position, etc. Tic marks along the axis indicate 0.5 Ue (one-half the edge velocity) associated with the profile immediately to the right of the tic.

1. Velocity Profiles

Figures 20 through 23 show mean velocity profiles for each of the four wind tunnel configurations. In the no grid case, Figure 20, the flow appears to be fully laminar up to the .30c position. Laminar profiles are characterized by a linear decrease in velocity near the wall. Turbulent profiles exhibit a much more non-linear decrease in velocity near the

38

wall. Transition to a turbulent boundary layer starts to occur just downstream of the 0.30c position as indicated by the fuller and much thicker velocity profile seen at the .35c position. At the .35c position, the profile appears to be nearly fully turbulent. The transition to turbulent flow in this case occurs over a small airfoil chord distance (<.05c), called the transition region.

The grid 4 case, shown in Figure 23, is similar to the no grid case in several ways. Grid 4 was the small-diameter wire grid generating the least turbulence intensity levels (approximately 0.5%) and had the smallest length scale (approximately 0.5 inches) of any of the grids used. Note that data for the .25c position were unavailable due to probe failure.

The profile at the .30c position appears to be nearly laminar though slightly transitional in the outer layer. Transition of the grid 4 boundary layer is evident at the .35c position as it was in the no grid case. The major difference between the two cases is seen at the .30c position, where the grid 4 profile appears to be more transitional than the no grid case. Both cases exhibit almost identical nearly turbulent profiles at the .40c position.

Similarities also exist between these two cases by comparing boundary layer growth rates (i.e., fullness or thickness). Growth rates for the two cases are nearly equal through the laminar and transitional region. However, the growth rate (thickness) for grid 4 profiles increases as the flow within the boundary becomes fully turbulent. At the aft-most

39

chord location, .65c, boundary layer thickness for grid 4 is approximately 0.0225c inches while for no grid the boundary layer appears to be approximately 0.02c inches--reflecting an increase of about 12% thickness for grid 4.

Profiles for the grid 1 and grid 3 cases, Figures 21 and 22, show differences from the two cases discussed above. At the .25c position, grid 1 already appears to be transitional while the grid 3 profile appears to be only nearly-transitional. Grids 1 and 3 produce T_u levels of approximately 3.5% and 1.9% respectively and approximate length scales of 1.8 and 1.2 inches (refer to Figures 1 and 2). In both these cases, freestream turbulence generated by the grids is prompting boundary layer transition to occur sooner than in the two previous cases. Fully-turbulent velocity profiles exist at the .35c position for grid 3 and at the .40c position for grid 1.

Comparison of boundary layer thicknesses for grids 1 and 3 show marked differences at the earlier chord locations. At .30c, thicknesses of approximately 0.009c and 0.008c inches exist for these grids while the no grid profile thickness at this same chord location is approximately 0.005c inches. However, at the .65c position, the boundary layer thicknesses for the two wooden grids and the no grid cases are all approximately equal.

As expected, freestream turbulence levels are seen to be directly related to transition of the boundary layer from laminar to turbulent flow. But for the test conditions encountered during this experiment, it appears that the effect of increased turbulence intensity is limited to

40
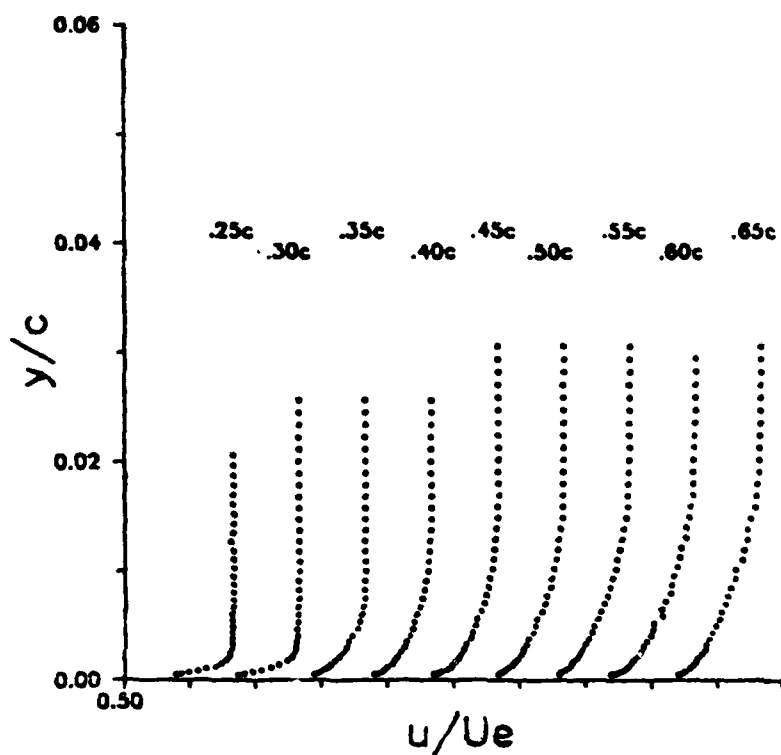
Figure 20. No Grid Velocity Profile
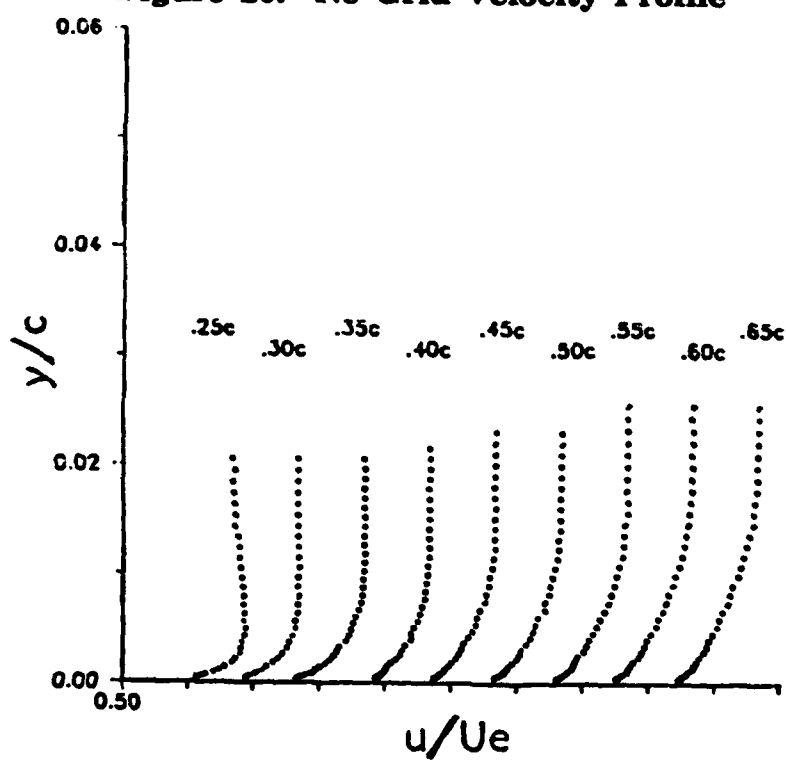
Figure 21. Grid 1 Velocity Profile

41
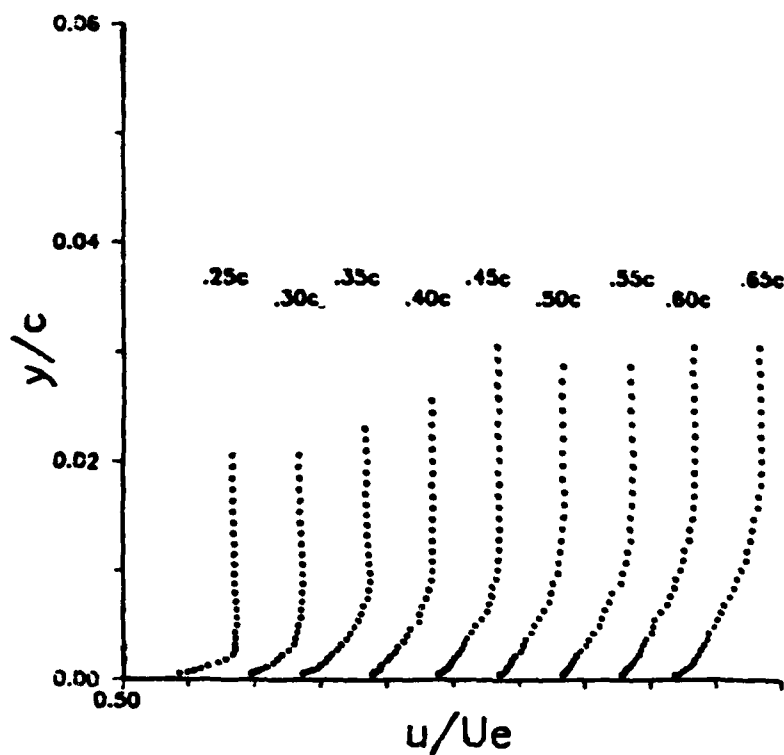
Figure 22. Grid 3 Velocity Profile
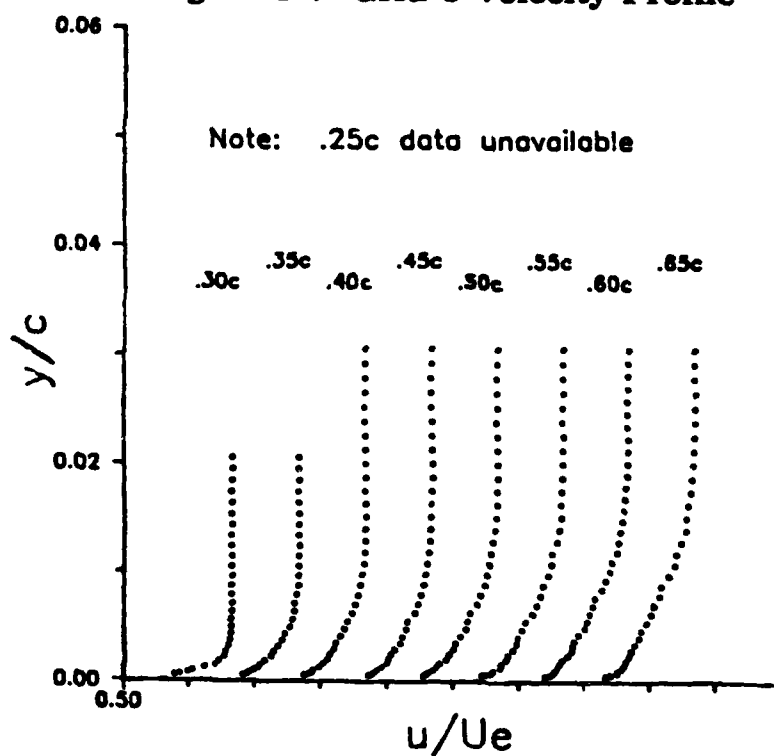
Figure 23. Grid 4 Velocity Profile

earlier transition of the boundary layer. Kline, Lisin, and Waitman
[Ref. 14] found, on the other hand, that boundary layer thicknesses were
very sensitive to increases in freestream turbulence. They found that
boundary layer thicknesses increased 50 to 100% at a Reynolds number
of approximately 2×10^6 at a local freestream turbulence level of 5.7%.
These experiments were performed over a flat plate with transition for
each case induced near the leading edge; the purpose was to separate the
direct effect of freestream turbulence on the turbulent boundary layer
growth from the variations in thicknesses due to a change in the
transition location with turbulence intensity. The growing boundary
layer actually experienced turbulence levels much higher than stated,
since the intensity decays with distance downstream. The sole intent
here is to note that the expected condition is that the turbulent boundary
layer would increase noticeably in thickness over the ambient turbulence
case with increases in freestream turbulence levels. Profiles obtained
during this research do not indicate this correlation between freestream
turbulence levels and boundary layer thickness.

It is postulated here that the lack of correlation found in this
experiment is due to turbulence length scale effects. For the highly
turbulent grids, grids 1 and 3, length scales reported by Roane [Ref. 3]
are close to an order of magnitude greater than the boundary layer
thickness. In order for turbulence in the freestream to effect boundary
layer behavior, its length scale value must be close to the boundary layer
thickness. In the grid 4 case, where length scales are relatively close to

43

boundary layer thickness, the greatest effect of freestream turbulence is seen, resulting in a 12% increase in boundary layer thickness. No length scale information is provided in the work by Kline et al.

More detailed comparisons can be made by taking a look at the two extreme cases, i.e. the no grid case and the grid 1 case, as shown in Figures 24 to 29. In this series of plots, differences in profile characteristics (laminar or turbulent, fullness, boundary layer thickness) are more easily seen. Note on the plots that the left side of the x-axis does not correspond to zero velocity. At chord locations up to .35c, shown in Figure 24 through 26, profiles for grid 1 show definitive turbulent characteristics. Profiles for the no grid case appear to be nearly turbulent only at the .35c position. Boundary layer thickness for the grid 1 case, particularly at the .30c position, is nearly twice that found in the no grid case.

As profiles are sampled farther aft along the chordline, shown in Figures 27 to 29, the profiles become more and more similar in both fullness and in thickness. Profiles at .50c and .60c, Figures 28 and 29, show nearly identical characteristics for these two extreme configurations.

The same trends discussed above are evident when comparing velocity profiles between the different grids. Figures 30 through 32 illustrate profile differences between the grids at three selected chord locations (.30c, .45c, and .60c). At the .30c position, grid 4 appears to be the most laminar-like and has the thinnest boundary layer, estimated to be approximately 0.005c inches. Significant differences between the
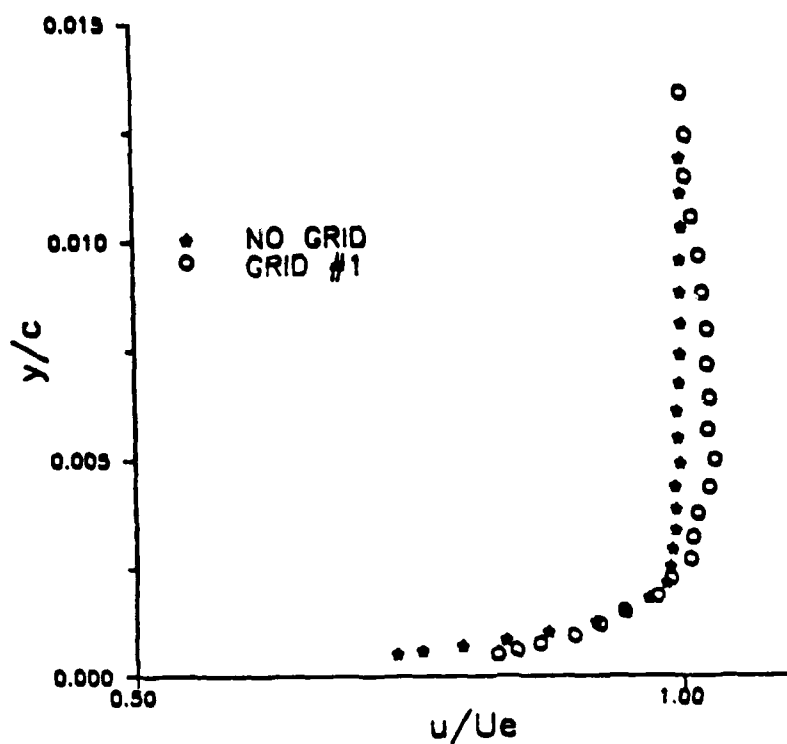
Figure 24.   No Grid vs Grid 1 Velocity Profile (.25c)
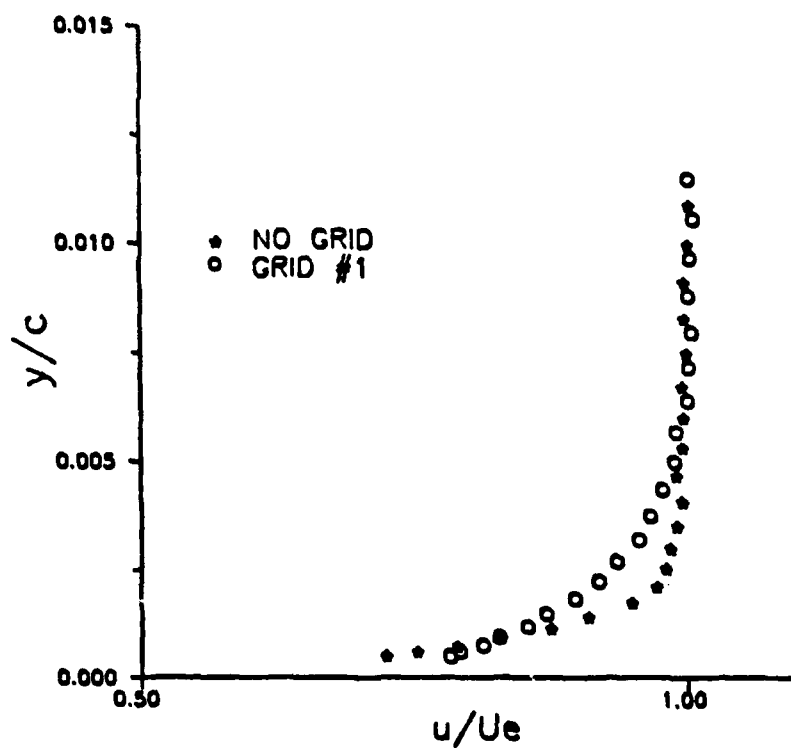
Figure 25.   No Grid vs Grid 1 Velocity Profile (.30c)

45
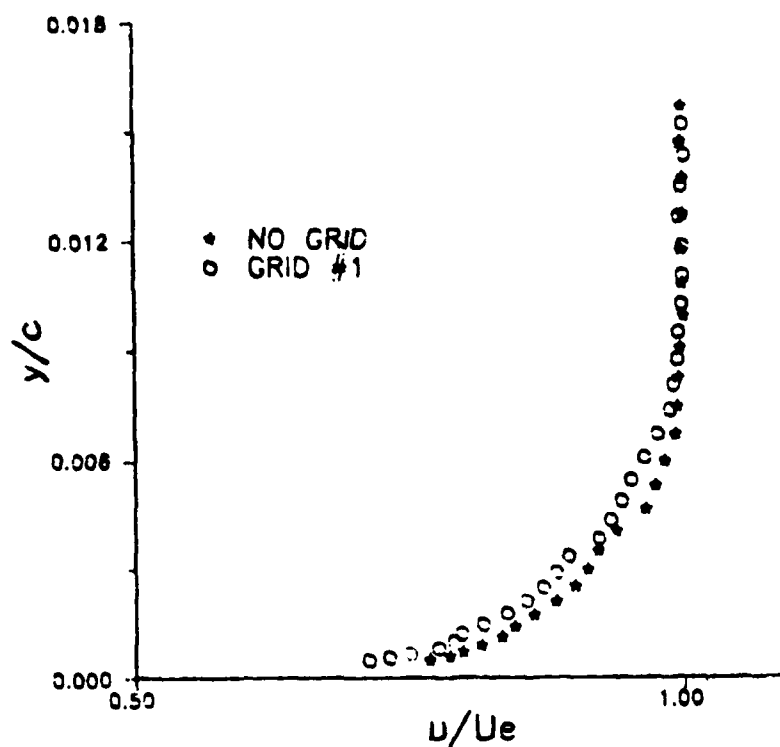
Figure 26. No Grid vs Grid 1 Velocity Profile (.35c)
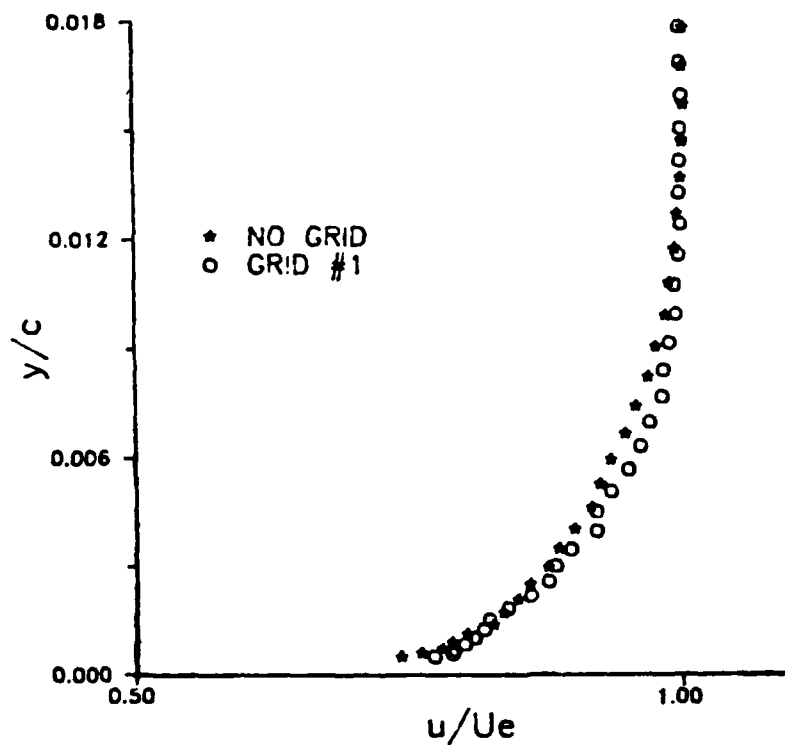
Figure 27. No Grid vs Grid 1 Velocity Profile (.40c)

46
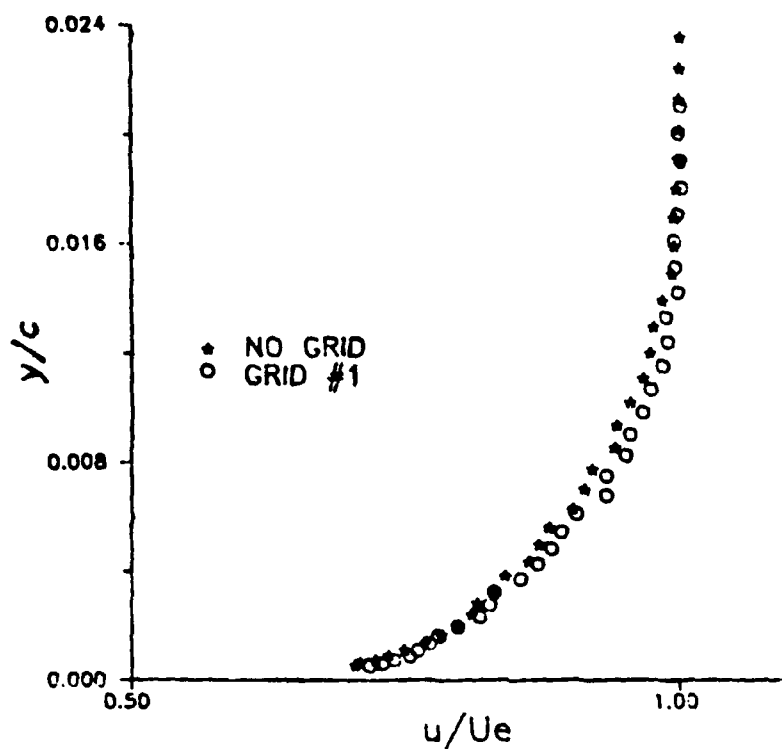
Figure 28. No Grid vs Grid 1 Velocity Profile (.50c)
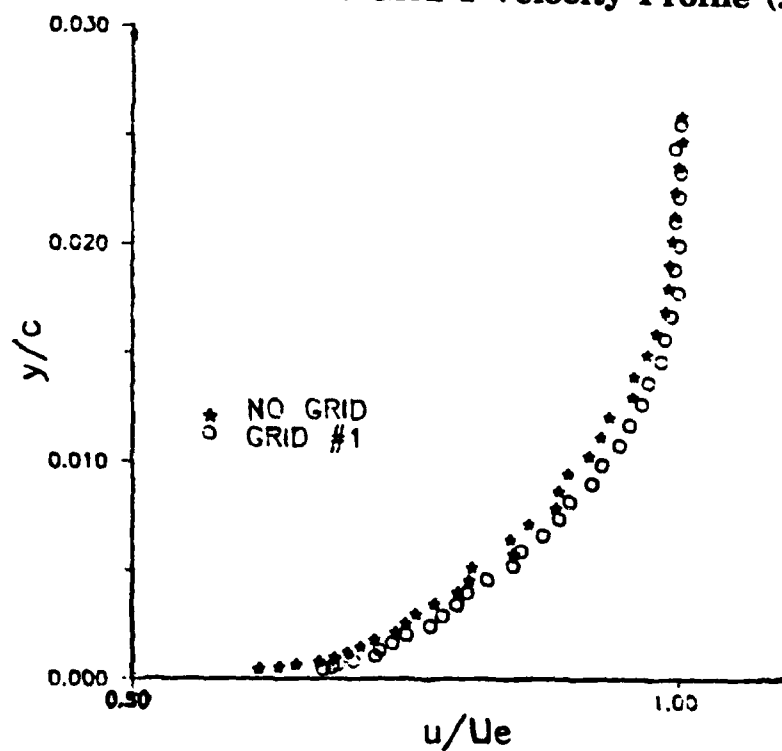
Figure 29. No Grid vs Grid 1 Velocity Profile (.60c)

47
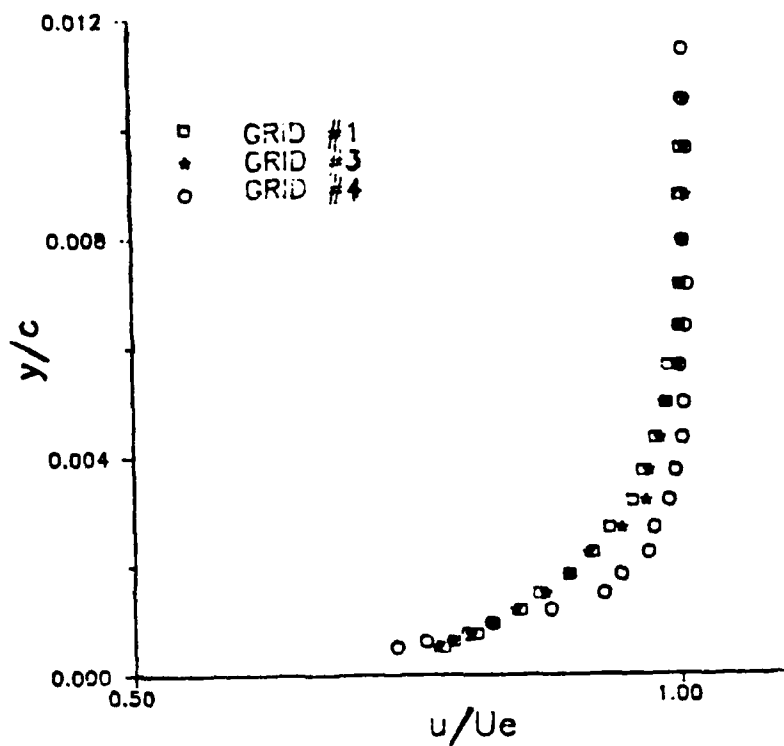
Figure 30. Velocity Profile Comparison (.30c)
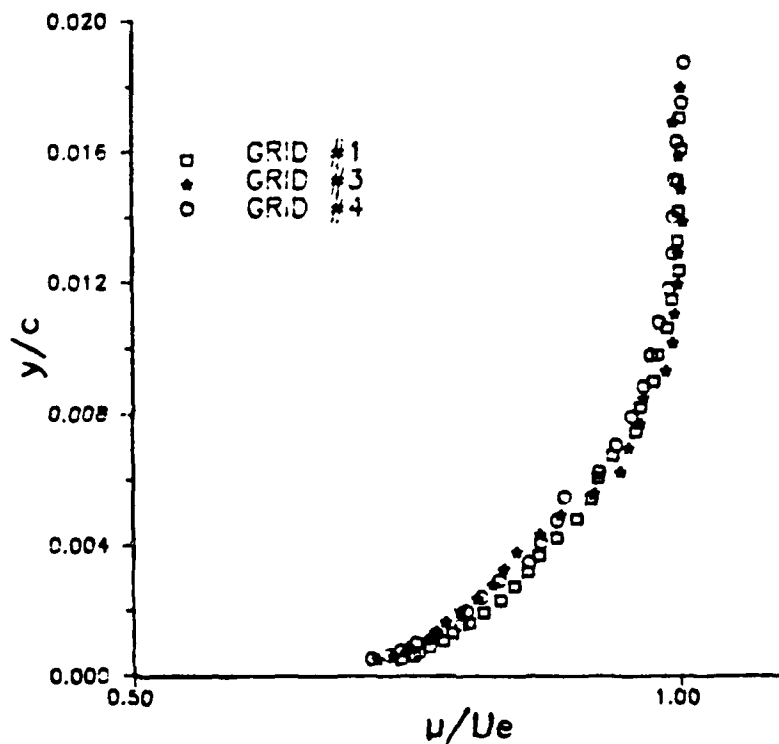
Figure 31. Velocity Profile Comparison (.45c)

48

profiles (laminar vs turbulent characteristics, boundary layer thickness, etc.) are readily observed at the early chord locations. At the .60c position, however, all profiles have the same basic turbulent shape, but grid 4 has the thickest boundary layer, estimated to be 0.0225c inches. This is believed to be a direct result of length scale.
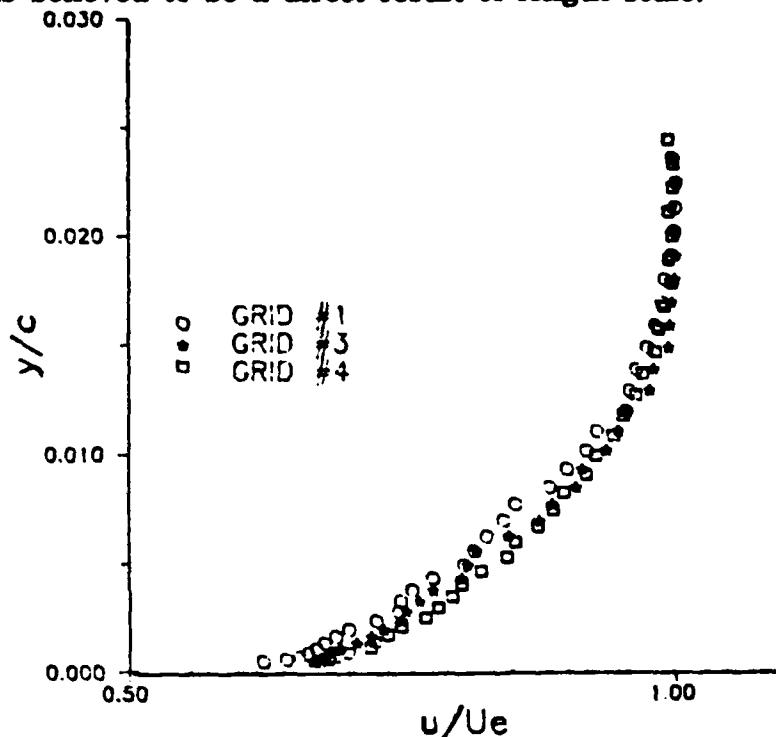
Figure 32. Velocity Profile Comparison (.60c)

Though grids 1 and 3 result in freestream turbulence levels much higher than for grid 4, the effect of the higher turbulence levels is only to transition the boundary layer earlier. The dissipation length scales of the turbulence for grids 1 and 3 are much larger than the boundary layer thickness and appear to have little or no effect on boundary layer growth rate. The lower turbulence intensity of grid 4 appears to have a

49

much more dominant effect on increasing the turbulent boundary layer thickness, up to an approximate increase of 12% in thickness, because the scale of these turbulent eddies more closely matches those of the turbulent boundary layer.

2. Turbulence Intensity Profiles

Turbulence intensity profiles, Figures 33 through 40, show relative turbulence levels present in the sampled boundary layers. Data for these plots were non-dimensionalized by dividing the rms value of the velocity fluctuation at a given data point by the edge velocity at each chord location. A mathematical definition of T_u can be written as:

$$T_u = u'/U_e \qquad (4)$$

where $\quad u'$ = rms of a velocity fluctuation
$\quad U_e$ = velocity at the edge of the boundary layer

The rms plots were formatted using the same constant as the velocity profiles (0.3) added to subsequent chord locations to spread the profiles along the axis. Tic marks on each plot indicate zero T_u for each profile. A scale is also provided for each plot.

The effects of the grids on T_u is readily apparent at the earlier chord positions (.25c to .35c). As with the velocity profiles, the most interesting boundary layer behavior will occur at or near the transitional region. In the transitional boundary layer, turbulence is generated near the wall as the transition process is occurring. Added to this turbulence is the grid-generated turbulence existing in the freestream. The addition

50

of the freestream turbulence will cause a rapid increase in T_u levels as shown on the plots. Kline et al. [Ref. 14] attribute both the increase in thickness and increase in T_u to the mixing occurring between the naturally-formed turbulence of a transitional boundary layer and the freestream turbulence entering the boundary layer. The boundary layer T_u levels must return to the approximate freestream values at the top of the layer; therefore a rapid decrease in T_u levels follows. The resultant is a T_u peak shown on the plots. The peak is located near the bottom of the boundary layer because the transition process, which naturally generates turbulence, begins at the wall and diffuses upward. At the bottom of the boundary layer, the T_u must go to zero because the velocity must also go to zero to satisfy the no slip condition at the wall boundary.

At the fully-turbulent chord locations (.50c to .65c), the decrease to approximate freestream T_u levels is much more gradual. The much thicker boundary layers found at the downstream chord locations allow for a more complete interaction between the freestream turbulence and the turbulence already generated near the wall in the turbulent boundary layer.
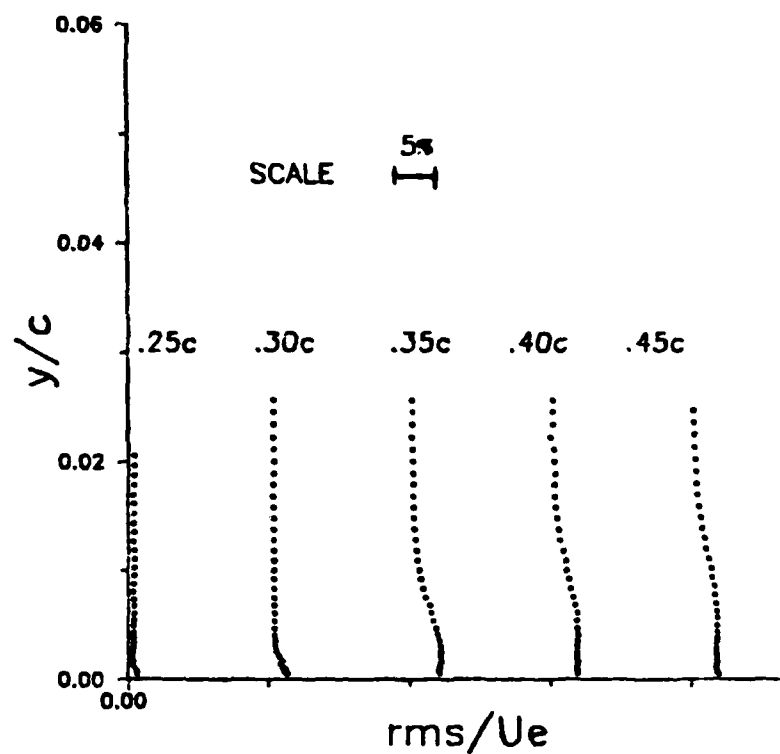
Figure 33. Turbulence Intensity Profile (NO Grid)
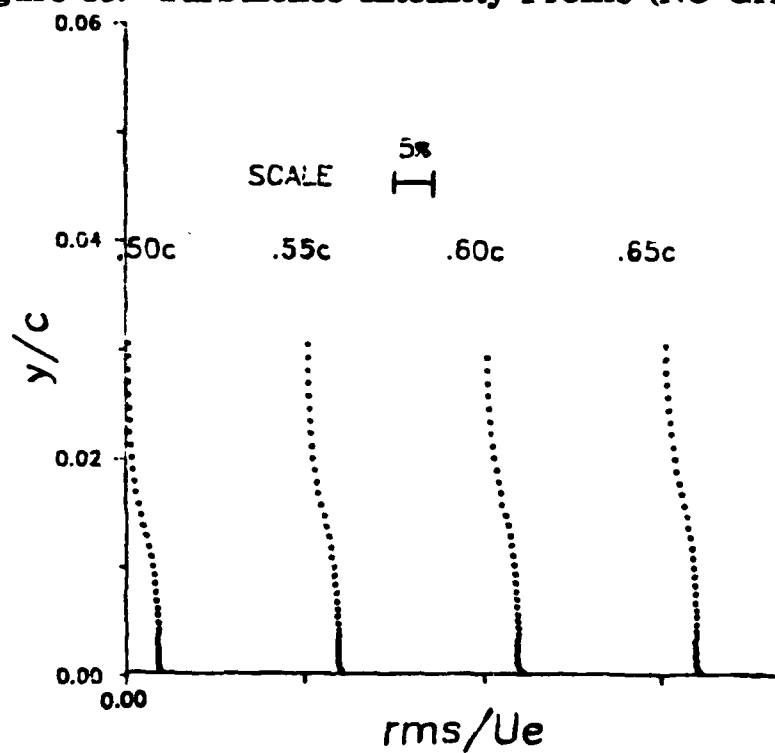
Figure 34. Turbulence Intensity Profile (No Grid)
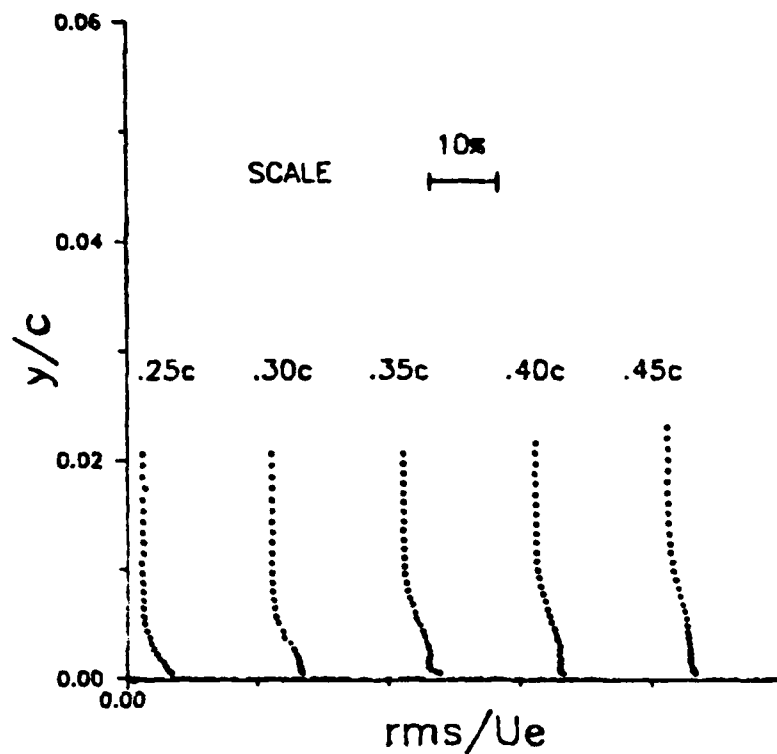
Figure 35. Turbulence Intensity Profile (Grid 1)
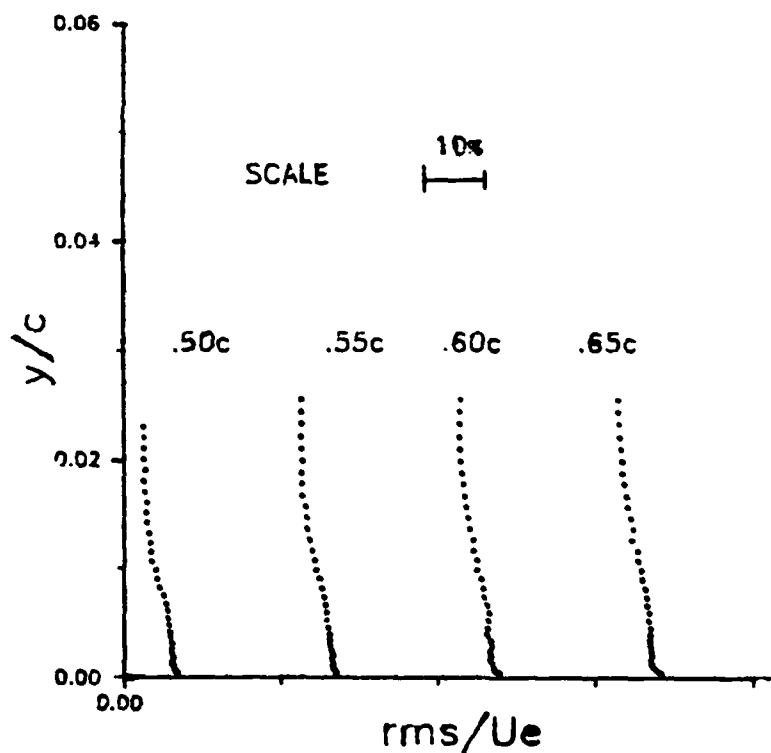
Figure 36. Turbulence Intensity Profile (Grid 1)
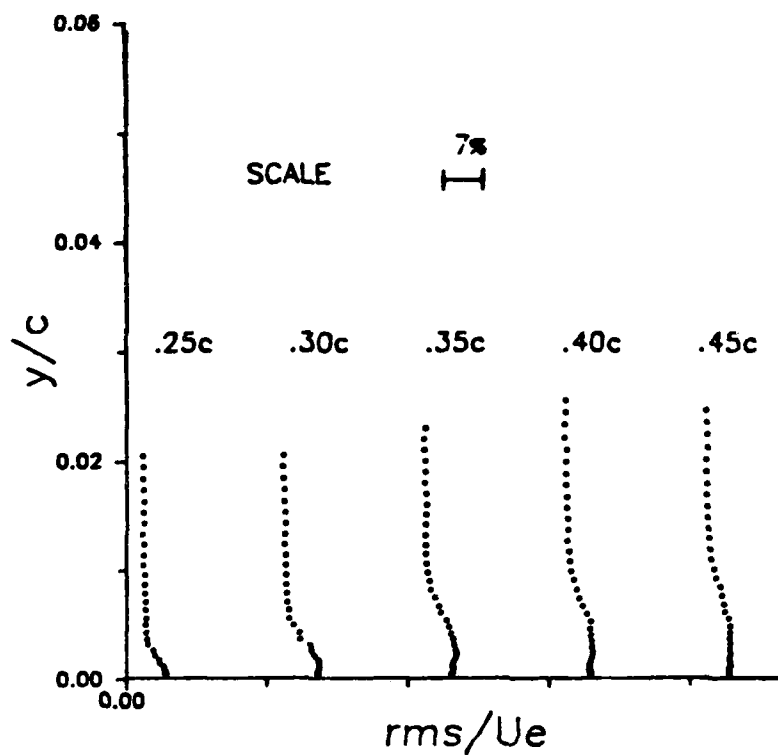
Figure 37. Turbulence Intensity Profile (Grid 3)
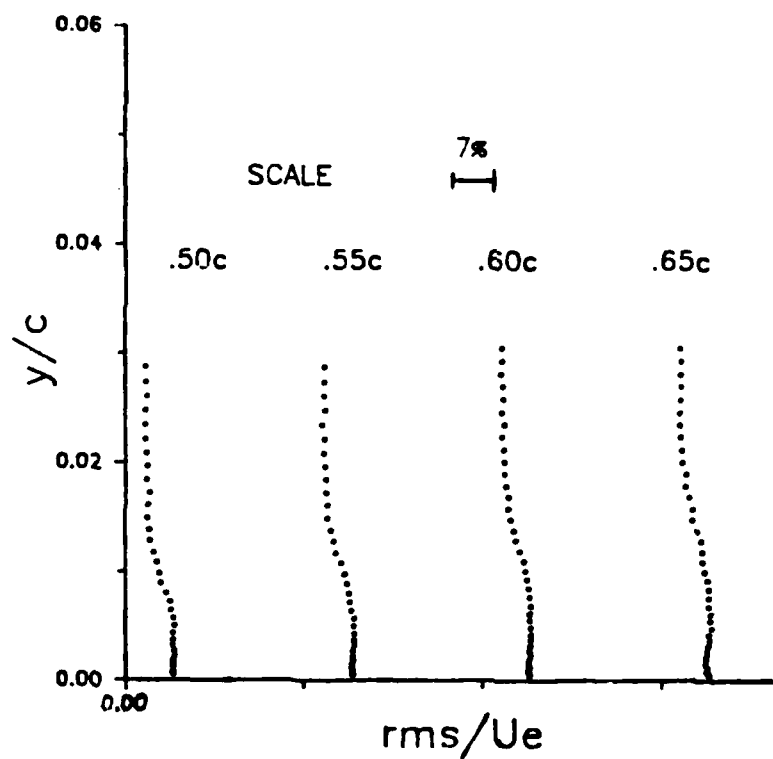
Figure 38. Turbulence Intensity Profile (Grid 3)
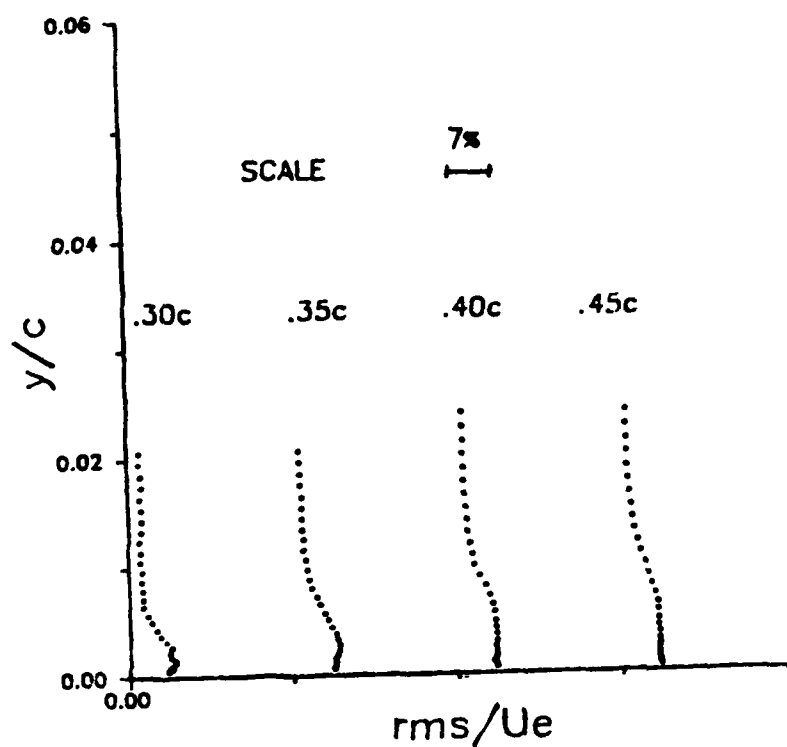
Figure 39. Turbulence Intensity Profile (Grid 4)
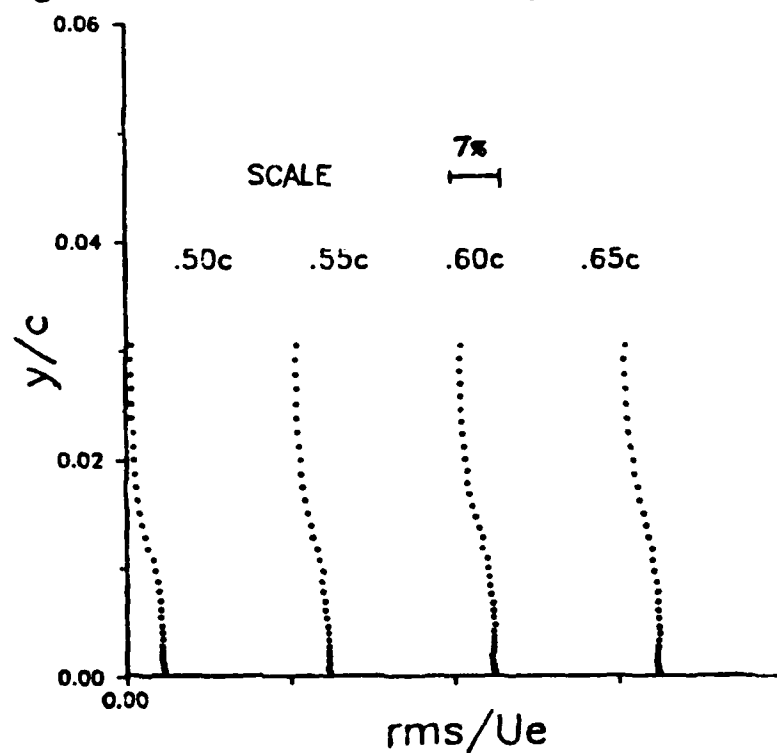
Figure 40. Turbulence Intensity Profile (Grid 4)

IV. CONCLUSIONS

The effects of freestream turbulence on boundary layer behavior has been shown to play a pivotal role in boundary layer transition from laminar to turbulent flow. As expected, increased levels of freestream turbulence caused an earlier transition to turbulent flow much sooner than would occur in a low freestream turbulence flow. In this experiment, the transition region was moved approximately .10c forward with freestream turbulence levels near 4%.

The contributions to boundary layer behavior due to length scale have also been postulated by these results. Although no direct correlation between boundary layer thickness and freestream turbulence levels is concluded from grid 1 or grid 3 data, this lack of correlation may be significant in itself.

It is known that freestream turbulence with a length scale much larger than the boundary layer thickness will not significantly affect the boundary layer. In this experiment, turbulence generated by grid 4 (whose length scale was on the order of boundary layer thickness) resulted in a 12% increase in boundary layer thickness at .65c measured against all other wind tunnel configurations. This increase occurred only in the grid 4 configuration indicating that higher T_u levels at length scales much greater than the boundary layer thickness do not

56

significantly affect boundary layer growth. Further research and experimentation are required to better understand these relationships.

V. RECOMMENDATIONS

During this experiment, wind tunnel velocity was set with a reference pressure differential obtained from a pitot-static probe installed in the upper portion of the wind tunnel test section. For all wind tunnel configurations, freestream velocity was set at approximately 98 ft/sec computed from the pressure differential using Equation 4. This velocity corresponded to a Reynolds number of approximately 500,000 based on airfoil chord.

Boundary layer edge velocities, however, were found to vary by as much as 45% for different tunnel configurations. This phenomenon was associated primarily with grid 1 and grid 3 installed. To check the validity of the pitot-static system used, pressure measurements were taken at all configurations with the pitot-static probe located near the bottom of the test section. No abnormal pressure readings were obtained which might have explained the variance in boundary layer edge velocities. It is recommended that in future research and experimentation with the turbulence grids, reference freestream velocity be set and checked using two different systems, e.g., a pressure differential system and a hot-wire voltage system. Additionally, a complete 3-D turbulence mapping of the NPS wind tunnel should be undertaken using both systems mentioned above. This mapping should

include both T_u and turbulence length scales to better characterize wind tunnel flow with the grids installed.

More research also needs to be undertaken to more fully understand low Reynolds numbers flows. Future investigations involving freestream turbulence should be done with an automated data collection system. Hot-wire voltage output fluctuations with turbulence grids installed was found to be as high as 20% making manual data collection difficult and time consuming. Future plans at NPS include experimentation in unsteady turbulent flow at low Reynolds numbers using an automated, high-frequency sampling technique in conjunction with the IFA-100 Anemometry System.

Other areas for future research should include quantitative studies of the effects of freestream turbulence on boundary layer growth and transition. This report addressed pre-selected chord locations (.25c to .65c) only. Future studies should include more frequent sampling along the chordline within a transitional boundary layer. Other factors for possible inclusion in future projects include airfoils at different angles of attack, including near-stall conditions, to study the effects of turbulence on flow separation, the effect of freestream turbulence on separation bubbles, and changing T_u and length scale parameters independently to differentiate their effects on the flow field.

APPENDIX A   AIRFOIL COORDINATES

TABLE A-1
EXPERIMENTAL AIRFOIL COORDINATES

x/c	y/c	x/c	y/c	x/c	y/c
1.0000	0.0000	0.1200	0.0785	0.5200	0.0061
0.9900	0.0008	0.1150	0.0773	0.5100	0.0059
0.9800	0.0015	0.1100	0.0760	0.5000	0.0056
0.9700	0.0022	0.1050	0.0746	0.4900	0.0053
0.9600	0.0030	0.1000	0.0731	0.4800	0.0050
0.9500	0.0039	0.0950	0.0716	0.4700	0.0047
0.9400	0.0050	0.0900	0.0700	0.4600	0.0044
0.9300	0.0064	0.0850	0.0684	0.4500	0.0040
0.9200	0.0080	0.0800	0.0666	0.4400	0.0036
0.9100	0.0100	0.0750	0.0647	0.4300	0.0031
0.9000	0.0121	0.0700	0.0628	0.4200	0.0027
0.8900	0.0142	0.0600	0.0585	0.4100	0.0022
0.8500	0.0220	0.0500	0.0537	0.4000	0.0018
0.8000	0.0310	0.0400	0.0481	0.3900	0.0013
0.7500	0.0400	0.0300	0.0415	0.3800	0.0009
0.7000	0.0483	0.0200	0.0335	0.3700	0.0004
0.6500	0.0561	0.0150	0.0286	0.3600	0.0000
0.6000	0.0635	0.0100	0.0233	0.3400	-0.0008
0.5500	0.0704	0.0050	0.0169	0.3200	-0.0015
0.5000	0.0766	1.0000	0.0000	0.3000	-0.0020
0.4500	0.0816	0.9900	-0.0002	0.2800	-0.0025
0.4000	0.0858	0.9800	-0.0005	0.2600	-0.0029
0.3500	0.0894	0.9700	-0.0008	0.2400	-0.0032
0.3000	0.0918	0.9600	-0.0010	0.2200	-0.0034
0.2500	0.0927	0.9500	-0.0011	0.2100	-0.0035
0.2400	0.0926	0.9400	-0.0011	0.2000	-0.0034
0.2300	0.0923	0.9300	-0.0009	0.1800	-0.0033
0.2200	0.0919	0.9200	-0.0007	0.1500	-0.0030
0.2100	0.0914	0.9100	-0.0003	0.1000	-0.0016
0.2000	0.0907	0.9000	0.0001	0.0800	-0.0008
0.1900	0.0900	0.8900	0.0006	0.0600	-0.0001
0.1800	0.0888	0.8800	0.0010	0.0500	0.0002
0.1700	0.0876	0.8500	0.0023	0.0400	0.0003
0.1600	0.0862	0.8000	0.0042	0.0300	0.0001
0.1550	0.0854	0.7500	0.0056	0.0250	-0.0002
0.1500	0.0846	0.7000	0.0066	0.0200	-0.0008
0.1450	0.0837	0.6500	0.0071	0.0150	-0.0016
0.1400	0.0828	0.6000	0.0072	0.0100	-0.0029
0.1350	0.0818	0.5500	0.0067	0.0050	-0.0044
0.1300	0.0808	0.5400	0.0065		
0.1250	0.0797	0.5300	0.0063		

x/c

y/c
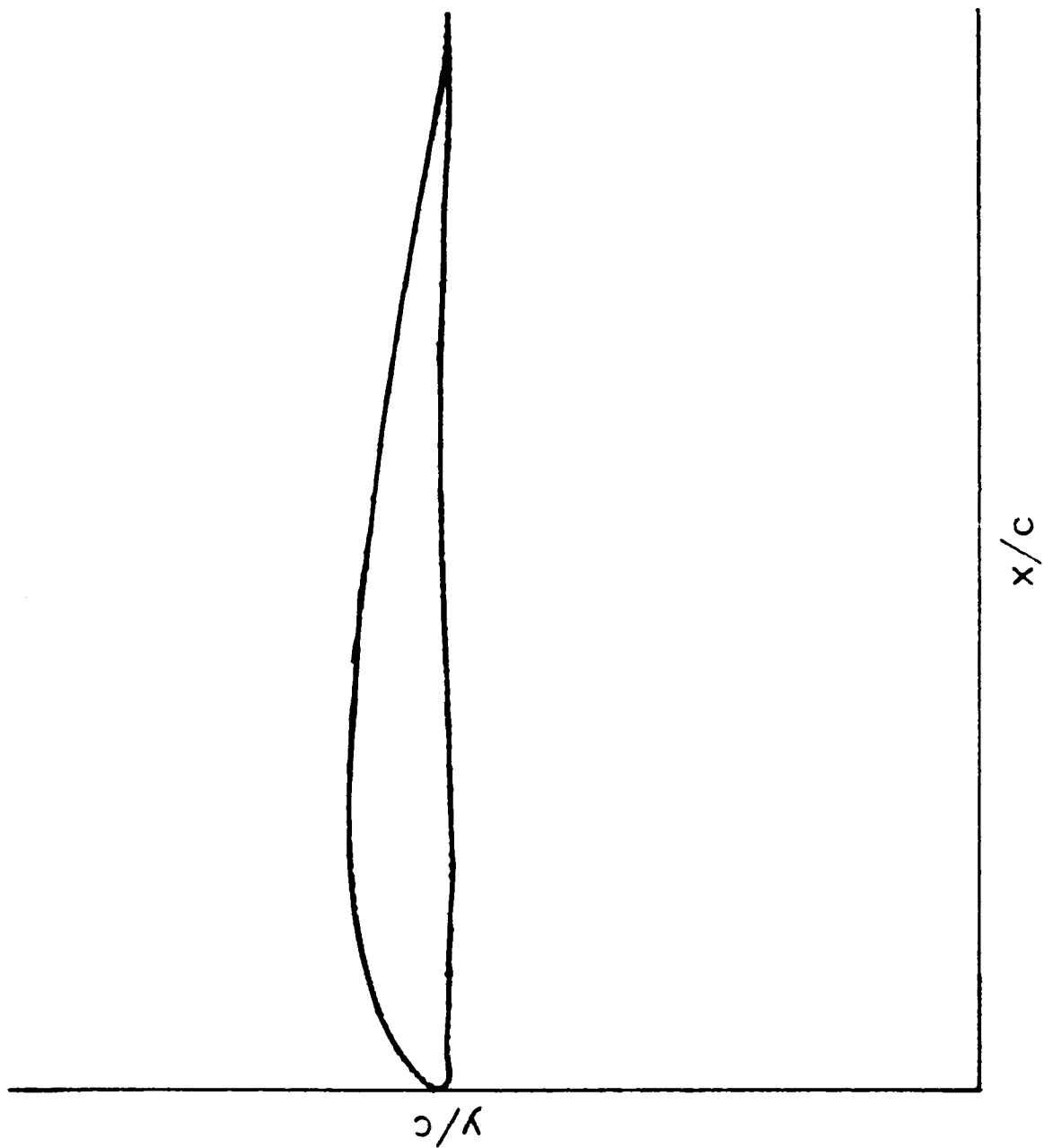
Figure A-1. Experimental Airfoil

61

APPENDIX B   CALIBRATION DATA

Table B-1
Grid 1 Calibration Data

Del-h (in)	HW Out (volts)	Velocity (ft/sec)
0.50	2.925	37.92
1.35	3.402	62.30
2.35	3.690	82.20
3.35	3.910	98.15
4.15	4.075	109.24
4.95	4.203	119.30
5.95	4.311	130.80
6.75	4.405	139.32
7.50	4.485	146.85
8.35	4.552	154.95

$$Y = 0.6518 * (X**0.4254)$$
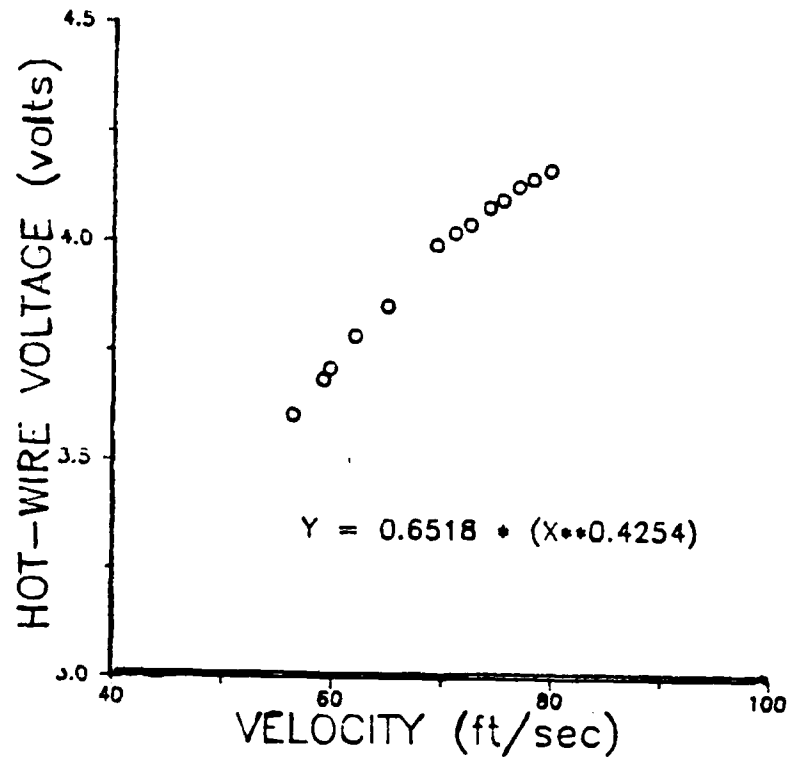
Figure B-1. Grid 1 Calibration Curve

Table B-2
Grids 3 and 4 Calibration Curve

Del-h (in)	HW Out (volts)	Velocity (ft/sec)
0.44	3.291	34.79
1.30	3.779	61.21
2.75	4.163	89.02
3.75	4.394	103.95
4.95	4.564	119.43
6.15	4.710	133.13
7.35	4.832	145.53
7.95	4.879	151.36

$$Y = 1.2472 * (X**0.2711)$$
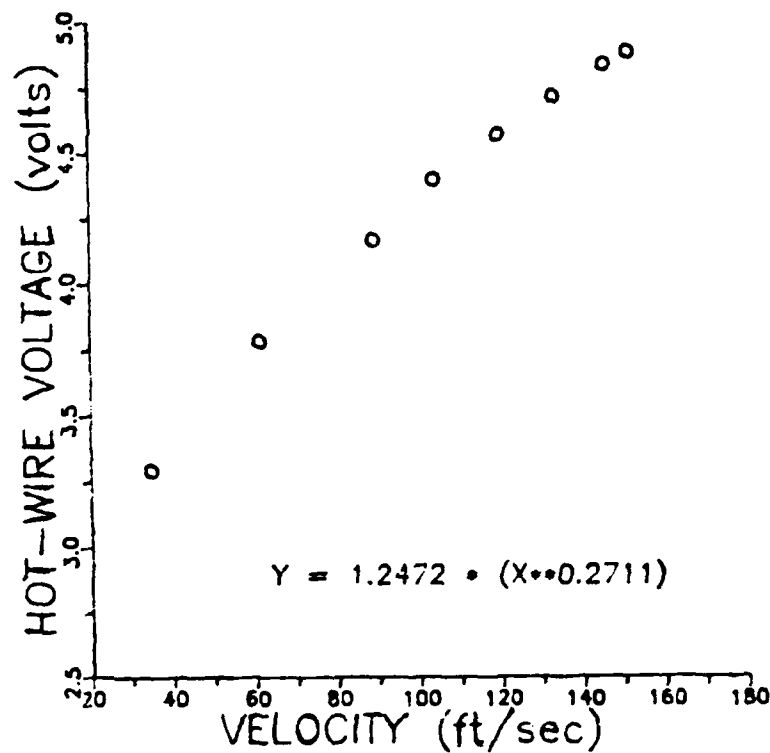
Figure B-2. Grids 3 and 4 Calibration Curve

APPENDIX C   DATA TABLES

TABLE C-1   NO GRID DATA .25c

y/c (in)	HOTWIRE (volt)	RMS (mV)	VELOC (ft/s)	RMS-V (ft/s)	NORMALIZED VELOC	NORMALIZED RMS-V
0.0005	4.023	41.0	95.51	2.50	0.738	0.026
0.0006	4.072	43.0	98.52	2.67	0.761	0.027
0.0007	4.148	40.0	103.30	2.55	0.798	0.025
0.0008	4.227	36.0	108.42	2.37	0.838	0.022
0.0010	4.302	27.0	113.42	1.82	0.877	0.016
0.0012	4.384	22.0	119.04	1.53	0.920	0.013
0.0015	4.432	19.0	122.41	1.35	0.946	0.011
0.0018	4.473	19.0	125.34	1.36	0.969	0.011
0.0021	4.501	19.0	127.36	1.38	0.984	0.011
0.0025	4.508	20.0	127.87	1.45	0.988	0.011
0.0029	4.512	22.0	128.16	1.60	0.990	0.012
0.0033	4.517	22.0	128.52	1.60	0.993	0.012
0.0038	4.519	22.0	128.67	1.61	0.994	0.012
0.0043	4.518	22.0	128.59	1.61	0.994	0.012
0.0049	4.526	22.0	129.18	1.61	0.998	0.012
0.0054	4.522	24.0	128.89	1.75	0.996	0.014
0.0060	4.521	23.0	128.81	1.68	0.995	0.013
0.0067	4.526	22.0	129.18	1.61	0.998	0.012
0.0073	4.527	22.0	129.25	1.61	0.999	0.012
0.0080	4.529	20.0	129.40	1.46	1.000	0.011
0.0087	4.529	22.0	129.40	1.61	1.000	0.012
0.0095	4.528	24.0	129.32	1.76	0.999	0.014
0.0102	4.531	23.0	129.54	1.69	1.001	0.013
0.0110	4.529	23.0	129.40	1.68	1.000	0.013
0.0118	4.530	23.0	129.47	1.69	1.001	0.013
0.0126	4.270	22.0	111.27	1.47	0.990	0.013
0.0135	4.527	24.0	129.25	1.76	0.999	0.014
0.0143	4.529	22.0	129.40	1.61	1.000	0.012
0.0152	4.531	23.0	129.54	1.69	1.001	0.013
0.0161	4.523	24.0	128.96	1.75	0.997	0.014
0.0169	4.523	21.0	128.96	1.53	0.997	0.012
0.0178	4.531	23.0	129.54	1.69	1.001	0.013
0.0187	4.528	23.0	129.32	1.68	0.999	0.013
0.0196	4.530	23.0	129.47	1.69	1.001	0.013
0.0205	4.529	23.0	129.40	1.68	1.000	0.013

TABLE C-2   NO GRID DATA .30c

y/c (in)	HOTWIRE (volt)	RMS (mV)	VELOC (ft/s)	RMS-V (ft/s)	NORMALIZED VELOC	RMS-V
0.0005	3.965	83.0	92.02	4.94	0.724	0.054
0.0006	4.025	78.0	95.63	4.75	0.753	0.050
0.0007	4.101	66.0	100.33	4.14	0.790	0.041
0.0009	4.179	69.0	105.29	4.46	0.829	0.042
0.0011	4.268	54.0	111.14	3.60	0.875	0.032
0.0014	4.333	45.0	115.53	3.08	0.909	0.027
0.0017	4.408	49.0	120.72	3.44	0.950	0.028
0.0021	4.448	38.0	123.55	2.71	0.972	0.022
0.0025	4.463	28.0	124.62	2.00	0.981	0.016
0.0030	4.470	24.0	125.12	1.72	0.985	0.014
0.0035	4.480	22.0	125.84	1.58	0.990	0.013
0.0040	4.489	20.0	126.49	1.44	0.995	0.011
0.0046	4.480	20.0	125.84	1.44	0.990	0.011
0.0053	4.490	20.0	126.56	1.45	0.996	0.011
0.0060	4.491	19.0	126.63	1.37	0.997	0.011
0.0067	4.489	19.0	126.49	1.37	0.995	0.011
0.0074	4.496	19.0	127.00	1.38	0.999	0.011
0.0082	4.493	19.0	126.78	1.37	0.998	0.011
0.0091	4.493	19.0	126.78	1.37	0.998	0.011
0.0099	4.498	18.0	127.14	1.30	1.001	0.010
0.0108	4.500	18.0	127.29	1.31	1.002	0.010
0.0117	4.497	18.0	127.07	1.30	1.000	0.010
0.0127	4.501	18.0	127.36	1.31	1.002	0.010
0.0137	4.502	18.0	127.43	1.31	1.003	0.010
0.0147	4.495	19.0	126.92	1.38	0.999	0.011
0.0157	4.498	18.0	127.14	1.30	1.001	0.010
0.0167	4.497	17.0	127.07	1.23	1.000	0.010
0.0178	4.498	17.0	127.14	1.23	1.001	0.010
0.0188	4.499	17.0	127.21	1.23	1.001	0.010
0.0199	4.497	19.0	127.07	1.38	1.000	0.011
0.0210	4.500	19.0	127.29	1.38	1.002	0.011
0.0221	4.495	19.0	126.92	1.38	0.999	0.011
0.0233	4.498	19.0	127.14	1.38	1.001	0.011
0.0244	4.492	19.0	126.71	1.37	0.997	0.011
0.0255	4.497	19.0	127.07	1.38	1.000	0.011

TABLE C-3   NO GRID DATA .35c

y/c (in)	HOTWIRE (volt)	RMS (mV)	VELOC (ft/s)	RMS-V (ft/s)	NORMALIZED VELOC	NORMALIZED RMS-V
0.0005	4.011	128.0	94.78	7.75	0.769	0.082
0.0006	4.048	124.0	97.04	7.62	0.788	0.079
0.0007	4.072	122.0	98.52	7.57	0.800	0.077
0.0009	4.105	122.0	100.58	7.66	0.816	0.076
0.0011	4.141	124.0	102.85	7.89	0.835	0.077
0.0014	4.164	124.0	104.33	7.96	0.847	0.076
0.0017	4.198	126.0	106.52	8.20	0.865	0.077
0.0021	4.236	124.0	109.01	8.18	0.885	0.075
0.0025	4.268	123.0	111.14	8.21	0.902	0.074
0.0030	4.291	120.0	112.68	8.08	0.915	0.072
0.0035	4.308	113.0	113.82	7.65	0.924	0.067
0.0040	4.338	104.0	115.87	7.12	0.941	0.061
0.0046	4.386	98.0	119.18	6.83	0.967	0.057
0.0053	4.402	87.0	120.30	6.09	0.977	0.051
0.0060	4.417	77.0	121.35	5.42	0.985	0.045
0.0067	4.430	74.0	122.63	4.99	0.990	0.042
0.0074	4.437	57.0	122.77	4.04	0.997	0.033
0.0082	4.439	48.0	122.91	3.41	0.998	0.028
0.0091	4.442	41.0	123.12	2.91	0.999	0.024
0.0099	4.447	34.0	123.48	2.42	1.002	0.020
0.0108	4.446	27.0	123.41	1.92	1.002	0.016
0.0117	4.444	24.0	123.26	1.71	1.001	0.014
0.0127	4.447	21.0	123.48	1.49	1.002	0.012
0.0137	4.446	17.0	123.41	1.21	1.002	0.010
0.0147	4.442	15.0	123.12	1.07	0.999	0.009
0.0157	4.445	15.0	123.34	1.07	1.001	0.009
0.0167	4.446	14.0	123.41	1.00	1.002	0.008
0.0178	4.448	13.0	123.55	0.93	1.003	0.007
0.0188	4.447	11.0	123.48	0.78	1.002	0.006
0.0199	4.449	10.0	123.62	0.71	1.003	0.006
0.0210	4.443	10.0	123.19	0.71	1.000	0.006
0.0221	4.444	9.0	123.26	0.64	1.001	0.005
0.0233	4.447	9.0	123.48	0.64	1.002	0.005
0.0244	4.443	9.0	123.19	0.64	1.000	0.005
0.0255	4.443	9.0	123.19	0.64	1.000	0.005

TABLE C-4   NO GRID DATA .40c

y/c (in)	HOTWIRE (volt)	RMS (mV)	VELOC (ft/s)	RMS-V (ft/s)	NORMALIZED VELOC	NORMALIZED RMS-V
0.0005	3.927	118.0	89.77	6.91	0.742	0.077
0.0006	3.965	117.0	92.02	6.96	0.761	0.076
0.0007	4.003	114.0	94.30	6.88	0.780	0.073
0.0009	4.020	112.0	95.33	6.81	0.788	0.071
0.0011	4.048	110.0	97.04	6.76	0.802	0.070
0.0014	4.095	109.0	99.95	6.82	0.827	0.068
0.0017	4.113	109.0	101.08	6.87	0.836	0.068
0.0021	4.138	107.0	102.66	6.80	0.849	0.066
0.0025	4.159	107.0	104.00	6.86	0.860	0.066
0.0030	4.190	107.0	106.00	6.94	0.877	0.065
0.0035	4.208	106.0	107.17	6.92	0.886	0.065
0.0040	4.235	106.0	108.95	6.99	0.901	0.064
0.0046	4.263	103.0	110.80	6.86	0.916	0.062
0.0053	4.277	101.0	111.74	6.76	0.924	0.061
0.0060	4.295	99.0	112.95	6.67	0.934	0.059
0.0067	4.319	91.0	114.57	6.19	0.947	0.054
0.0074	4.335	83.0	115.66	5.68	0.956	0.049
0.0082	4.355	74.0	117.04	5.10	0.968	0.044
0.0091	4.368	68.0	117.93	4.71	0.975	0.040
0.0099	4.383	55.0	118.97	3.83	0.984	0.032
0.0108	4.389	54.0	119.39	3.77	0.987	0.032
0.0117	4.398	44.0	120.02	3.08	0.992	0.026
0.0127	4.402	32.0	120.30	2.24	0.995	0.019
0.0137	4.408	28.0	120.72	1.97	0.998	0.016
0.0147	4.411	23.0	120.93	1.62	1.000	0.013
0.0157	4.413	19.0	121.07	1.34	1.001	0.011
0.0167	4.411	16.0	120.93	1.12	1.000	0.009
0.0178	4.413	14.0	121.07	0.98	1.001	0.008
0.0188	4.409	14.0	120.79	0.98	0.999	0.008
0.0199	4.410	11.0	120.86	0.77	0.999	0.006
0.0210	4.409	10.0	120.79	0.70	0.999	0.006
0.0221	4.410	0.9	120.86	0.06	0.999	0.001
0.0233	4.410	9.0	120.86	0.63	0.999	0.005
0.0244	4.409	9.0	120.79	0.63	0.999	0.005
0.0255	4.411	9.0	120.93	0.63	1.000	0.005

TABLE C-5   NO GRID DATA .45c

y/c (in)	HOTWIRE (volt)	RMS (mV)	VELOC (ft/s)	RMS-V (ft/s)	NORMALIZED VELOC	RMS-V
0.0005	3.825	122.0	83.92	6.86	0.710	0.082
0.0006	3.871	117.0	86.53	6.70	0.732	0.077
0.0007	3.895	113.0	87.91	6.54	0.744	0.074
0.0009	3.950	108.0	91.13	6.39	0.771	0.070
0.0011	3.985	105.0	93.21	6.30	0.789	0.068
0.0013	3.998	105.0	93.99	6.33	0.796	0.067
0.0016	4.025	104.0	95.63	6.33	0.809	0.066
0.0020	4.058	104.0	97.65	6.42	0.827	0.066
0.0024	4.075	103.0	98.70	6.40	0.835	0.065
0.0028	4.094	103.0	99.89	6.44	0.846	0.064
0.0033	4.117	103.0	101.33	6.50	0.858	0.064
0.0038	4.154	102.0	103.68	6.53	0.878	0.063
0.0043	4.171	101.0	104.78	6.50	0.887	0.062
0.0049	4.197	100.0	106.46	6.50	0.901	0.061
0.0056	4.208	99.0	107.17	6.46	0.907	0.060
0.0062	4.240	96.0	109.28	6.34	0.925	0.058
0.0069	4.263	92.0	110.80	6.13	0.938	0.055
0.0077	4.279	87.0	111.87	5.83	0.947	0.052
0.0085	4.297	85.0	113.08	5.73	0.957	0.051
0.0093	4.309	77.0	113.89	5.22	0.964	0.046
0.0101	4.330	72.0	115.32	4.92	0.976	0.043
0.0110	4.341	63.0	116.07	4.32	0.983	0.037
0.0119	4.347	52.0	116.48	3.57	0.986	0.031
0.0129	4.355	48.0	117.04	3.31	0.991	0.028
0.0138	4.363	38.0	117.59	2.63	0.995	0.022
0.0148	4.370	34.0	118.07	2.35	0.999	0.020
0.0158	4.370	28.0	118.07	1.94	0.999	0.016
0.0169	4.379	22.0	118.70	1.53	1.005	0.013
0.0179	4.379	19.0	118.70	1.32	1.005	0.011
0.0190	4.374	15.0	118.35	1.04	1.002	0.009
0.0201	4.380	13.0	118.76	0.90	1.005	0.008
0.0212	4.380	11.0	118.76	0.76	1.005	0.006
0.0224	4.379	11.0	118.70	0.76	1.005	0.006
0.0235	4.378	10.0	118.63	0.69	1.004	0.006
0.0246	4.373	9.0	118.28	0.62	1.001	0.005
0.0258	4.374	9.0	118.35	0.62	1.002	0.005
0.0270	4.376	8.0	118.49	0.56	1.003	0.005
0.0281	4.372	8.0	118.21	0.55	1.001	0.005
0.0293	4.369	8.0	118.00	0.55	0.999	0.005
0.0305	4.371	8.0	118.14	0.55	1.000	0.005

TABLE C-6   NO GRID DATA .50c

y/c (in)	HOTWIRE (volt)	RMS (mV)	VELOC (ft/s)	RMS-V (ft/s)	NORMALIZED VELOC	NORMALIZED RMS-V
0.0005	3.786	123.0	81.74	6.81	0.705	0.083
0.0006	3.795	121.0	82.24	6.72	0.709	0.082
0.0007	3.824	116.0	83.86	6.52	0.723	0.078
0.0009	3.848	114.0	85.22	6.47	0.735	0.076
0.0011	3.878	109.0	86.93	6.26	0.749	0.072
0.0013	3.915	108.0	89.07	6.30	0.768	0.071
0.0016	3.945	107.0	90.83	6.32	0.783	0.070
0.0020	3.972	105.0	92.44	6.26	0.797	0.068
0.0024	3.998	105.0	93.99	6.33	0.810	0.067
0.0028	4.008	104.0	94.60	6.29	0.815	0.067
0.0033	4.036	102.0	96.30	6.24	0.830	0.065
0.0038	4.056	102.0	97.53	6.29	0.841	0.064
0.0043	4.097	101.0	100.08	6.32	0.863	0.063
0.0049	4.114	100.0	101.14	6.30	0.872	0.062
0.0056	4.131	99.0	102.22	6.28	0.881	0.061
0.0062	4.170	97.0	104.71	6.24	0.903	0.060
0.0069	4.190	93.0	106.00	6.03	0.914	0.057
0.0077	4.203	90.0	106.85	5.86	0.921	0.055
0.0085	4.239	86.0	109.21	5.68	0.941	0.052
0.0093	4.242	83.0	109.41	5.49	0.943	0.050
0.0101	4.264	78.0	110.87	5.20	0.956	0.047
0.0110	4.285	73.0	112.27	4.90	0.968	0.044
0.0119	4.295	66.0	112.95	4.45	0.974	0.039
0.0129	4.301	57.0	113.35	3.85	0.977	0.034
0.0138	4.314	48.0	114.23	3.26	0.985	0.029
0.0148	4.329	42.0	115.25	2.87	0.994	0.025
0.0158	4.333	37.0	115.53	2.53	0.996	0.022
0.0169	4.332	28.0	115.46	1.91	0.995	0.017
0.0179	4.335	24.0	115.66	1.64	0.997	0.014
0.0190	4.339	20.0	115.94	1.37	0.999	0.012
0.0201	4.340	18.0	116.00	1.23	1.000	0.011
0.0212	4.340	14.0	116.00	0.96	1.000	0.008
0.0224	4.341	12.0	116.07	0.82	1.001	0.007
0.0235	4.342	11.0	116.14	0.75	1.001	0.006
0.0246	4.341	10.0	116.07	0.69	1.001	0.006
0.0258	4.340	9.0	116.00	0.62	1.000	0.005
0.0270	4.338	9.0	115.87	0.62	0.999	0.005
0.0281	4.339	8.0	115.94	0.55	0.999	0.005
0.0293	4.338	8.0	115.87	0.55	0.999	0.005
0.0305	4.340	8.0	116.00	0.55	1.000	0.005

TABLE C-7   NO GRID DATA .55c

y/c (in)	HOTWIRE (volt)	RMS (mV)	VELOC (ft/s)	RMS-V (ft/s)	NORMALIZED VELOC	NORMALIZED RMS-V
0.0005	3.695	130.0	76.80	6.93	0.680	0.090
0.0006	3.702	128.0	77.17	6.84	0.683	0.089
0.0007	3.718	125.0	78.03	6.72	0.690	0.086
0.0009	3.750	118.0	79.76	6.43	0.706	0.081
0.0011	3.785	115.0	81.69	6.36	0.723	0.078
0.0013	3.810	113.0	83.08	6.32	0.735	0.076
0.0016	3.827	112.0	84.03	6.30	0.744	0.075
0.0020	3.868	111.0	86.36	6.35	0.764	0.074
0.0024	3.883	109.0	87.22	6.28	0.772	0.072
0.0028	3.905	109.0	88.49	6.33	0.783	0.072
0.0033	3.935	107.0	90.24	6.29	0.799	0.070
0.0038	3.962	107.0	91.84	6.36	0.813	0.069
0.0043	3.993	105.0	93.69	6.32	0.829	0.067
0.0049	4.015	104.0	95.02	6.31	0.841	0.066
0.0056	4.045	102.0	96.85	6.26	0.857	0.065
0.0062	4.065	102.0	98.08	6.31	0.868	0.064
0.0069	4.093	99.0	99.83	6.19	0.883	0.062
0.0077	4.117	97.0	101.33	6.12	0.897	0.060
0.0085	4.141	90.0	102.85	5.73	0.910	0.056
0.0093	4.162	86.0	104.20	5.52	0.922	0.053
0.0101	4.188	84.0	105.87	5.44	0.937	0.051
0.0110	4.195	77.0	106.33	5.00	0.941	0.047
0.0119	4.221	75.0	108.03	4.92	0.956	0.046
0.0129	4.237	67.0	109.08	4.42	0.965	0.041
0.0138	4.251	60.0	110.00	3.98	0.973	0.036
0.0148	4.267	55.0	111.07	3.67	0.983	0.033
0.0158	4.285	46.0	112.27	3.09	0.993	0.028
0.0169	4.277	36.0	111.74	2.41	0.989	0.022
0.0179	4.283	34.0	112.14	2.28	0.992	0.020
0.0190	4.289	27.0	112.54	1.82	0.996	0.016
0.0201	4.293	22.0	112.81	1.48	0.998	0.013
0.0212	4.296	19.0	113.01	1.28	1.000	0.011
0.0224	4.297	16.0	113.08	1.08	1.001	0.010
0.0235	4.293	14.0	112.81	0.94	0.998	0.008
0.0246	4.295	12.0	112.95	0.81	0.999	0.007
0.0258	4.295	11.0	112.95	0.74	0.999	0.007
0.0270	4.294	10.0	112.88	0.67	0.999	0.006
0.0281	4.296	9.0	113.01	0.61	1.000	0.005
0.0293	4.294	9.0	112.88	0.61	0.999	0.005
0.0305	4.296	8.0	113.01	0.54	1.000	0.005

TABLE C-8   NO GRID DATA .60c

y/c (in)	HOTWIRE (volt)	RMS (mV)	VELOC (ft/s)	RMS-V (ft/s)	NORMALIZED VELOC	NORMALIZED RMS-V
0.0005	3.527	148.0	68.17	7.33	0.616	0.108
0.0006	3.567	141.0	70.16	7.11	0.634	0.101
0.0007	3.601	138.0	71.89	7.06	0.650	0.098
0.0008	3.645	127.0	74.16	6.62	0.670	0.089
0.0010	3.675	123.0	75.74	6.50	0.684	0.086
0.0013	3.701	118.0	77.12	6.30	0.697	0.082
0.0015	3.725	115.0	78.41	6.20	0.709	0.079
0.0019	3.750	115.0	79.76	6.27	0.721	0.079
0.0022	3.789	113.0	81.91	6.26	0.740	0.076
0.0026	3.808	112.0	82.97	6.25	0.750	0.075
0.0030	3.827	112.0	84.03	6.30	0.759	0.075
0.0035	3.860	111.0	85.90	6.33	0.776	0.074
0.0040	3.899	111.0	88.14	6.43	0.796	0.073
0.0046	3.919	110.0	89.31	6.43	0.807	0.072
0.0052	3.925	109.0	89.66	6.38	0.810	0.071
0.0058	3.995	108.0	93.81	6.50	0.848	0.069
0.0065	3.990	105.0	93.51	6.31	0.845	0.067
0.0072	4.020	103.0	95.33	6.26	0.861	0.066
0.0079	4.065	98.0	98.08	6.06	0.886	0.062
0.0087	4.070	96.0	98.39	5.95	0.889	0.060
0.0095	4.086	94.0	99.39	5.86	0.898	0.059
0.0103	4.119	90.0	101.46	5.68	0.917	0.056
0.0112	4.138	86.0	102.66	5.47	0.928	0.053
0.0121	4.151	80.0	103.49	5.11	0.935	0.049
0.0130	4.188	75.0	105.87	4.86	0.957	0.046
0.0140	4.190	70.0	106.00	4.54	0.958	0.043
0.0149	4.211	63.0	107.37	4.12	0.970	0.038
0.0159	4.225	54.0	108.29	3.55	0.978	0.033
0.0170	4.239	48.0	109.21	3.17	0.987	0.029
0.0180	4.243	42.0	109.47	2.78	0.989	0.025
0.0191	4.245	38.0	109.61	2.52	0.990	0.023
0.0202	4.248	30.0	109.81	1.99	0.992	0.018
0.0213	4.252	25.0	110.07	1.66	0.995	0.015
0.0224	4.254	20.0	110.20	1.33	0.996	0.012
0.0235	4.258	16.0	110.47	1.06	0.998	0.010
0.0247	4.264	14.0	110.87	0.93	1.002	0.008
0.0259	4.262	12.0	110.74	0.80	1.001	0.007
0.0270	4.262	11.0	110.74	0.73	1.001	0.007
0.0282	4.263	10.0	110.80	0.67	1.001	0.006
0.0294	4.260	10.0	110.60	0.67	0.999	0.006
0.0306	4.261	9.0	110.67	0.60	1.000	0.005
0.0318	4.260	9.0	110.60	0.60	0.999	0.005
0.0331	4.262	9.0	110.74	0.60	1.001	0.005
0.0343	4.260	9.0	110.60	0.60	0.999	0.005
0.0355	4.261	8.0	110.67	0.53	1.000	0.005

TABLE C-9   NO GRID DATA .65c

y/c (in)	HOTWIRE (volt)	RMS (mV)	VELOC (ft/s)	RMS-V (ft/s)	NORMALIZED VELOC	RMS-V
0.0005	3.525	150.0	68.07	7.42	0.623	0.109
0.0006	3.565	145.0	70.06	7.30	0.641	0.104
0.0007	3.570	135.0	70.32	6.82	0.643	0.097
0.0009	3.595	131.0	71.58	6.69	0.655	0.093
0.0011	3.635	129.0	73.64	6.70	0.674	0.091
0.0013	3.665	123.0	75.21	6.47	0.688	0.086
0.0016	3.695	125.0	76.80	6.66	0.703	0.087
0.0020	3.708	119.0	77.49	6.37	0.709	0.082
0.0024	3.745	120.0	79.49	6.53	0.727	0.082
0.0028	3.778	117.0	81.30	6.45	0.744	0.079
0.0033	3.785	115.0	81.69	6.36	0.748	0.078
0.0038	3.815	117.0	83.36	6.55	0.763	0.079
0.0043	3.842	114.0	84.88	6.46	0.777	0.076
0.0049	3.875	115.0	86.76	6.60	0.794	0.076
0.0056	3.905	117.0	88.49	6.80	0.810	0.077
0.0062	3.920	115.0	89.37	6.72	0.818	0.075
0.0069	3.955	110.0	91.42	6.52	0.837	0.071
0.0077	3.975	109.0	92.61	6.51	0.848	0.070
0.0085	4.000	105.0	94.11	6.33	0.861	0.067
0.0093	4.035	102.0	96.24	6.24	0.881	0.065
0.0101	4.040	98.0	96.55	6.00	0.884	0.062
0.0110	4.095	94.0	99.95	5.88	0.915	0.059
0.0119	4.108	92.0	100.77	5.78	0.922	0.057
0.0129	4.132	84.0	102.28	5.33	0.936	0.052
0.0138	4.140	78.0	102.79	4.96	0.941	0.048
0.0148	4.160	74.0	104.07	4.75	0.952	0.046
0.0158	4.195	68.0	106.33	4.42	0.973	0.042
0.0169	4.201	58.0	106.72	3.78	0.977	0.035
0.0179	4.210	52.0	107.31	3.40	0.982	0.032
0.0190	4.225	43.0	108.29	2.83	0.991	0.026
0.0201	4.225	40.0	108.29	2.63	0.991	0.024
0.0212	4.230	33.0	108.62	2.17	0.994	0.020
0.0224	4.235	28.0	108.95	1.85	0.997	0.017
0.0235	4.235	23.0	108.95	1.52	0.997	0.014
0.0246	4.235	20.0	108.95	1.32	0.997	0.012
0.0258	4.238	18.0	109.14	1.19	0.999	0.011
0.0270	4.239	16.0	109.21	1.06	0.999	0.010
0.0281	4.238	14.0	109.14	0.92	0.999	0.008
0.0293	4.239	13.0	109.21	0.86	0.999	0.008
0.0305	4.240	12.0	109.28	0.79	1.000	0.007

TABLE C-10   GRID #1 DATA .25c

y/c (in)	HOTWIRE (volt)	RMS (mV)	VELOC (ft/s)	RMS-V (ft/s)	NORMALIZED VELOC	RMS-V
======	======	=======	=====	=====	======	======
0.0005	3.528	142.0	53.15	4.98	0.851	0.080
0.0006	3.560	137.0	54.28	4.86	0.869	0.078
0.0007	3.598	130.0	55.64	4.68	0.891	0.075
0.0009	3.653	131.0	57.64	4.81	0.923	0.077
0.0012	3.694	127.0	59.15	4.73	0.947	0.076
0.0015	3.733	123.0	60.61	4.64	0.971	0.074
0.0018	3.783	109.0	62.52	4.19	1.001	0.067
0.0022	3.803	104.0	63.29	4.03	1.014	0.064
0.0027	3.833	92.0	64.46	3.60	1.032	0.058
0.0032	3.837	82.0	64.61	3.21	1.035	0.051
0.0037	3.845	78.0	64.93	3.06	1.040	0.049
0.0043	3.863	68.0	65.64	2.69	1.051	0.043
0.0050	3.871	61.0	65.95	2.42	1.056	0.039
0.0056	3.860	60.0	65.52	2.37	1.049	0.038
0.0064	3.864	59.0	65.68	2.33	1.052	0.037
0.0071	3.860	57.0	65.52	2.25	1.049	0.036
0.0079	3.861	57.0	65.56	2.25	1.050	0.036
0.0087	3.855	56.0	65.32	2.21	1.046	0.035
0.0096	3.849	53.0	65.09	2.08	1.042	0.033
0.0105	3.839	52.0	64.69	2.04	1.036	0.033
0.0114	3.830	57.0	64.34	2.23	1.030	0.036
0.0124	3.831	57.0	64.38	2.23	1.031	0.036
0.0133	3.823	53.0	64.07	2.07	1.026	0.033
0.0143	3.802	56.0	63.25	2.17	1.013	0.035
0.0153	3.803	55.0	63.29	2.13	1.014	0.034
0.0163	3.799	51.0	63.14	1.97	1.011	0.032
0.0174	3.197	53.0	42.27	1.63	0.677	0.026
0.0184	3.790	53.0	62.79	2.04	1.006	0.033
0.0195	3.799	54.0	63.14	2.09	1.011	0.033
0.0205	3.781	53.0	62.44	2.04	1.000	0.033

TABLE C-11 GRID #1 DATA .30c

y/c (in)	HOTWIRE (volt)	RMS (mV)	VELOC (ft/s)	RMS-V (ft/s)	NORMALIZED VELOC	NORMALIZED RMS-V
0.0005	3.842	156.0	64.81	6.12	0.783	0.074
0.0006	3.861	151.0	65.56	5.96	0.792	0.072
0.0007	3.905	152.0	67.31	6.09	0.813	0.074
0.0009	3.935	155.0	68.52	6.28	0.827	0.076
0.0012	3.987	150.0	70.64	6.18	0.853	0.075
0.0015	4.022	151.0	72.09	6.29	0.871	0.076
0.0018	4.075	150.0	74.32	6.36	0.897	0.077
0.0022	4.117	143.0	76.11	6.15	0.919	0.074
0.0027	4.148	133.0	77.45	5.78	0.935	0.070
0.0032	4.187	123.0	79.16	5.41	0.956	0.065
0.0037	4.206	100.0	80.00	4.42	0.966	0.053
0.0043	4.228	97.0	80.97	4.32	0.978	0.052
0.0050	4.248	80.0	81.87	3.59	0.989	0.043
0.0056	4.251	71.0	82.00	3.19	0.990	0.038
0.0064	4.270	68.0	82.86	3.07	1.001	0.037
0.0071	4.272	60.0	82.95	2.71	1.002	0.033
0.0079	4.277	58.0	83.17	2.62	1.004	0.032
0.0087	4.271	57.0	82.90	2.57	1.001	0.031
0.0096	4.275	57.0	83.08	2.58	1.003	0.031
0.0105	4.280	56.0	83.31	2.53	1.006	0.031
0.0114	4.271	55.0	82.90	2.48	1.001	0.030
0.0124	4.271	56.0	82.90	2.53	1.001	0.031
0.0133	4.270	57.0	82.86	2.57	1.001	0.031
0.0143	4.272	55.0	82.95	2.48	1.002	0.030
0.0153	4.271	55.0	82.90	2.48	1.001	0.030
0.0163	4.267	54.0	82.72	2.43	0.999	0.029
0.0174	4.270	57.0	82.86	2.57	1.001	0.031
0.0184	4.269	57.0	82.81	2.57	1.000	0.031
0.0195	4.268	53.0	82.77	2.39	0.999	0.029
0.0205	4.269	52.0	82.81	2.35	1.000	0.028

TABLE C-12   GRID #1 DATA .35c

y/c (in)	HOTWIRE (volt)	RMS (mV)	VELOC (ft/s)	RMS-V (ft/s)	NORMALIZED VELOC	NORMALIZED RMS-V
0.0005	3.653	168.0	57.64	6.16	0.715	0.076
0.0006	3.694	153.0	59.15	5.70	0.734	0.071
0.0007	3.735	150.0	60.69	5.67	0.753	0.070
0.0008	3.789	143.0	62.75	5.51	0.778	0.068
0.0010	3.818	138.0	63.87	5.37	0.792	0.067
0.0012	3.833	142.0	64.46	5.55	0.800	0.069
0.0015	3.873	138.0	66.03	5.47	0.819	0.068
0.0018	3.918	144.0	67.83	5.80	0.841	0.072
0.0021	3.953	147.0	69.25	5.99	0.859	0.074
0.0025	3.983	145.0	70.48	5.97	0.874	0.074
0.0029	4.008	142.0	71.51	5.89	0.887	0.073
0.0033	4.030	132.0	72.43	5.52	0.898	0.068
0.0038	4.083	131.0	74.66	5.57	0.926	0.069
0.0043	4.104	126.0	75.56	5.39	0.937	0.067
0.0049	4.122	116.0	76.33	5.00	0.947	0.062
0.0054	4.139	104.0	77.06	4.50	0.956	0.056
0.0060	4.161	99.0	78.02	4.32	0.968	0.054
0.0067	4.185	88.0	79.07	3.87	0.981	0.048
0.0073	4.205	79.0	79.95	3.49	0.992	0.043
0.0080	4.211	71.0	80.22	3.15	0.995	0.039
0.0087	4.217	68.0	80.48	3.02	0.998	0.037
0.0095	4.219	63.0	80.57	2.80	0.999	0.035
0.0102	4.224	62.0	80.79	2.76	1.002	0.034
0.0110	4.226	60.0	80.88	2.67	1.003	0.033
0.0118	4.227	60.0	80.93	2.67	1.004	0.033
0.0126	4.220	59.0	80.62	2.62	1.000	0.033
0.0135	4.223	58.0	80.75	2.58	1.002	0.032
0.0143	4.229	60.0	81.02	2.67	1.005	0.033
0.0152	4.227	57.0	80.93	2.54	1.004	0.031
0.0160	4.223	58.0	80.75	2.58	1.002	0.032
0.0169	4.229	57.0	81.02	2.54	1.005	0.032
0.0178	4.227	58.0	80.93	2.58	1.004	0.032
0.0187	4.229	60.0	81.02	2.67	1.005	0.033
0.0196	4.225	57.0	80.84	2.54	1.003	0.031
0.0205	4.220	56.0	80.62	2.49	1.000	0.031

TABLE C-13   GRID #1 DATA .40c

y/c (in)	HOTWIRE (volt)	RMS (mV)	VELOC (ft/s)	RMS-V (ft/s)	NORMALIZED VELOC	RMS-V
0.0005	3.735	144.0	60.69	5.44	0.773	0.069
0.0006	3.769	138.0	61.98	5.28	0.790	0.067
0.0007	3.773	135.0	62.14	5.17	0.792	0.066
0.0008	3.792	134.0	62.87	5.17	0.801	0.066
0.0010	3.809	137.0	63.52	5.31	0.809	0.068
0.0013	3.827	138.0	64.22	5.39	0.818	0.069
0.0015	3.838	137.0	64.65	5.37	0.824	0.068
0.0018	3.871	142.0	65.95	5.63	0.840	0.072
0.0022	3.912	138.0	67.59	5.54	0.861	0.071
0.0026	3.944	138.0	68.88	5.61	0.877	0.071
0.0030	3.957	141.0	69.41	5.75	0.884	0.073
0.0035	3.983	132.0	70.48	5.43	0.898	0.069
0.0040	4.028	130.0	72.34	5.43	0.922	0.069
0.0045	4.028	124.0	72.34	5.18	0.922	0.066
0.0051	4.052	113.0	73.35	4.76	0.934	0.061
0.0057	4.083	108.0	74.66	4.59	0.951	0.059
0.0063	4.102	102.0	75.47	4.36	0.961	0.056
0.0070	4.118	93.0	76.16	4.00	0.970	0.051
0.0077	4.138	84.0	77.02	3.64	0.981	0.046
0.0084	4.140	78.0	77.11	3.38	0.982	0.043
0.0092	4.151	72.0	77.58	3.13	0.988	0.040
0.0099	4.161	67.0	78.02	2.92	0.994	0.037
0.0107	4.159	62.0	77.93	2.70	0.993	0.034
0.0115	4.166	63.0	78.24	2.75	0.997	0.035
0.0124	4.169	61.0	78.37	2.67	0.998	0.034
0.0132	4.167	62.0	78.28	2.71	0.997	0.035
0.0141	4.169	62.0	78.37	2.71	0.998	0.035
0.0150	4.170	60.0	78.41	2.62	0.999	0.033
0.0159	4.171	60.0	78.46	2.62	0.999	0.033
0.0168	4.170	58.0	78.41	2.54	0.999	0.032
0.0178	4.169	60.0	78.37	2.62	0.998	0.033
0.0187	4.172	56.0	78.50	2.45	1.000	0.031
0.0196	4.172	59.0	78.50	2.58	1.000	0.033
0.0206	4.173	56.0	78.54	2.45	1.001	0.031
0.0215	4.172	60.0	78.50	2.63	1.000	0.033

TABLE C-14   GRID #1 DATA .45c

y/c (in)	HOTWIRE (volt)	RMS (mV)	VELOC (ft/s)	RMS-V (ft/s)	NORMALIZED VELOC	RMS-V
======	======	=======	=====	=====	======	======
0.0005	3.652	141.0	57.60	5.17	0.743	0.067
0.0006	3.678	142.0	58.56	5.26	0.755	0.068
0.0007	3.687	134.0	58.89	4.98	0.759	0.064
0.0009	3.706	137.0	59.60	5.12	0.769	0.066
0.0011	3.731	133.0	60.54	5.02	0.781	0.065
0.0013	3.748	131.0	61.18	4.97	0.789	0.064
0.0016	3.779	131.0	62.37	5.03	0.804	0.065
0.0019	3.806	133.0	63.41	5.15	0.818	0.066
0.0023	3.837	131.0	64.61	5.13	0.833	0.066
0.0027	3.863	130.0	65.64	5.14	0.846	0.066
0.0032	3.887	129.0	66.59	5.14	0.859	0.066
0.0037	3.906	128.0	67.35	5.13	0.869	0.066
0.0042	3.937	126.0	68.60	5.11	0.885	0.066
0.0048	3.973	126.0	70.07	5.17	0.904	0.067
0.0054	3.998	125.0	71.10	5.17	0.917	0.067
0.0061	4.009	118.0	71.55	4.90	0.923	0.063
0.0067	4.035	109.0	72.64	4.56	0.937	0.059
0.0075	4.074	103.0	74.28	4.37	0.958	0.056
0.0082	4.080	98.0	74.53	4.16	0.961	0.054
0.0090	4.103	90.0	75.51	3.85	0.974	0.050
0.0098	4.110	81.0	75.81	3.47	0.978	0.045
0.0106	4.126	78.0	76.50	3.36	0.987	0.043
0.0115	4.133	70.0	76.80	3.03	0.990	0.039
0.0123	4.146	69.0	77.37	2.99	0.998	0.039
0.0132	4.142	66.0	77.19	2.86	0.996	0.037
0.0142	4.145	64.0	77.32	2.78	0.997	0.036
0.0151	4.143	61.0	77.24	2.64	0.996	0.034
0.0160	4.150	62.0	77.54	2.69	1.000	0.035
0.0170	4.147	59.0	77.41	2.56	0.998	0.033
0.0180	4.143	60.0	77.24	2.60	0.996	0.034
0.0190	4.147	62.0	77.41	2.69	0.998	0.035
0.0200	4.147	61.0	77.41	2.65	0.998	0.034
0.0210	4.146	62.0	77.37	2.69	0.998	0.035
0.0220	4.143	59.0	77.24	2.56	0.996	0.033
0.0230	4.150	59.0	77.54	2.56	1.000	0.033

TABLE C-15   GRID #1 DATA .50c

y/c (in)	HOTWIRE (volt)	RMS (mV)	VELOC (ft/s)	RMS-V (ft/s)	NORMALIZED VELOC	NORMALIZED RMS-V
0.0005	3.698	148.0	59.30	5.52	0.716	0.067
0.0006	3.724	142.0	60.28	5.35	0.728	0.065
0.0007	3.747	145.0	61.14	5.50	0.738	0.066
0.0009	3.778	140.0	62.33	5.37	0.753	0.065
0.0011	3.795	142.0	62.98	5.48	0.761	0.066
0.0013	3.817	134.0	63.83	5.21	0.771	0.063
0.0016	3.834	138.0	64.50	5.40	0.779	0.065
0.0019	3.870	141.0	65.91	5.58	0.796	0.067
0.0023	3.912	137.0	67.59	5.50	0.816	0.066
0.0027	3.931	139.0	68.36	5.62	0.825	0.068
0.0032	3.939	140.0	68.68	5.68	0.829	0.069
0.0037	3.988	137.0	70.68	5.65	0.854	0.068
0.0042	4.019	137.0	71.97	5.71	0.869	0.069
0.0048	4.044	135.0	73.01	5.67	0.882	0.068
0.0054	4.063	132.0	73.81	5.58	0.891	0.067
0.0061	4.089	131.0	74.92	5.58	0.905	0.067
0.0067	4.142	128.0	77.19	5.55	0.932	0.067
0.0075	4.142	122.0	77.19	5.29	0.932	0.064
0.0082	4.177	109.0	78.72	4.78	0.951	0.058
0.0090	4.183	102.0	78.98	4.48	0.954	0.054
0.0098	4.205	100.0	79.95	4.42	0.965	0.053
0.0106	4.220	86.0	80.62	3.82	0.974	0.046
0.0115	4.238	84.0	81.42	3.75	0.983	0.045
0.0123	4.248	83.0	81.87	3.72	0.989	0.045
0.0132	4.245	79.0	81.73	3.54	0.987	0.043
0.0142	4.264	71.0	82.59	3.20	0.997	0.039
0.0151	4.260	69.0	82.41	3.10	0.995	0.037
0.0160	4.259	71.0	82.36	3.19	0.995	0.039
0.0170	4.263	64.0	82.54	2.88	0.997	0.035
0.0180	4.270	62.0	82.86	2.80	1.001	0.034
0.0190	4.269	66.0	82.81	2.98	1.000	0.036
0.0200	4.265	61.0	82.63	2.75	0.998	0.033
0.0210	4.268	63.0	82.77	2.84	0.999	0.034
0.0220	4.274	64.0	83.04	2.89	1.003	0.035
0.0230	4.269	60.0	82.81	2.71	1.000	0.033

TABLE C-16   GRID #1 DATA .55c

y/c (in)	HOTWIRE (volt)	RMS (mV)	VELOC (ft/s)	RMS-V (ft/s)	NORMALIZED VELOC	NORMALIZED RMS-V
======	======	=======	=====	=====	======	======
0.0005	3.634	149.0	56.94	5.43	0.702	0.067
0.0006	3.670	150.0	58.26	5.54	0.718	0.068
0.0007	3.684	148.0	58.78	5.49	0.724	0.068
0.0009	3.719	144.0	60.09	5.41	0.740	0.0u7
0.0011	3.741	145.0	60.92	5.49	0.751	0.068
0.0014	3.777	146.0	62.29	5.60	0.768	0.069
0.0017	3.792	141.0	62.87	5.44	0.775	0.067
0.0021	3.809	148.0	63.52	5.74	0.783	0.071
0.0025	3.831	143.0	64.38	5.59	0.793	0.069
0.0030	3.881	141.0	66.35	5.61	0.818	0.069
0.0035	3.905	142.0	67.31	5.69	0.829	0.070
0.0040	3.923	143.0	68.03	5.77	0.838	0.071
0.0046	3.960	139.0	69.53	5.68	0.857	0.070
0.0053	3.991	136.0	70.81	5.61	0.873	0.069
0.0060	4.019	136.0	71.97	5.66	0.887	0.070
0.0067	4.055	134.0	73.48	5.65	0.905	0.070
0.0074	4.088	131.0	74.87	5.58	0.923	0.069
0.0082	4.108	125.0	75.73	5.36	0.933	0.066
0.0091	4.134	120.0	76.85	5.19	0.947	0.064
0.0099	4.153	109.0	77.67	4.74	0.957	0.058
0.0108	4.169	105.0	78.37	4.59	0.966	0.057
0.0117	4.190	97.0	79.29	4.27	0.977	0.053
0.0127	4.203	90.0	79.86	3.98	0.984	0.049
0.0137	4.207	83.0	80.04	3.67	0.986	0.045
0.0147	4.214	80.0	80.35	3.55	0.990	0.044
0.0157	4.235	77.0	81.29	3.44	1.002	0.042
0.0167	4.238	68.0	81.42	3.04	1.003	0.037
0.0178	4.230	67.0	81.06	2.99	0.999	0.037
0.0188	4.229	64.0	81.02	2.85	0.998	0.035
0.0199	4.230	69.0	81.06	3.08	0.999	0.038
0.0210	4.231	65.0	81.11	2.90	0.999	0.036
0.0221	4.230	64.0	81.06	2.85	0.999	0.035
0.0233	4.231	65.0	81.11	2.90	0.999	0.036
0.0244	4.230	64.0	81.06	2.85	0.999	0.035
0.0255	4.232	66.0	81.15	2.94	1.000	0.036

TABLE C-17   GRID #1 DATA .60c

y/c (in)	HOTWIRE (volt)	RMS (mV)	VELOC (ft/s)	RMS-V (ft/s)	NORMALIZED VELOC	NORMALIZED RMS-V
0.0005	3.570	165.0	54.64	5.87	0.674	0.072
0.0006	3.589	162.0	55.32	5.81	0.682	0.072
0.0007	3.601	153.0	55.75	5.51	0.688	0.068
0.0009	3.631	151.0	56.83	5.50	0.701	0.068
0.0011	3.675	151.0	58.45	5.58	0.721	0.069
0.0014	3.684	149.0	58.78	5.53	0.725	0.068
0.0017	3.710	143.0	59.75	5.36	0.737	0.066
0.0021	3.737	147.0	60.77	5.56	0.750	0.069
0.0025	3.784	145.0	62.56	5.57	0.772	0.069
0.0030	3.808	153.0	63.48	5.93	0.783	0.073
0.0035	3.835	150.0	64.54	5.87	0.796	0.072
0.0040	3.853	141.0	65.24	5.55	0.805	0.068
0.0046	3.890	145.0	66.71	5.78	0.823	0.071
0.0053	3.938	148.0	68.64	6.00	0.847	0.074
0.0060	3.953	150.0	69.25	6.11	0.854	0.075
0.0067	3.993	145.0	70.89	5.99	0.875	0.074
0.0074	4.021	137.0	72.05	5.71	0.889	0.070
0.0082	4.040	136.0	72.85	5.70	0.899	0.070
0.0091	4.079	131.0	74.49	5.56	0.919	0.069
0.0099	4.097	119.0	75.26	5.08	0.928	0.063
0.0108	4.127	120.0	76.55	5.18	0.944	0.064
0.0117	4.144	109.0	77.28	4.73	0.953	0.058
0.0127	4.165	110.0	78.19	4.80	0.965	0.059
0.0137	4.176	100.0	78.68	4.38	0.971	0.054
0.0147	4.198	94.0	79.64	4.15	0.982	0.051
0.0157	4.203	88.0	79.86	3.89	0.985	0.048
0.0167	4.214	84.0	80.35	3.72	0.991	0.046
0.0178	4.226	80.0	80.88	3.56	0.998	0.044
0.0188	4.221	74.0	80.66	3.29	0.995	0.041
0.0199	4.227	71.0	80.93	3.16	0.998	0.039
0.0210	4.220	70.0	80.62	3.11	0.995	0.038
0.0221	4.228	68.0	80.97	3.03	0.999	0.037
0.0233	4.229	67.0	81.02	2.99	0.999	0.037
0.0244	4.220	68.0	80.62	3.02	0.995	0.037
0.0255	4.230	70.0	81.06	3.12	1.000	0.038

TABLE C-18   GRID #1 DATA .65c

y/c (in)	HOTWIRE (volt)	RMS (mV)	VELOC (ft/s)	RMS-V (ft/s)	NORMALIZED VELOC	NORMALIZED RMS-V
========	========	========	=======	=======	=======	=======
0.0005	3.530	174.0	53.22	6.10	0.659	0.076
0.0006	3.561	170.0	54.32	6.03	0.673	0.075
0.0007	3.571	161.0	54.67	5.73	0.677	0.071
0.0009	3.611	161.0	56.11	5.82	0.695	0.072
0.0011	3.629	155.0	56.76	5.64	0.703	0.070
0.0014	3.671	153.0	58.30	5.65	0.722	0.070
0.0017	3.689	150.0	58.97	5.58	0.730	0.069
0.0021	3.711	155.0	59.79	5.81	0.740	0.072
0.0025	3.740	154.0	60.88	5.83	0.754	0.072
0.0030	3.775	153.0	62.21	5.86	0.770	0.073
0.0035	3.803	153.0	63.29	5.92	0.784	0.073
0.0040	3.815	156.0	63.76	6.06	0.790	0.075
0.0046	3.848	158.0	65.05	6.21	0.806	0.077
0.0053	3.891	154.0	66.75	6.14	0.827	0.076
0.0060	3.911	156.0	67.55	6.27	0.837	0.078
0.0067	3.937	149.0	68.60	6.04	0.850	0.075
0.0074	3.985	151.0	70.56	6.22	0.874	0.077
0.0082	3.998	148.0	71.10	6.12	0.880	0.076
0.0091	4.021	140.0	72.05	5.83	0.892	0.072
0.0099	4.073	138.0	74.24	5.85	0.919	0.072
0.0108	4.089	128.0	74.92	5.45	0.928	0.068
0.0117	4.108	128.0	75.73	5.49	0.938	0.068
0.0127	4.135	112.0	76.89	4.84	0.952	0.060
0.0137	4.155	117.0	77.76	5.09	0.963	0.063
0.0147	4.188	109.0	79.20	4.79	0.981	0.059
0.0157	4.185	99.0	79.07	4.35	0.979	0.054
0.0167	4.200	98.0	79.73	4.33	0.987	0.054
0.0178	4.219	90.0	80.57	4.00	0.998	0.050
0.0188	4.219	83.0	80.57	3.69	0.998	0.046
0.0199	4.214	84.0	80.35	3.72	0.995	0.046
0.0210	4.220	80.0	80.62	3.55	0.998	0.044
0.0221	4.220	77.0	80.62	3.42	0.998	0.042
0.0233	4.225	72.0	80.84	3.20	1.001	0.040
0.0244	4.227	70.0	80.93	3.12	1.002	0.039
0.0255	4.223	71.0	80.75	3.16	1.000	0.039

TABLE C-19   GRID #3 DATA .25c

y/c (in)	HOTWIRE (volt)	RMS (mV)	VELOC (ft/s)	RMS-V (ft/s)	NORMALIZED VELOC	NORMALIZED RMS-V
0.0005	3.589	111.0	49.40	5.62	0.759	0.086
0.0006	3.638	103.0	51.93	5.41	0.798	0.083
0.0007	3.674	103.0	53.84	5.55	0.827	0.085
0.0009	3.709	96.0	55.75	5.31	0.857	0.082
0.0012	3.749	92.0	58.00	5.24	0.891	0.080
0.0015	3.801	79.0	61.02	4.67	0.938	0.072
0.0018	3.839	76.0	63.29	4.61	0.973	0.071
0.0022	3.874	64.0	65.44	3.98	1.006	0.061
0.0027	3.885	60.0	66.13	3.76	1.016	0.058
0.0032	3.879	49.0	65.75	3.06	1.011	0.047
0.0037	3.883	47.0	66.00	2.94	1.014	0.045
0.0043	3.880	45.0	65.81	2.81	1.011	0.043
0.0050	3.892	42.0	66.57	2.64	1.023	0.041
0.0056	3.890	45.0	66.44	2.83	1.021	0.043
0.0064	3.889	42.0	66.38	2.64	1.020	0.041
0.0071	3.886	44.0	66.19	2.76	1.017	0.042
0.0079	3.880	42.0	65.81	2.62	1.011	0.040
0.0087	3.879	42.0	65.75	2.62	1.011	0.040
0.0096	3.879	43.0	65.75	2.68	1.011	0.041
0.0105	3.880	39.0	65.81	2.43	1.011	0.037
0.0114	3.877	41.0	65.63	2.55	1.009	0.039
0.0124	3.878	42.0	65.69	2.62	1.010	0.040
0.0133	3.874	37.0	65.44	2.30	1.006	0.035
0.0143	3.877	40.0	65.63	2.49	1.009	0.038
0.0153	3.873	39.0	65.38	2.42	1.005	0.037
0.0163	3.870	41.0	65.19	2.54	1.002	0.039
0.0174	3.869	39.0	65.13	2.42	1.001	0.037
0.0184	3.867	38.0	65.01	2.35	0.999	0.036
0.0195	3.870	39.0	65.19	2.42	1.002	0.037
0.0205	3.868	38.0	65.07	2.35	1.000	0.036

TABLE C-20   GRID #3 DATA .30c

y/c (in)	HOTWIRE (volt)	RMS (mV)	VELOC (ft/s)	RMS-V (ft/s)	NORMALIZED VELOC	NORMALIZED RMS-V
0.0005	3.624	138.0	51.19	7.17	0.786	0.110
0.0006	3.641	132.0	52.08	6.95	0.800	0.107
0.0007	3.662	131.0	53.20	7.00	0.817	0.108
0.0009	3.688	132.0	54.60	7.19	0.838	0.110
0.0012	3.712	131.0	55.92	7.26	0.859	0.111
0.0015	3.745	128.0	57.77	7.27	0.887	0.112
0.0018	3.768	124.0	59.09	7.15	0.907	0.110
0.0022	3.789	112.0	60.31	6.56	0.926	0.101
0.0027	3.824	103.0	62.38	6.18	0.958	0.095
0.0032	3.848	99.0	63.84	6.04	0.980	0.093
0.0037	3.852	76.0	64.08	4.65	0.984	0.071
0.0043	3.863	73.0	64.76	4.50	0.994	0.069
0.0050	3.867	60.0	65.01	3.71	0.998	0.057
0.0056	3.881	49.0	65.88	3.06	1.011	0.047
0.0064	3.882	49.0	65.94	3.06	1.012	0.047
0.0071	3.884	45.0	66.06	2.82	1.014	0.043
0.0079	3.885	44.0	66.13	2.76	1.015	0.042
0.0087	3.890	42.0	66.44	2.64	1.020	0.041
0.0096	3.889	43.0	66.38	2.70	1.019	0.041
0.0105	3.890	43.0	66.44	2.70	1.020	0.041
0.0114	3.886	43.0	66.19	2.69	1.016	0.041
0.0124	3.884	41.0	66.06	2.57	1.014	0.039
0.0133	3.883	41.0	66.00	2.56	1.013	0.039
0.0143	3.880	42.0	65.81	2.62	1.011	0.040
0.0153	3.876	41.0	65.56	2.55	1.007	0.039
0.0163	3.877	39.0	65.63	2.43	1.008	0.037
0.0174	3.872	40.0	65.32	2.48	1.003	0.038
0.0184	3.874	38.0	65.44	2.36	1.005	0.036
0.0195	3.870	37.0	65.19	2.29	1.001	0.035
0.0205	3.869	39.0	65.13	2.42	1.000	0.037

TABLE C-21   GRID #3 DATA .35c

y/c (in)	HOTWIRE (volt)	RMS (mV)	VELOC (ft/s)	RMS-V (ft/s)	NORMALIZED VELOC	NORMALIZED RMS-V
========	========	========	=======	=======	========	========
0.0005	3.548	123.0	47.35	6.04	0.721	0.092
0.0006	3.557	126.0	47.80	6.23	0.728	0.095
0.0007	3.584	125.0	49.14	6.31	0.748	0.096
0.0009	3.611	123.0	50.52	6.33	0.769	0.096
0.0011	3.638	122.0	51.93	6.41	0.790	0.098
0.0013	3.649	116.0	52.51	6.14	0.799	0.093
0.0016	3.677	117.0	54.00	6.32	0.822	0.096
0.0019	3.693	122.0	54.87	6.67	0.835	0.102
0.0023	3.711	124.0	55.86	6.87	0.850	0.105
0.0027	3.742	118.0	57.60	6.68	0.877	0.102
0.0032	3.761	113.0	58.69	6.49	0.893	0.099
0.0037	3.788	109.0	60.25	6.38	0.917	0.097
0.0042	3.806	101.0	61.31	5.99	0.933	0.091
0.0048	3.823	95.0	62.32	5.70	0.949	0.087
0.0054	3.848	88.0	63.84	5.37	0.972	0.082
0.0061	3.861	75.0	64.64	4.62	0.984	0.070
0.0067	3.872	70.0	65.32	4.34	0.994	0.066
0.0075	3.891	61.0	66.50	3.84	1.012	0.058
0.0082	3.898	51.0	66.94	3.22	1.019	0.049
0.0090	3.904	49.0	67.32	3.11	1.025	0.047
0.0098	3.905	45.0	67.39	2.86	1.026	0.043
0.0106	3.899	43.0	67.01	2.72	1.020	0.041
0.0115	3.895	42.0	66.76	2.65	1.016	0.040
0.0123	3.893	42.0	66.63	2.64	1.014	0.040
0.0132	3.890	40.0	66.44	2.51	1.011	0.038
0.0142	3.893	40.0	66.63	2.52	1.014	0.038
0.0151	3.889	42.0	66.38	2.64	1.010	0.040
0.0160	3.887	43.0	66.25	2.70	1.009	0.041
0.0170	3.881	42.0	65.88	2.62	1.003	0.040
0.0180	3.888	39.0	66.31	2.45	1.010	0.037
0.0190	3.887	41.0	66.25	2.57	1.009	0.039
0.0200	3.888	41.0	66.31	2.57	1.010	0.039
0.0210	3.881	39.0	65.88	2.44	1.003	0.037
0.0220	3.880	38.0	65.81	2.37	1.002	0.036
0.0230	3.878	41.0	65.69	2.56	1.000	0.039

TABLE C-22   GRID #3 DATA .40c

y/c (in)	HOTWIRE (volt)	RMS (mV)	VELOC (ft/s)	RMS-V (ft/s)	NORMALIZED VELOC	RMS-V
======	======	=======	=====	=====	======	======
0.0005	3.597	118.0	49.80	6.01	0.733	0.088
0.0006	3.611	115.0	50.52	5.92	0.743	0.087
0.0007	3.612	117.0	50.57	6.03	0.744	0.089
0.0009	3.643	109.0	52.19	5.75	0.768	0.085
0.0011	3.647	112.0	52.40	5.92	0.771	0.087
0.0014	3.655	109.0	52.82	5.80	0.777	0.085
0.0017	3.688	110.0	54.60	5.99	0.803	0.088
0.0021	3.704	113.0	55.48	6.23	0.816	0.092
0.0025	3.731	113.0	56.98	6.35	0.838	0.093
0.0030	3.743	109.0	57.66	6.18	0.848	0.091
0.0035	3.776	106.0	59.55	6.15	0.876	0.091
0.0040	3.794	102.0	60.60	5.99	0.892	0.088
0.0046	3.811	99.0	61.61	5.89	0.907	0.087
0.0053	3.854	98.0	64.21	6.01	0.945	0.088
0.0060	3.857	88.0	64.39	5.41	0.947	0.080
0.0067	3.869	78.0	65.13	4.83	0.958	0.071
0.0074	3.889	69.0	66.38	4.33	0.977	0.064
0.0082	3.903	63.0	67.26	3.99	0.990	0.059
0.0091	3.918	56.0	68.22	3.59	1.004	0.053
0.0099	3.919	50.0	68.28	3.21	1.005	0.047
0.0108	3.922	48.0	68.47	3.08	1.008	0.045
0.0117	3.920	47.0	68.35	3.02	1.006	0.044
0.0127	3.921	42.0	68.41	2.70	1.007	0.040
0.0137	3.923	42.0	68.54	2.70	1.008	0.040
0.0147	3.924	42.0	68.60	2.70	1.009	0.040
0.0157	3.925	40.0	68.67	2.57	1.010	0.038
0.0167	3.923	41.0	68.54	2.64	1.008	0.039
0.0178	3.918	39.0	68.22	2.50	1.004	0.037
0.0188	3.926	39.0	68.73	2.51	1.011	0.037
0.0199	3.921	40.0	68.41	2.57	1.007	0.038
0.0210	3.919	42.0	68.28	2.69	1.005	0.040
0.0221	3.918	37.0	68.22	2.37	1.004	0.035
0.0233	3.917	36.0	68.15	2.30	1.003	0.034
0.0244	3.919	39.0	68.28	2.50	1.005	0.037
0.0255	3.914	39.0	67.96	2.49	1.000	0.037

TABLE C-23   GRID #3 DATA .45c

y/c (in)	HOTWIRE (volt)	RMS (mV)	VELOC (ft/s)	RMS-V (ft/s)	NORMALIZED VELOC	NORMALIZED RMS-V
======	======	=======	=====	=====	======	======
0.0005	3.622	113.0	51.09	5.86	0.731	0.084
0.0006	3.641	109.0	52.08	5.74	0.745	0.082
0.0007	3.657	110.0	52.93	5.86	0.757	0.084
0.0009	3.659	108.0	53.04	5.76	0.759	0.082
0.0011	3.682	106.0	54.27	5.75	0.776	0.082
0.0013	3.693	111.0	54.87	6.07	0.785	0.087
0.0016	3.704	108.0	55.48	5.95	0.794	0.085
0.0020	3.721	104.0	56.42	5.80	0.807	0.083
0.0024	3.741	107.0	57.54	6.06	0.823	0.087
0.0028	3.759	103.0	58.57	5.90	0.838	0.084
0.0033	3.771	104.0	59.26	6.01	0.848	0.086
0.0038	3.785	101.0	60.08	5.90	0.859	0.084
0.0043	3.811	99.0	61.61	5.89	0.881	0.084
0.0049	3.834	98.0	62.99	5.92	0.901	0.085
0.0056	3.869	92.0	65.13	5.70	0.932	0.082
0.0062	3.896	81.0	66.82	5.11	0.956	0.073
0.0069	3.905	79.0	67.39	5.02	0.964	0.072
0.0077	3.917	74.0	68.15	4.74	0.975	0.068
0.0085	3.920	71.0	68.35	4.55	0.978	0.065
0.0093	3.942	60.0	69.77	3.91	0.998	0.056
0.0101	3.949	55.0	70.23	3.60	1.005	0.051
0.0110	3.951	49.0	70.36	3.21	1.007	0.046
0.0119	3.955	47.0	70.62	3.09	1.010	0.044
0.0129	3.955	44.0	70.62	2.89	1.010	0.041
0.0138	3.960	40.0	70.95	2.64	1.015	0.038
0.0148	3.958	39.0	70.82	2.57	1.013	0.037
0.0158	3.956	39.0	70.68	2.56	1.011	0.037
0.0169	3.950	38.0	70.29	2.49	1.006	0.036
0.0179	3.957	39.0	70.75	2.57	1.012	0.037
0.0190	3.952	38.0	70.42	2.49	1.007	0.036
0.0201	3.955	38.0	70.62	2.50	1.010	0.036
0.0212	3.953	42.0	70.49	2.76	1.008	0.039
0.0224	3.947	41.0	70.09	2.68	1.003	0.038
0.0235	3.945	39.0	69.96	2.54	1.001	0.036
0.0246	3.951	38.0	70.36	2.49	1.007	0.036
0.0258	3.948	40.0	70.16	2.62	1.004	0.037
0.0270	3.943	39.0	69.83	2.54	0.999	0.036
0.0281	3.948	37.0	70.16	2.42	1.004	0.035
0.0293	3.944	39.0	69.90	2.54	1.000	0.036
0.0305	3.944	37.0	69.90	2.41	1.000	0.035

TABLE C-24   GRID #3 DATA .50c

y/c (in)	HOTWIRE (volt)	RMS (mV)	VELOC (ft/s)	RMS-V (ft/s)	NORMALIZED VELOC	RMS-V
0.0005	3.645	115.0	52.29	6.07	0.710	0.082
0.0006	3.663	111.0	53.25	5.94	0.723	0.081
0.0007	3.679	107.0	54.11	5.79	0.735	0.079
0.0009	3.688	110.0	54.60	5.99	0.742	0.081
0.0012	3.695	109.0	54.98	5.97	0.747	0.081
0.0015	3.717	108.0	56.20	6.01	0.763	0.082
0.0018	3.722	106.0	56.48	5.92	0.767	0.080
0.0022	3.743	109.0	57.66	6.18	0.783	0.084
0.0027	3.776	105.0	59.55	6.09	0.809	0.083
0.0032	3.788	101.0	60.25	5.91	0.818	0.080
0.0037	3.803	101.0	61.13	5.97	0.830	0.081
0.0043	3.837	98.0	63.17	5.94	0.858	0.081
0.0050	3.852	101.0	64.08	6.18	0.870	0.084
0.0057	3.878	97.0	65.69	6.05	0.892	0.082
0.0064	3.905	89.0	67.39	5.65	0.915	0.077
0.0072	3.929	86.0	68.92	5.55	0.936	0.075
0.0080	3.941	78.0	69.70	5.08	0.947	0.069
0.0089	3.950	68.0	70.29	4.45	0.955	0.060
0.0098	3.979	64.0	72.21	4.27	0.981	0.058
0.0108	3.981	59.0	72.34	3.94	0.983	0.054
0.0117	3.989	53.0	72.88	3.56	0.990	0.048
0.0128	3.995	46.0	73.28	3.10	0.995	0.042
0.0138	4.001	45.0	73.69	3.05	1.001	0.041
0.0149	4.009	41.0	74.23	2.79	1.008	0.038
0.0161	4.010	41.0	74.30	2.80	1.009	0.038
0.0172	4.090	42.0	79.90	3.02	1.085	0.041
0.0184	4.000	39.0	73.62	2.64	1.000	0.036
0.0196	4.001	41.0	73.69	2.78	1.001	0.038
0.0208	3.997	39.0	73.42	2.64	0.997	0.036
0.0221	4.003	37.0	73.82	2.51	1.003	0.034
0.0234	3.999	37.0	73.55	2.50	0.999	0.034
0.0247	3.998	38.0	73.49	2.57	0.998	0.035
0.0260	3.995	40.0	73.28	2.70	0.995	0.037
0.0273	3.994	38.0	73.22	2.56	0.994	0.035
0.0287	4.001	37.0	73.69	2.51	1.001	0.034
0.0300	3.998	38.0	73.49	2.57	0.998	0.035
0.0314	3.995	36.0	73.28	2.43	0.995	0.033
0.0328	3.997	37.0	73.42	2.50	0.997	0.034
0.0341	3.993	34.0	73.15	2.29	0.994	0.031
0.0355	4.000	39.0	73.62	2.64	1.000	0.036

TABLE C-25   GRID #3 DATA .55c

y/c (in)	HOTWIRE (volt)	RMS (mV)	VELOC (ft/s)	RMS-V (ft/s)	NORMALIZED VELOC	NORMALIZED RMS-V
======	======	=======	=====	=====	======	======
0.0005	3.656	117.0	52.88	6.23	0.699	0.082
0.0006	3.673	115.0	53.79	6.20	0.711	0.082
0.0007	3.676	113.0	53.95	6.10	0.714	0.081
0.0009	3.689	113.0	54.66	6.16	0.723	0.081
0.0012	3.704	110.0	55.48	6.06	0.734	0.080
0.0015	3.714	110.0	56.03	6.11	0.741	0.081
0.0018	3.728	112.0	56.81	6.28	0.751	0.083
0.0022	3.745	109.0	57.77	6.19	0.764	0.082
0.0027	3.768	108.0	59.09	6.23	0.782	0.082
0.0032	3.798	109.0	60.84	6.42	0.805	0.085
0.0037	3.818	107.0	62.03	6.40	0.820	0.085
0.0043	3.843	106.0	63.53	6.45	0.840	0.085
0.0050	3.878	102.0	65.69	6.36	0.869	0.084
0.0057	3.892	103.0	66.57	6.48	0.880	0.086
0.0064	3.909	94.0	67.64	5.98	0.895	0.079
0.0072	3.930	90.0	68.99	5.81	0.913	0.077
0.0080	3.942	88.0	69.77	5.73	0.923	0.076
0.0089	3.992	81.0	73.08	5.46	0.967	0.072
0.0098	4.002	76.0	73.76	5.15	0.976	0.068
0.0108	4.021	69.0	75.05	4.74	0.993	0.063
0.0117	4.027	59.0	75.47	4.07	0.998	0.054
0.0128	4.043	55.0	76.58	3.83	1.013	0.051
0.0138	4.040	50.0	76.37	3.48	1.010	0.046
0.0149	4.043	44.0	76.58	3.07	1.013	0.041
0.0161	4.049	43.0	77.00	3.01	1.018	0.040
0.0172	4.050	40.0	77.07	2.80	1.019	0.037
0.0184	4.049	40.0	77.00	2.80	1.018	0.037
0.0196	4.053	38.0	77.28	2.67	1.022	0.035
0.0208	4.052	36.0	77.21	2.52	1.021	0.033
0.0221	4.047	38.0	76.86	2.66	1.017	0.035
0.0234	4.045	33.0	76.72	2.30	1.015	0.030
0.0247	4.040	39.0	76.37	2.71	1.010	0.036
0.0260	4.042	36.0	76.51	2.51	1.012	0.033
0.0273	4.039	37.0	76.30	2.57	1.009	0.034
0.0287	4.037	38.0	76.16	2.64	1.007	0.035
0.0300	4.031	35.0	75.74	2.42	1.002	0.032
0.0314	4.036	36.0	76.09	2.50	1.006	0.033
0.0328	4.031	40.0	75.74	2.77	1.002	0.037
0.0341	4.027	37.0	75.47	2.55	0.998	0.034
0.0355	4.029	42.0	75.60	2.90	1.000	0.038

TABLE C-26   GRID #3 DATA .60c

y/c (in)	HOTWIRE (volt)	RMS (mV)	VELOC (ft/s)	RMS-V (ft/s)	NORMALIZED VELOC	RMS-V
======	======	=======	=====	=====	======	======
0.0005	3.695	117.0	54.98	6.41	0.670	0.078
0.0006	3.706	117.0	55.59	6.46	0.677	0.079
0.0007	3.713	115.0	55.98	6.38	0.682	0.078
0.0009	3.721	111.0	56.42	6.19	0.687	0.075
0.0011	3.732	111.0	57.04	6.24	0.695	0.076
0.0013	3.754	113.0	58.28	6.46	0.710	0.079
0.0016	3.773	109.0	59.38	6.31	0.723	0.077
0.0020	3.789	109.0	60.31	6.38	0.735	0.078
0.0024	3.812	111.0	61.67	6.61	0.751	0.080
0.0028	3.818	107.0	62.03	6.40	0.756	0.078
0.0033	3.834	108.0	62.99	6.53	0.767	0.080
0.0038	3.851	108.0	64.02	6.61	0.780	0.080
0.0043	3.887	106.0	66.25	6.65	0.807	0.081
0.0049	3.894	105.0	66.69	6.62	0.813	0.081
0.0056	3.905	102.0	67.39	6.48	0.821	0.079
0.0062	3.942	99.0	69.77	6.45	0.850	0.079
0.0069	3.977	98.0	72.08	6.53	0.878	0.080
0.0077	3.992	94.0	73.08	6.33	0.890	0.077
0.0085	4.018	91.0	74.85	6.24	0.912	0.076
0.0093	4.025	87.0	75.33	5.99	0.918	0.073
0.0101	4.051	82.0	77.14	5.74	0.940	0.070
0.0110	4.064	79.0	78.05	5.58	0.951	0.068
0.0119	4.069	71.0	78.40	5.03	0.955	0.061
0.0129	4.097	62.0	80.41	4.48	0.980	0.055
0.0138	4.101	59.0	80.70	4.27	0.983	0.052
0.0148	4.117	52.0	81.86	3.80	0.997	0.046
0.0158	4.118	47.0	81.94	3.44	0.998	0.042
0.0169	4.120	47.0	82.08	3.45	1.000	0.042
0.0179	4.123	42.0	82.30	3.08	1.003	0.038
0.0190	4.124	39.0	82.38	2.87	1.004	0.035
0.0201	4.124	39.0	82.38	2.87	1.004	0.035
0.0212	4.120	38.0	82.08	2.79	1.000	0.034
0.0224	4.126	34.0	82.52	2.50	1.005	0.030
0.0235	4.123	40.0	82.30	2.94	1.003	0.036
0.0246	4.119	35.0	82.01	2.56	0.999	0.031
0.0258	4.119	37.0	82.01	2.71	0.999	0.033
0.0270	4.121	36.0	82.16	2.64	1.001	0.032
0.0281	4.109	33.0	81.28	2.40	0.990	0.029
0.0293	4.113	35.0	81.57	2.55	0.994	0.031
0.0305	4.120	35.0	82.08	2.57	1.000	0.031

89

TABLE C-27   GRID #3 DATA .65c

y/c (in)	HOTWIRE (volt)	RMS (mV)	VELOC (ft/s)	RMS-V (ft/s)	NORMALIZED VELOC	NORMALIZED RMS-V
======	======	=======	=====	=====	======	======
0.0005	3.682	132.0	54.27	7.16	0.612	0.081
0.0006	3.718	127.0	56.25	7.07	0.634	0.080
0.0007	3.728	126.0	56.81	7.06	0.640	0.080
0.0009	3.741	118.0	57.54	6.68	0.649	0.075
0.0011	3.763	118.0	58.80	6.78	0.663	0.076
0.0013	3.795	116.0	60.66	6.82	0.684	0.077
0.0016	3.818	109.0	62.03	6.52	0.699	0.073
0.0020	3.825	110.0	62.45	6.61	0.704	0.074
0.0024	3.850	109.0	63.96	6.66	0.721	0.075
0.0028	3.861	110.0	64.64	6.78	0.729	0.076
0.0033	3.883	112.0	66.00	7.00	0.744	0.079
0.0038	3.905	114.0	67.39	7.24	0.760	0.082
0.0043	3.916	111.0	68.09	7.10	0.767	0.080
0.0049	3.949	115.0	70.23	7.52	0.792	0.085
0.0056	3.972	109.0	71.74	7.24	0.809	0.082
0.0062	3.993	109.0	73.15	7.35	0.824	0.083
0.0069	4.008	103.0	74.16	7.01	0.836	0.079
0.0077	4.041	101.0	76.44	7.03	0.862	0.079
0.0085	4.068	99.0	78.33	7.01	0.883	0.079
0.0093	4.088	95.0	79.76	6.82	0.899	0.077
0.0101	4.110	88.0	81.35	6.41	0.917	0.072
0.0110	4.137	82.0	83.34	6.08	0.939	0.069
0.0119	4.142	82.0	83.71	6.10	0.943	0.069
0.0129	4.161	79.0	85.13	5.95	0.960	0.067
0.0138	4.174	70.0	86.11	5.31	0.971	0.060
0.0148	4.182	60.0	86.72	4.58	0.977	0.052
0.0158	4.203	59.0	88.33	4.56	0.996	0.051
0.0169	4.203	51.0	88.33	3.94	0.996	0.044
0.0179	4.217	44.0	89.42	3.43	1.008	0.039
0.0190	4.219	46.0	89.58	3.59	1.010	0.041
0.0201	4.219	38.0	89.58	2.97	1.010	0.033
0.0212	4.215	38.0	89.27	2.96	1.006	0.033
0.0224	4.214	36.0	89.19	2.80	1.005	0.032
0.0235	4.212	34.0	89.03	2.64	1.004	0.030
0.0246	4.214	34.0	89.19	2.65	1.005	0.030
0.0258	4.212	34.0	89.03	2.64	1.004	0.030
0.0270	4.209	36.0	88.80	2.79	1.001	0.031
0.0281	4.208	35.0	88.72	2.72	1.000	0.031
0.0293	4.203	36.0	88.33	2.78	0.996	0.031
0.0305	4.208	34.0	88.72	2.64	1.000	0.030

TABLE C-28   GRID #4 DATA .30c

y/c (in)	HOTWIRE (volt)	RMS (mV)	VELOC (ft/s)	RMS-V (ft/s)	NORMALIZED VELOC	NORMALIZED RMS-V
0.0005	4.029	108.0	75.60	7.46	0.735	0.072
0.0006	4.068	103.0	78.33	7.30	0.761	0.071
0.0007	4.122	111.0	82.23	8.15	0.799	0.079
0.0009	4.152	101.0	84.45	7.56	0.821	0.073
0.0012	4.225	108.0	90.05	8.47	0.875	0.082
0.0015	4.288	104.0	95.09	8.49	0.924	0.082
0.0018	4.307	93.0	96.65	7.68	0.939	0.075
0.0022	4.338	88.0	99.23	7.41	0.964	0.072
0.0027	4.345	93.0	99.82	7.86	0.970	0.076
0.0032	4.361	80.0	101.18	6.83	0.983	0.066
0.0037	4.369	68.0	101.87	5.83	0.990	0.057
0.0043	4.377	60.0	102.56	5.17	0.997	0.050
0.0050	4.379	49.0	102.73	4.23	0.998	0.041
0.0056	4.375	37.7	102.39	0.00	0.995	0.000
0.0064	4.381	30.0	102.90	2.59	1.000	0.025
0.0071	4.384	30.0	103.16	2.60	1.003	0.025
0.0079	4.378	29.0	102.64	2.50	0.997	0.024
0.0087	4.378	27.0	102.64	2.33	0.997	0.023
0.0096	4.384	30.0	103.16	2.60	1.003	0.025
0.0105	4.379	26.0	102.73	2.24	0.998	0.022
0.0114	4.381	28.0	102.90	2.42	1.000	0.024
0.0124	4.376	23.0	102.47	1.98	0.996	0.019
0.0133	4.375	28.0	102.39	2.41	0.995	0.023
0.0143	4.379	30.0	102.73	2.59	0.998	0.025
0.0153	4.376	29.0	102.47	2.50	0.996	0.024
0.0163	4.380	26.0	102.82	2.25	0.999	0.022
0.0174	4.376	32.0	102.47	2.76	0.996	0.027
0.0184	4.378	29.0	102.64	2.50	0.997	0.024
0.0195	4.382	25.0	102.99	2.16	1.001	0.021
0.0205	4.381	27.0	102.90	2.33	1.000	0.023

TABLE C-29   GRID #4 DATA .35c

y/c (in)	HOTWIRE (volt)	RMS (mV)	VELOC (ft/s)	RMS-V (ft/s)	NORMALIZED VELOC	NORMALIZED RMS-V
0.0005	4.018	106.0	74.85	7.27	0.749	0.073
0.0006	4.044	103.0	76.65	7.18	0.767	0.072
0.0007	4.059	101.0	77.70	7.11	0.777	0.071
0.0009	4.088	103.0	79.76	7.39	0.798	0.074
0.0012	4.114	101.0	81.64	7.37	0.816	0.074
0.0015	4.126	99.0	82.52	7.29	0.825	0.073
0.0018	4.154	103.0	84.60	7.72	0.846	0.077
0.0022	4.193	105.0	87.56	8.07	0.876	0.081
0.0027	4.208	104.0	88.72	8.07	0.887	0.081
0.0032	4.235	98.0	90.83	7.73	0.908	0.077
0.0037	4.259	93.0	92.74	7.45	0.927	0.075
0.0043	4.276	83.0	94.11	6.72	0.941	0.067
0.0050	4.304	74.0	96.40	6.10	0.964	0.061
0.0056	4.318	67.0	97.56	5.57	0.976	0.056
0.0064	4.327	55.0	98.31	4.60	0.983	0.046
0.0071	4.329	49.0	98.48	4.10	0.985	0.041
0.0079	4.341	38.0	99.49	3.20	0.995	0.032
0.0087	4.352	33.0	100.42	2.80	1.004	0.028
0.0096	4.349	30.0	100.16	2.54	1.002	0.025
0.0105	4.350	28.0	100.25	2.37	1.003	0.024
0.0114	4.351	23.0	100.33	1.95	1.003	0.020
0.0124	4.353	22.0	100.50	1.87	1.005	0.019
0.0133	4.350	19.0	100.25	1.61	1.003	0.016
0.0143	4.348	19.0	100.08	1.61	1.001	0.016
0.0153	4.350	19.0	100.25	1.61	1.003	0.016
0.0163	4.348	20.0	100.08	1.69	1.001	0.017
0.0174	4.346	17.0	99.91	1.44	0.999	0.014
0.0184	4.350	17.0	100.25	1.44	1.003	0.014
0.0195	4.347	16.0	99.99	1.35	1.000	0.014
0.0205	4.347	15.0	99.99	1.27	1.000	0.013

TABLE C-30   GRID #4 DATA .40c

y/c (in)	HOTWIRE (volt)	RMS (mV)	VELOC (ft/s)	RMS-V (ft/s)	NORMALIZED VELOC	NORMALIZED RMS-V
======	======	=======	=====	=====	======	======
0.0005	3.959	102.0	70.88	6.72	0.727	0.069
0.0006	3.980	98.0	72.28	6.55	0.741	0.067
0.0008	4.008	96.0	74.16	6.54	0.760	0.067
0.0010	4.017	89.0	74.78	6.10	0.766	0.062
0.0013	4.058	92.0	77.63	6.48	0.796	0.066
0.0016	4.081	93.0	79.26	6.65	0.812	0.068
0.0020	4.107	90.0	81.13	6.54	0.832	0.067
0.0024	4.123	88.0	82.30	6.46	0.844	0.066
0.0029	4.148	90.0	84.15	6.72	0.863	0.069
0.0035	4.162	89.0	85.20	6.70	0.873	0.069
0.0041	4.189	86.0	87.26	6.59	0.894	0.068
0.0047	4.211	84.0	88.95	6.53	0.912	0.067
0.0055	4.227	80.0	90.20	6.28	0.925	0.064
0.0062	4.253	75.0	92.26	5.99	0.946	0.061
0.0070	4.272	68.0	93.79	5.49	0.961	0.056
0.0079	4.289	59.0	95.17	4.82	0.976	0.049
0.0088	4.299	48.0	95.99	3.94	0.984	0.040
0.0098	4.307	37.0	96.65	3.05	0.991	0.031
0.0108	4.318	33.0	97.56	2.74	1.000	0.028
0.0118	4.323	26.0	97.98	2.17	1.004	0.022
0.0129	4.323	21.0	97.98	1.75	1.004	0.018
0.0140	4.321	21.0	97.81	1.75	1.003	0.018
0.0151	4.325	19.0	98.14	1.59	1.006	0.016
0.0163	4.324	17.0	98.06	1.42	1.005	0.015
0.0175	4.320	15.0	97.73	1.25	1.002	0.013
0.0187	4.323	16.0	97.98	1.33	1.004	0.014
0.0200	4.321	14.0	97.81	1.17	1.003	0.012
0.0212	4.322	16.0	97.89	1.33	1.003	0.014
0.0225	4.319	14.0	97.64	1.16	1.001	0.012
0.0238	4.317	13.0	97.48	1.08	0.999	0.011
0.0251	4.316	12.0	97.39	1.00	0.998	0.010
0.0265	4.317	12.0	97.48	1.00	0.999	0.010
0.0278	4.317	12.0	97.48	1.00	0.999	0.010
0.0292	4.319	13.0	97.64	1.08	1.001	0.011
0.0305	4.318	13.0	97.56	1.08	1.000	0.011

TABLE C-31   GRID #4 DATA .45c

y/c (in)	HOTWIRE (volt)	RMS (mV)	VELOC (ft/s)	RMS-V (ft/s)	NORMALIZED VELOC	NORMALIZED RMS-V
0.0005	3.929	101.0	68.92	6.52	0.719	0.068
0.0006	3.952	99.0	70.42	6.49	0.735	0.068
0.0008	3.967	95.0	71.41	6.29	0.745	0.066
0.0010	3.988	94.0	72.81	6.31	0.760	0.066
0.0013	4.014	90.0	74.57	6.15	0.778	0.064
0.0016	4.046	89.0	76.79	6.21	0.801	0.065
0.0020	4.053	88.0	77.28	6.17	0.806	0.064
0.0024	4.072	89.0	78.62	6.32	0.820	0.066
0.0029	4.094	87.0	80.19	6.27	0.837	0.065
0.0035	4.129	86.0	82.74	6.34	0.863	0.066
0.0041	4.143	82.0	83.78	6.10	0.874	0.064
0.0047	4.163	82.0	85.28	6.18	0.890	0.064
0.0055	4.172	79.0	85.96	5.99	0.897	0.062
0.0062	4.211	77.0	88.95	5.98	0.928	0.062
0.0070	4.231	70.0	90.52	5.51	0.945	0.058
0.0079	4.248	62.0	91.87	4.93	0.959	0.051
0.0088	4.261	57.0	92.90	4.57	0.970	0.048
0.0098	4.269	51.0	93.55	4.11	0.976	0.043
0.0108	4.278	40.0	94.28	3.24	0.984	0.034
0.0118	4.289	33.0	95.17	2.69	0.993	0.028
0.0129	4.293	26.0	95.50	2.13	0.997	0.022
0.0140	4.294	23.0	95.58	1.88	0.997	0.020
0.0151	4.295	21.0	95.66	1.72	0.998	0.018
0.0163	4.298	18.0	95.91	1.48	1.001	0.015
0.0175	4.303	15.0	96.32	1.24	1.005	0.013
0.0187	4.305	14.0	96.48	1.15	1.007	0.012
0.0200	4.305	14.0	96.48	1.15	1.007	0.012
0.0212	4.303	15.0	96.32	1.24	1.005	0.013
0.0225	4.300	12.0	96.07	0.99	1.003	0.010
0.0238	4.301	12.0	96.15	0.99	1.003	0.010
0.0251	4.297	12.0	95.83	0.98	1.000	0.010
0.0265	4.293	11.0	95.50	0.90	0.997	0.009
0.0278	4.291	12.0	95.33	0.98	0.995	0.010
0.0292	4.300	11.0	96.07	0.90	1.003	0.009
0.0305	4.297	11.0	95.83	0.90	1.000	0.009

94

TABLE C-32   GRID #4 DATA .50c

y/c (in)	HOTWIRE (volt)	RMS (mV)	VELOC (ft/s)	RMS-V (ft/s)	NORMALIZED VELOC	NORMALIZED RMS-V
======	======	=======	=====	=====	======	======
0.0005	3.831	109.0	62.81	6.57	0.666	0.070
0.0006	3.852	105.0	64.08	6.43	0.680	0.068
0.0008	3.863	103.0	64.76	6.35	0.687	0.067
0.0010	3.897	99.0	66.88	6.25	0.709	0.066
0.0013	3.921	97.0	68.41	6.23	0.726	0.066
0.0016	3.939	93.0	69.57	6.04	0.738	0.064
0.0020	3.983	91.0	72.48	6.09	0.769	0.065
0.0024	4.002	90.0	73.76	6.10	0.782	0.065
0.0029	4.029	86.0	75.60	5.94	0.802	0.063
0.0035	4.043	88.0	76.58	6.13	0.812	0.065
0.0041	4.073	85.0	78.69	6.04	0.835	0.064
0.0047	4.108	82.0	81.21	5.96	0.861	0.063
0.0055	4.117	79.0	81.86	5.78	0.868	0.061
0.0062	4.131	79.0	82.89	5.83	0.879	0.062
0.0070	4.172	75.0	85.96	5.69	0.912	0.060
0.0079	4.193	72.0	87.56	5.53	0.929	0.059
0.0088	4.215	68.0	89.27	5.30	0.947	0.056
0.0098	4.225	61.0	90.05	4.78	0.955	0.051
0.0108	4.238	57.0	91.07	4.51	0.966	0.048
0.0118	4.247	45.0	91.79	3.58	0.974	0.038
0.0129	4.255	40.0	92.42	3.20	0.980	0.034
0.0140	4.266	31.0	93.31	2.49	0.990	0.026
0.0151	4.273	26.0	93.87	2.10	0.996	0.022
0.0163	4.279	23.0	94.36	1.87	1.001	0.020
0.0175	4.279	20.0	94.36	1.62	1.001	0.017
0.0187	4.282	17.0	94.60	1.38	1.003	0.015
0.0200	4.281	14.0	94.52	1.14	1.003	0.012
0.0212	4.280	13.0	94.44	1.06	1.002	0.011
0.0225	4.279	13.0	94.36	1.05	1.001	0.011
0.0238	4.272	11.0	93.79	0.89	0.995	0.009
0.0251	4.280	10.0	94.44	0.81	1.002	0.009
0.0265	4.274	11.0	93.95	0.89	0.997	0.009
0.0278	4.271	10.0	93.71	0.81	0.994	0.009
0.0292	4.278	9.0	94.28	0.73	1.000	0.008
0.0305	4.278	10.0	94.28	0.81	1.000	0.009

TABLE C-33   GRID #4 DATA .55c

y/c (in)	HOTWIRE (volt)	RMS (mV)	VELOC (ft/s)	RMS-V (ft/s)	NORMALIZED VELOC	RMS-V
0.0005	3.756	113.0	58.40	6.46	0.632	0.070
0.0006	3.785	110.0	60.08	6.42	0.650	0.070
0.0008	3.821	103.0	62.21	6.17	0.673	0.067
0.0010	3.839	103.0	63.29	6.25	0.685	0.068
0.0013	3.887	103.0	66.25	6.46	0.717	0.070
0.0016	3.889	100.0	66.38	6.28	0.718	0.068
0.0020	3.923	99.0	68.54	6.36	0.742	0.069
0.0024	3.935	96.0	69.31	6.22	0.750	0.067
0.0029	3.969	94.0	71.54	6.23	0.774	0.067
0.0035	3.992	91.0	73.08	6.13	0.791	0.066
0.0041	3.998	92.0	73.49	6.22	0.795	0.067
0.0047	4.027	88.0	75.47	6.07	0.817	0.066
0.0055	4.048	84.0	76.93	5.87	0.832	0.064
0.0062	4.091	79.0	79.98	5.68	0.865	0.061
0.0070	4.115	77.0	81.72	5.63	0.884	0.061
0.0079	4.139	71.0	83.48	5.27	0.903	0.057
0.0088	4.153	67.0	84.53	5.02	0.915	0.054
0.0098	4.180	70.0	86.57	5.33	0.937	0.058
0.0108	4.198	61.0	87.95	4.70	0.952	0.051
0.0118	4.203	56.0	88.33	4.33	0.956	0.047
0.0129	4.227	46.0	90.20	3.61	0.976	0.039
0.0140	4.237	41.0	90.99	3.24	0.985	0.035
0.0151	4.248	34.0	91.87	2.71	0.994	0.029
0.0163	4.245	30.0	91.63	2.38	0.991	0.026
0.0175	4.251	25.0	92.10	1.99	0.997	0.022
0.0187	4.253	20.0	92.26	1.60	0.998	0.017
0.0200	4.256	18.0	92.50	1.44	1.001	0.016
0.0212	4.258	15.0	92.66	1.20	1.003	0.013
0.0225	4.260	12.0	92.82	0.96	1.004	0.010
0.0238	4.252	11.0	92.18	0.88	0.997	0.009
0.0251	4.257	11.0	92.58	0.88	1.002	0.010
0.0265	4.258	12.0	92.66	0.96	1.003	0.010
0.0278	4.255	10.0	92.42	0.80	1.000	0.009
0.0292	4.257	10.0	92.58	0.80	1.002	0.009
0.0305	4.255	10.0	92.42	0.80	1.000	0.009

TABLE C-34   GRID #4 DATA .60c

y/c (in)	HOTWIRE (volt)	RMS (mV)	VELOC (ft/s)	RMS-V (ft/s)	NORMALIZED VELOC	NORMALIZED RMS-V
0.0005	3.729	118.0	56.87	6.62	0.622	0.072
0.0006	3.763	113.0	58.80	6.50	0.643	0.071
0.0007	3.783	114.0	59.96	6.65	0.656	0.073
0.0009	3.794	109.0	60.60	6.41	0.663	0.070
0.0011	3.806	109.0	61.31	6.46	0.670	0.071
0.0013	3.817	105.0	61.97	6.27	0.677	0.069
0.0016	3.833	102.0	62.93	6.16	0.688	0.067
0.0020	3.851	99.0	64.02	6.06	0.700	0.066
0.0024	3.888	101.0	66.31	6.34	0.725	0.069
0.0028	3.917	99.0	68.15	6.34	0.745	0.069
0.0033	3.920	99.0	68.35	0.00	0.747	0.000
0.0038	3.935	99.0	69.31	6.42	0.758	0.070
0.0043	3.962	96.0	71.08	6.34	0.777	0.069
0.0049	4.001	98.0	73.69	6.64	0.806	0.073
0.0056	4.014	92.0	74.57	6.29	0.815	0.069
0.0062	4.029	92.0	75.60	6.35	0.827	0.069
0.0069	4.049	89.0	77.00	6.23	0.842	0.068
0.0077	4.063	84.0	77.98	5.93	0.853	0.065
0.0085	4.103	78.0	80.84	5.65	0.884	0.062
0.0093	4.123	76.0	82.30	5.58	0.900	0.061
0.0101	4.145	73.0	83.93	5.44	0.918	0.059
0.0110	4.157	71.0	84.83	5.33	0.927	0.058
0.0119	4.189	59.0	87.26	4.52	0.954	0.049
0.0129	4.193	60.0	87.56	4.61	0.957	0.050
0.0138	4.200	51.0	88.10	3.94	0.963	0.043
0.0148	4.212	43.0	89.03	3.34	0.973	0.037
0.0158	4.221	37.0	89.73	2.89	0.981	0.032
0.0169	4.228	31.0	90.28	2.44	0.987	0.027
0.0179	4.231	26.0	90.52	2.05	0.990	0.022
0.0190	4.238	25.0	91.07	1.98	0.996	0.022
0.0201	4.241	20.0	91.31	1.58	0.998	0.017
0.0212	4.242	18.0	91.39	1.43	0.999	0.016
0.0224	4.243	15.0	91.47	1.19	1.000	0.013
0.0235	4.239	13.0	91.15	1.03	0.997	0.011
0.0246	4.239	12.0	91.15	0.95	0.997	0.010
0.0258	4.240	12.0	91.23	0.95	0.997	0.010
0.0270	4.239	12.0	91.15	0.95	0.997	0.010
0.0281	4.240	10.0	91.23	0.79	0.997	0.009
0.0293	4.242	11.0	91.39	0.87	0.999	0.010
0.0305	4.243	11.0	91.47	0.87	1.000	0.010

TABLE C-35   GRID #4 DATA .65c

y/c (in)	HOTWIRE (volt)	RMS (mV)	VELOC (ft/s)	RMS-V (ft/s)	NORMALIZED VELOC	NORMALIZED RMS-V
0.0005	3.685	123.0	54.44	6.69	0.601	0.074
0.0006	3.723	115.0	56.53	6.43	0.625	0.071
0.0008	3.766	111.0	58.97	6.40	0.651	0.071
0.0010	3.769	112.0	59.15	6.47	0.653	0.071
0.0013	3.798	108.0	60.84	6.37	0.672	0.070
0.0016	3.814	104.0	61.79	6.20	0.683	0.068
0.0020	3.827	104.0	62.57	6.26	0.691	0.069
0.0024	3.849	102.0	63.90	6.23	0.706	0.069
0.0029	3.865	104.0	64.88	6.42	0.717	0.071
0.0035	3.889	103.0	66.38	6.47	0.733	0.071
0.0041	3.918	105.0	68.22	6.73	0.754	0.074
0.0047	3.932	101.0	69.12	6.53	0.764	0.072
0.0055	3.964	98.0	71.21	6.48	0.787	0.072
0.0062	3.992	95.0	73.08	6.40	0.807	0.071
0.0070	4.012	93.0	74.44	6.35	0.822	0.070
0.0079	4.047	91.0	76.86	6.36	0.849	0.070
0.0088	4.055	87.0	77.42	6.11	0.855	0.068
0.0098	4.097	79.0	80.41	5.70	0.888	0.063
0.0108	4.129	74.0	82.74	5.46	0.914	0.060
0.0118	4.139	74.0	83.48	5.49	0.922	0.061
0.0129	4.164	64.0	85.35	4.83	0.943	0.053
0.0140	4.188	57.0	87.18	4.37	0.963	0.048
0.0151	4.191	52.0	87.41	3.99	0.966	0.044
0.0163	4.202	44.0	88.26	3.40	0.975	0.038
0.0175	4.218	40.0	89.50	3.12	0.989	0.034
0.0187	4.221	31.0	89.73	2.42	0.991	0.027
0.0200	4.226	28.0	90.13	2.20	0.996	0.024
0.0212	4.231	23.0	90.52	1.81	1.000	0.020
0.0225	4.233	19.0	90.68	1.50	1.002	0.017
0.0238	4.238	17.0	91.07	1.34	1.006	0.015
0.0251	4.239	15.0	91.15	1.19	1.007	0.013
0.0265	4.238	14.0	91.07	1.11	1.006	0.012
0.0278	4.231	12.0	90.52	0.94	1.000	0.010
0.0292	4.233	11.0	90.68	0.87	1.002	0.010
0.0305	4.231	12.0	90.52	0.94	1.000	0.010

APPENDIX D   PROGRAM TRAVERSE

```
1000 REM ************* PROGRAM TRAVERSE ******************
1010 REM
1020 REM    OPEN THE COM PORT AND INITIALIZE THE MOTOR SETTINGS
1030 OPEN "com1:1200,n,8,1,rs,cs,ds,cd" AS #1
1040 REM SET MOTOR DEFAULT VALUES
1050 DATA 1000,1000,1000,2,2,2,0.000125,0.000125,0.000125
1060 READ V1,V2,V3,R1,R2,R3,C1,C2,C3
1070 DIM Z(100),Z1(100),HWV(100),RMS(100),VEL(100),NDVEL(100),VRMS(100)
1080 PI=3.141592654#
1090 REM DEFINE CHARACTERS FOR DATA REDUCTION ALGORITHM
1100 RN2$="RENAME A:MOTOR.DAT "
1110 RN3$="RENAME A:CALCDAT.DAT "
1120 EX$=".DAT"
1130 ID2$="RAW"
1140 ID3$="CAL"
1150 PRINT
1160 PRINT "*********************************************"
1170 PRINT "** USER MUST SELECT 'CAPS LOCK' FUNCTION **"
1180 PRINT "*********************************************"
1190 REM          DISPLAY MOTOR DEFAULT SETTINGS
1200 PRINT "      ***********************************"
1210 PRINT "         INITIALIZED VALUES FOR ALL MOTOR SETTINGS:"
1220 PRINT "            VELOCITY = 1000 STEPS/SEC"
1230 PRINT "         RAMP(MOTOR ACCELERATION) = 2   (6000 STEPS/SEC^2)"
1240 PRINT "            DEFAULT INCREMENTAL UNITS ARE INCHES"
1250 PRINT "      ***********************************"
1260 PRINT
1270 PRINT "DO YOU WANT TO INPUT YOUR OWN INCREMENT EACH TIME OR
          HAVE THE"
1280 PRINT "COMPUTER COMPUTE MOVEMENTS THROUGH A BOUNDARY
          LAYER FOR YOU ?"
1290 PRINT
1300 PRINT "        ********** NOTE *************"
1310 PRINT "FOR COMPUTED BOUNDARY LAYER MOVEMENT, YOU MUST
          KNOW:"
1320 PRINT "     1. WHICH MOTOR WILL MOVE THE APPROPRIATE
          DIRECTION."
1330 PRINT "     2. HOW THICK (IN INCHES) IS THE B.L.
1340 PRINT "     3. HOW MANY DATA COLLECTION POINTS DO YOU WANT
          IN THE B.L."
1350 PRINT "      ***************************"
1360 PRINT
1370 PRINT "NOTE!! USE MANUAL CONTROL TO INITIALIZE PROBE
          POSITION BEFORE"
1380 PRINT "        SELECTING COMPUTER CONTROLLED MOVEMENT.     "
1390 PRINT
1400 INPUT "MANUAL CONTROL OR COMPUTER CONTROL (ENTER 'MAN' or
    'CP')";CON$
1410 IF CON$="CP" THEN 3200
1420 REM  OPTION TO CHANGE DEFAULT SETTINGS OF VELOCITY OR
          ACCELERATION RAMP
1430 PRINT
```

```
1440 PRINT
1450 PRINT " DO YOU WANT TO CHANGE THE VELOCITY OR
         ACCELERATION RAMP"
1460 PRINT "         DEFAULT SETTINGS? (Y or N)"
1470 PRINT
1480 PRINT "IF 'NO', THIS PROGRAM WILL THEN LET YOU DEFINE THE"
1490 PRINT "DISTANCE YOU WANT TO MOVE (IN INCHES). IF 'YES',"
1500 PRINT "YOU CAN CHANGE ANY OR ALL OF THE DEFAULT SETTINGS
         FOR ANY MOTOR."
1510 PRINT
1520 PRINT
1530 PRINT
1540 INPUT "DO YOU WANT TO CHANGE ANY OF THE DEFAULT
         SETTINGS? (Y or N)";D$
1550 IF D$="Y" THEN 1590
1560 IF D$="N" THEN 2220
1570 REM
1580 REM    **** OPERATOR SELECTED MOTOR VARIABLES *****
1590 PRINT
1600 PRINT
1610 INPUT "WHICH DEFAULT VALUE? (ENTER '1'FOR VELOC OR '2' FOR
         ACCEL RAMP)";L
1620 ON L GOTO 1690,1930
1630 PRINT "DO YOU WANT TO CHANGE THE DEFAULT VELOCITY? (Y OR
         N)"
1640 INPUT V$
1650 IF V$="Y" THEN 1690
1660 PRINT "DO YOU WANT TO CHANGE THE DEFAULT ACCELERATION
         RAMP? (Y or N)"
1670 IF R$="Y" THEN 1990
1680 IF R$="N" THEN 1450
1690 PRINT
1700 PRINT
1710 INPUT "WHICH MOTOR VELOCITY DO YOU WISH TO CHANGE? (1,2, or
         3)";J
1720 ON J GOTO 1730,1830,1880
1730 PRINT
1740 PRINT
1750 INPUT "ENTER DESIRED VELOCITY OF MOTOR #1";V1
   ?0 PRINT
1770 PRINT
1780 PRINT
1790 PRINT "DO YOU WANT TO CHANGE VELOCITY OF ANOTHER MOTOR?
         (Y OR N)"
1800 INPUT V$
1810 IF V$="Y" THEN 1690
1820 IF V$="N" THEN 1430
1830 PRINT
1840 PRINT
1850 INPUT "ENTER DESIRED VELOCITY OF MOTOR 2";V2
1860 PRINT
1870 GOTO 1780
1880 PRINT
1890 PRINT
1900 INPUT "ENTER DESIRED VELOCITY OF MOTOR #3";V3
1910 PRINT
1920 GOTO 1780
1930 PRINT
```

```
1940 PRINT
1950 INPUT "WHICH MOTOR ACCEL RAMP DO YOU WANT TO CHANGE? (1,
        2, or 3)";K
1960 ON K GOTO 1970,2060,2120
1970 PRINT
1980 PRINT
1990 INPUT "ENTER DESIRED ACCELERATION RAMP OF MOTOR #1";R1
2000 PRINT
2010 PRINT
2020 PRINT "DO YOU WANT TO CHANGE THE ACCEL RAMP OF ANOTHER
        MOTOR? (Y or N)?"
2030 INPUT RM$
2040 IF RM$="Y" THEN 1930
2050 IF RM$="N" THEN 1450
2060 PRINT
2070 PRINT
2080 INPUT "ENTER DESIRED ACCELERATION RAMP OF MOTOR #2";R2
2090 PRINT
2100 PRINT
2110 GOTO 2000
2120 PRINT
2130 PRINT
2140 INPUT "ENTER DESIRED ACCELERATION RAMP OF MOTOR #3";R3
2150 PRINT
2160 PRINT
2170 GOTO 2000
2180 REM
2190 REM DEFINE DISTANCE TO MOVE MOTOR
2200 PRINT
2210 PRINT
2220 PRINT
2230 REM INITIALIZE MOTOR INCREMENTS TO ZERO
2240 I1=0
2250 I2=0
2260 I3=0
2270 PRINT
2280 PRINT " ***************************************************************"
2290 PRINT " **      DEFINE WHICH MOTOR YOU WANT TO MOVE       **"
2300 PRINT " **                                               **"
2310 PRINT " **      NOTE!!!  A POSITIVE ('+') INCREMENT TO A MOTOR   **"
2320 PRINT " ** MOVES TRAVERSER AWAY FROM THAT PARTICULAR
        MOTOR
2330 PRINT " **                                               **"
2340 PRINT " **  -- MOTOR #1 MOVES THE PROBE UPSTREAM AGAINST
        THE FLOW **"
2350 PRINT " **  -- MOTOR #2 MOVES THE PROBE TOWARD THE ACCESS
        WINDOW   **"
2360 PRINT " **  -- MOTOR #3 MOVES THE PROBE VERTICALLY
        DOWNWARD       **"
2370 PRINT " ***************************************************************"
2380 PRINT
2390 PRINT
2400 INPUT "WHICH MOTOR DO YOU WANT TO MOVE? (1,2, or 3)";L
2410 ON L GOTO 2420,2530,2600
2420 PRINT
2430 PRINT
2440 PRINT "HOW FAR DO YOU WANT TO MOVE MOTOR #1?"
2450 PRINT " ********* (ENTER DISTANCE IN INCHES) *********"
```

```
2460 INPUT I1
2470 PRINT
2480 PRINT
2490 PRINT "DO YOU WANT TO MOVE ANOTHER MOTOR ALSO? (Y or N)?"
2500 INPUT C$
2510 IF C$="Y" THEN 2370
2520 IF C$="N" THEN 2670
2530 PRINT
2540 PRINT
2550 PRINT "HOW FAR DO YOU WANT TO MOVE MOTOR #2?"
2560 PRINT " ********* (ENTER DISTANCE IN INCHES) *********"
2570 INPUT I2
2580 PRINT
2590 GOTO 2480
2600 PRINT
2610 PRINT
2620 PRINT "HOW FAR DO YOU WANT TO MOVE MOTOR #3?"
2630 PRINT " ********* (ENTER DISTANCE IN INCHES) *********"
2640 INPUT I3
2650 PRINT
2660 GOTO 2470
2670 PRINT
2680 PRINT
2690 REM DISPLAY OPERATOR SELECTED MOTOR VARIABLES
2700 PRINT" ********************************"
2710 PRINT
2720 PRINT "SUMMARY OF OPERATOR INPUTS:"
2730 PRINT "          MOTOR #1   VELOCITY = ";V1
2740 PRINT "                     ACCELERATION RAMP = ";R1
2750 PRINT "                     INCREMENTAL DISTANCE = ";I1;"INCHES"
2760 PRINT "          MOTOR #2   VELOCITY = ";V2
2770 PRINT "                     ACCELERATION RAMP = ";R2
2780 PRINT "                     INCREMENTAL DISTANCE = ";I2;"INCHES"
2790 PRINT "          MOTOR #3   VELOCITY = ";V3
2800 PRINT "                     ACCELERATION RAMP = ";R3
2810 PRINT "                     INCREMENTAL DISTANCE = ";I3;"INCHES"
2820 PRINT
2830 PRINT" ********************************"
2840 PRINT
2850 PRINT
2860 PRINT "DO YOU WANT TO CHANGE ANY OF THESE VALUES? (Y or N)" 2870
PRINT
2880 PRINT "ENTER 'N' TO START MOTOR MOVEMENT.  ENTER 'Y' TO
          RETURN"
2890 PRINT "TO VARIABLE SELECTION SUBROUTINE."
2900 INPUT V$
2910 IF V$="Y" THEN 1430
2920 GOSUB 3130
2930 PRINT
2940 PRINT
2950 INPUT "DO YOU WANT TO INPUT ANOTHER MANUAL MOTOR
      MOVEMENT (Y or N)";M$
2960 IF M$="Y" THEN 2210
2970 PRINT
2980 PRINT "DO YOU WANT TO INPUT COMPUTER CONTROLLED MOTOR
      MOVEMENT?"
2990 PRINT "       ********* NOTE!!! ********* "
```

```
3000 PRINT " ALL PREVIOUS MOTOR INCREMENT INPUTS HAVE BEEN
         ZEROIZED."
3010 PRINT "PROGAM WILL LET YOU CHOOSE MANUAL OR
         CP-CONTROLLED B.L. MOVEMENT."
3020 PRINT "***** (IF 'NO', THE PROGRAM WILL END). *****"
3030 PRINT
3040 INPUT "DO YOU WANT COMPUTER CONTROLLED MOTOR MOVEMENT
         (Y or N)";N$
3050 IF N$="Y" THEN 1290
3060 PRINT
3070 PRINT
3080 PRINT
3090 PRINT "   ******************************"
3100 PRINT "       THE PROGRAM HAS ENDED."
3110 PRINT "   ******************************"
3120 END
3130 REM   ******* MOTOR MOVEMENT SUBROUTINE *********
3140 PRINT #1, "&"   :PRINT #1, "E";"C1=";C1;":C2=";C2;":C3=";C3
3150 PRINT #1, "I1=";I1;":V1=";V1;":R1=";R1;
3160 PRINT #1, ":I2=";I2;":V2=";V2;":R2=";R2
3170 PRINT #1, "I3=";I3;":V3=";V3;":R3=";R3;":@"
3180 RETURN
3190 REM   ********************************************
3200 PRINT
3210 REM ******* COMPUTER CONTROLLED BOUNDARY LAYER
         MOVEMENT *******
3220 PRINT
3230 PRINT "BOUNDARY LAYER AND HOTWIRE DATA WILL BE WRITTEN
         TO TWO SEPARATE"
3240 PRINT " FILES ON DRIVE 'A' NAMED   '***RAW.DAT' AND '***CAL.DAT'" 3250
PRINT
3260 PRINT "YOU WILL BE ASKED TO INPUT FILE NAMES FOR THESE."
3270 PRINT
3280 INPUT "IS A FORMATTED DISK IN DRIVE 'A'?  PRESS 'ENTER' TO
         CONTINUE";D$
3290 PRINT
3300 INPUT "ENTER 'RAW' DATA FILE NAME (5 CHARACTERS MAX -- NO
         EXTENSION)";F2$
3310 PRINT
3320 INPUT "ENTER 'REDUCED' DATA FILE NAME (5 CHAR MAX - NO
         EXTENSION)";F3$
3330 PRINT
3340 PRINT
3350 FI2$=(F2$+ID2$+EX$)
3360 FI3$=(F3$+ID3$+EX$)
3370 PRINT "THE 'RAW' DATA FILE FOR THIS RUN WILL BE  ";FI2$
3380 PRINT
3390 PRINT "THE 'CALCULATED' (REDUCED) DATA FILE WILL BE ";FI3$
3400 PRINT
3410 PRINT
3420 PRINT "   ***********************************************"
3430 PRINT "   **            NOTE !!!            **"
3440 PRINT "   ** COMPUTER CONTROLLED BOUNDARY LAYER **"
3450 PRINT "   **   MOVEMENT IS PROGRAMMED WITH A    **"
3460 PRINT "   ** DEFAULTED NEGATIVE MOTOR INCREMENT **"
3470 PRINT "   **  (i.e. MOTOR #3 WILL MOVE UPWARD   **"
3480 PRINT "   **  BY ENTERING A (+) B.L. DISTANCE). **"
3490 PRINT "   ***********************************************"
```

```
3500 PRINT
3510 REM SET INITIAL BL HEIGHT AND NUMBER OF DATA POINTS TO 0
3520 N=0
3530 BL=0
3540 PRINT
3550 INPUT "ENTER ESTIMATED INITIAL POINT DISTANCE ABOVE
         SURFACE (INCHES)";ZIP
3560 PRINT
3570 INPUT "WHAT IS THE B.L. THICKNESS (IN INCHES) THAT YOU WANT
         TO MEASURE";BL
3580 PRINT
3590 INPUT "HOW MANY DATA POINTS DO YOU WANT TO SAMPLE IN THE
         B.L.";N
3600 PRINT
3610 INPUT "WHICH MOTOR WILL MOVE YOU THROUGH THE B.L. (1,2, or
         3)";MN
3620 ON MN GOTO 3630,4280,4920
3630 PRINT
3640 PRINT
3650 REM  MOTOR 1 CP-CONTROLLED MOTOR MOVEMENT
3660 Z(1)=0
3670 I1=0
3680 I2=0
3690 I3=0
3700 FOR J=1 TO N
3710 IF J=1 THEN 3750
3720 Z(J)=BL*(1-(SIN((PI/2)*(1+(J/N)))))
3730 Z1(J)=Z(J)-Z(J-1)
3740 I1 = -Z1(J)
3750 PRINT
3760 PRINT
3770 PRINT
3780 PRINT "   ************************"
3790 PRINT
3800 PRINT "   DATA POINT ";J
3810 PRINT
3820 GOSUB 3130
3830 PRINT
3840 INPUT "ENTER HOTWIRE VOLTAGE";HWV(J)
3850 PRINT
3860 INPUT "ENTER RMS VOLTAGE";RMS(J)
3870 PRINT
3880 IF J=N THEN 3910
3890 INPUT "PRESS 'ENTER' FOR NEXT MOVEMENT";MOVE$
3900 NEXT J
3910 PRINT "ALL MOVEMENTS COMPLETE"
3920 OPEN "A:\MOTOR.DAT" FOR OUTPUT AS #2
3930 REM OPEN 'RAW' DATA FILE
3940 PRINT #2,"BL DISTANCE","HW VOLTS"","RMS VOLTS""
3950 DF2$=RN2$+FI2$
3960 FOR J=1 TO N
3970 PRINT #2, Z(J)+ZIP,HWV(J),RMS(J)
3980 NEXT J
3990 CLOSE #2
4000 REM RENAME 'RAW' DATA FILE
4010 SHELL DF2$
4020 REM OPEN 'CALCULATED' DATA FILE
4030 OPEN "A:\CALCDAT.DAT" FOR OUTPUT AS #3
```

```
4040 PRINT #3, "NORM DIST","UMEAN","URMS","N/D VEL","N/D RMS"
4050 DF3$=RN3$+F13$
4060 FOR J=1 TO N
4070 REM **** USE CALIBRATION CURVE EQUATION *********
4080 VEL(J) = 1.316021*(HWV(J)^3.14759)
4090 REM **** USE CALIBRATE CURVE SLOPE *****
4100 VRMS(J) = 4.1423*(HWV(J)^2.14659)*RMS(J)
4110 NEXT J
4120 FOR J=1 TO N
4130 PRINT #3, (Z(J)+ZIP)/10,VEL(J),VRMS(J),VEL(J)/VEL(N),VRMS(J)/VEL(N)
4140 NEXT J
4150 CLOSE #3
4160 REM RENAME 'REDUCED' DATA FILE
4170 SHELL DF3$
4180 PRINT
4190 PRINT
4200 PRINT "YOU WANT TO REPOSITION TRAVERSER FOR ANOTHER
        MOVEMENT (Y OR N)?"
4210 PRINT
4220 PRINT "IF 'Y', THE PROGRAM WILL TAKE YOU TO MANUAL CONTROL
        SUBROUTINE."
4230 PRINT "IF 'N', THE PROGRAM WILL END."
4240 PRINT
4250 INPUT "ANOTHER MOVEMENT";R$
4260 IF R$ = "Y" THEN 1360
4270 IF R$ = "N" THEN 3060
4280 PRINT
4290 PRINT
4300 REM CP-CONTROLLED MOTOR MOVEMENT FOR MOTOR 2
4310 Z(1)=0
4320 I1=0
4330 I2=0
4340 I3=0
4350 FOR J=1 TO N
4360 IF J=1 THEN 4400
4370 Z(J)=BL*(1-(SIN((PI/2)*(1+(J/N)))))
4380 Z1(J)=Z(J)-Z(J-1)
4390 I2 = -Z1(J)
4400 PRINT
4410 PRINT
4420 PRINT
4430 PRINT "    ***********************"
4440 PRINT
4450 PRINT "   DATA POINT ";J
4460 PRINT
4470 GOSUB 3130
4480 PRINT
4490 INPUT "ENTER HOTWIRE VOLTAGE";HWV(J)
4500 PRINT
4510 INPUT "ENTER RMS VOLTAGE";RMS(J)
4520 PRINT
4530 IF J=N THEN 4560
4540 INPUT "PRESS ENTER FOR NEXT MOVEMENT";MOVE$
4550 NEXT J
4560 PRINT "ALL MOVEMENTS COMPLETED"
4570 REM OPEN 'RAW' DATA FILE
4580 OPEN "A:\MOTOR.DAT" FOR OUTPUT AS #2
4590 PRINT #2,"BL DISTANCE","HW VOLTS","RMS VOLTS"
```

```
4600 DF2$=RN2$+FI2$
4610 FOR J=1 TO N
4620 PRINT #2, Z(J)+ZIP,HWV(J),RMS(J)
4630 NEXT J
4640 CLOSE #2
4650 REM RENAME 'RAW' DATA FILE
4660 SHELL DF2$
4670 REM OPEN 'REDUCED' DATA FILE
4680 OPEN "A:\CALCDAT.DAT" FOR OUTPUT AS #3
4690 PRINT #3, "NORM DIST","UMEAN","URMS","N/D VEL","N/D RMS"
4700 DF3$=RN3$+FI3$
4710 FOR J=1 TO N
4720 REM **** USE CALIBRATION CURVE EQUATION *********
4730 VEL(J) = 1.316021*(HWV(J)^3.14759)
4740 VRMS(J) = 4.1423*(HWV(J)^2.14659)*RMS(J)
4750 NEXT J
4760 FOR J=1 TO N
4770 PRINT #3, (Z(J)+ZIP)/10,VEL(J),VRMS(J),VEL(J)/VEL(N),VRMS(J)/VEL(N)
4780 NEXT J
4790 CLOSE #3
4800 REM RENAME 'REDUCED' DATA FILE
4810 SHELL DF3$
4820 PRINT
4830 PRINT
4840 PRINT "YOU WANT TO REPOSITION TRAVERSER FOR ANOTHER
          MOVEMENT (Y OR N)?";R$
4850 PRINT
4860 PRINT "IF 'Y', THE PROGRAM WILL TAKE YOU TO MANUAL CONTROL
             SUBROUTINE."
4870 PRINT "IF 'N', THE PROGRAM WILL END."
4880 PRINT
4890 INPUT "ANOTHER MOVEMENT";R$
4900 IF R$ = "Y" THEN 1360
4910 IF R$ = "N" THEN 3060
4920 PRINT
4930 PRINT
4940 REM CP-CONTROLLED MOTOR MOVEMENT FOR MOTOR 3
4950 Z(1)=0
4960 I1=0
4970 I2=0
4980 I3=0
4990 FOR J=1 TO N
5000 IF J=1 THEN 5040
5010 Z(J)=BL*(1-(SIN((PI/2)*(1+(J/N)))))
5020 Z1(J)=Z(J)-Z(J-1)
5030 I3 = -Z1(J)
5040 PRINT
5050 PRINT
5060 PRINT
5070 PRINT "    **********************"
5080 PRINT
5090 PRINT "   DATA POINT ";J
5100 PRINT
5110 GOSUB 3130
5120 PRINT
5130 INPUT "ENTER HOTWIRE VOLTAGE";HWV(J)
5140 PRINT
5150 INPUT "ENTER RMS VOLTAGE";RMS(J)
```

```
5160 PRINT
5170 IF J=N THEN 5200
5180 INPUT "PRESS 'ENTER' FOR NEXT MOTOR MOVEMENT";MOVE$
5190 NEXT J
5200 PRINT "ALL MOVEMENTS COMPLETED"
5210 REM OPEN 'RAW' DATA FILE
5220 OPEN "A:\MOTOR.DAT" FOR OUTPUT AS #2
5230 PRINT #2,"BL DISTANCE","HW VOLTS","RMS VOLTS"
5240 DF2$=RN2$+FI2$
5250 FOR J=1 TO N
5260 PRINT #2, Z(J)+ZIP,HWV(J),RMS(J)
5270 NEXT J
5280 CLOSE #2
5290 REM RENAME 'RAW' DATA FILE
5300 SHELL DF2$
5310 REM OPEN 'REDUCED' DATA FILE
5320 OPEN "A:\CALCDAT.DAT" FOR OUTPUT AS #3
5330 PRINT #3, "NORM DIST","UMEAN","URMS","N/D VEL","N/D RMS"
5340 DF3$=RN3$+FI3$
5350 FOR J=1 TO N
5360 REM **** USE CALIBRATION CURVE EQUATION *********
5370 VEL(J) = 1.316021*(HWV(J)^3.14759)
5380 VRMS(J) = 4.1423*(HWV(J)^2.14659)*RMS(J)
5390 NEXT J
5400 FOR J=1 TO N
5410 PRINT #3, (Z(J)+ZIP)/10,VEL(J),VRMS(J),VEL(J)/VEL(N),VRMS(J)/VEL(N)
5420 NEXT J
5430 CLOSE #3
5440 REM RENAME 'REDUCED' DATA FILE
5450 SHELL DF3$
5460 PRINT
5470 PRINT
5480 PRINT "YOU WANT TO REPOSITION TRAVERSER FOR ANOTHER
           MOVEMENT (Y OR N)?";R$
5490 PRINT
5500 PRINT "IF 'Y', THE PROGRAM WILL TAKE YOU TO MANUAL CONTROL
           SUBROUTINE."
5510 PRINT "IF 'N', THE PROGRAM WILL END."
5520 PRINT
5530 INPUT "ANOTHER MOVEMENT";R$
5540 IF R$ = "Y" THEN 1360
5550 IF R$ = "N" THEN 3060
```

List of References

1. Mueller, T. J., *Low Reynolds Numbers Vehicles*, AGARDograph 288, AGARD-AG-288, pp. 1-16, February 1985.

2. Bradshaw, P., *An Introduction to Turbulence and Its Measurement*, pp. 8-154, Pergamon Press, New York, NY, 1971.

3. Roane, D. P. Jr., *The Effect of a Turbulent Airstream on a Vertically-Launched Missile at High Angles of Attack*, Master's Thesis, Naval Postgraduate School, Monterey, CA, December 1987.

4. *Laboratory Manual for Low-Speed Wind Tunnel Testing*, pp. 3-1 to 3-8, Department of Aeronautics and Astronautics, Naval Postgraduate School, Monterey, CA, September 1983.

5. Pope, A., and Harper, J. J., *Low Speed Wind Tunnel Testing*, pp. 113-121, Wiley, New York, NY, 1966.

6. Bastedo, W. G. Jr., and Mueller, T. J., "Performance of Finite Wings at Low Reynolds Numbers", pp. 195-203, *Proceedings of the Conference on Low Reynolds Number Airfoil Aerodynamics*, University of Notre Dame, Report UNDAS-CP-77B123, June 1985.

7. American Institute of Aeronautics and Astronautics, AIAA-87-0495, *Boundary Layer Measurements on an Airfoil at Low Reynolds Numbers*, by Brendel, M. and Mueller, T. J., pp. 1-5, January 1987.

8. Brendel, M., and Mueller, T. J., "Preliminary Experiments in Unsteady Flow on Airfoils at Low Reynolds Numbers", pp. 281-292, *Proceedings of the Conference on Low Reynolds Number Airfoil Aerodynamics*, University of Notre Dame, Report UNDAS-CP-77B123, June 1985.

9. Schmidt, G. S., O'Meara, M. W., and Mueller, T. J., "An Analysis of a Separation Bubble Transition Criterion at Low Reynolds Numbers", pp. 125-134, *Proceedings of the Conference on Low Reynolds Number Airfoil Aerodynamics*, University of Notre Dame, Report UNDAS-CP-77B123, June 1985.

10. American Institute of Aeronautics and Astronautics, AIAA-86-0012, *Oscillating Hot-Wire Measurements Above an FX63-137 Airfoil*, by Crouch, J. D. and Saric, W. S., pp. 1-12, January 1986.

11. TSI, Inc., *IFA-100 System, Intelligent Flow Analyzer Instruction Manual*, pp. 1-1 to 4-11, Revision C, St. Paul, MN, August 1987.

12. Velmex, Inc., *User's Guide to 8300 Series Stepping Motor Controller/Drivers*, East Bloomfield, NY, January 1985.

13. Rabang, M. P., *Turbulence Effects on the High Angle of Attack Aerodynamics of a Vertically Launched Missile*, Master's Thesis, Naval Postgraduate School, Monterey, CA, June 1988.

14. National Aeronautics and Space Administration Technical Note D-368, *Preliminary Experimental Investigation of Effect of Freestream Turbulence on Turbulent Boundary Layer Growth*, by Kline, S. J., Lisin, A. V., and Waitman, B. A., pp. 1-60, March 1960.

INITIAL DISTRIBUTION LIST

		No. Copies
1.	Defense Technical Information Center Cameron Station Alexandria, VA 22304-6145	2
2.	Library, Code 0142 Naval Postgraduate School Monterey, CA 93943-5002	2
3.	Chairman Department of Aeronautics and Astronautics, Code 67 Naval Postgraduate School Monterey, CA 93943-5000	1
4.	Commander Naval Air Systems Command Washington, D.C. 20360	1
5.	Naval Research Laboratory, Code 5712 4555 Overlook Avenue, S.W. Washington, D.C. 20375	1
6.	NASA Langley Research Center MS/185 Technical Library Hampton, VA 23665	1
7.	NASA Ames Research Center Technical Library Moffett Field, CA 94035	1
8.	Prof. R.M. Howard Department of Aeronautics and Astronautics, Code 67HO Naval Postgraduate School Monterey, CA 93943-5000	10
9.	LT. David W. Kindelspire No. 4 Village Dr. East St. Charles, MO 63303	2